A unique role of E-cadherin among the cadherin family members co-expressed in the neural crest?

Zur Erlangung des akademischen Grades eines

DOKTORS DER NATURWISSENSCHAFTEN

(Dr. rer. nat.)

Fakultät für Chemie und Biowissenschaften

Karlsruher Institut für Technologie (KIT) – Universitätsbereich

genehmigte

DISSERTATION

von

Chaolie Huang

aus

Zhejiang (China)

Dekan: Prof. Dr. Peter Roesky

Referentin: Prof. Dr. Doris Wedlich

Korreferent: Dr. habil. Clemens Franz

Tag der mündlichen Prüfung: 18. Juli 2014

This work was performed at the Zoological Institute, Department of Cell and Developmental Biology at Karlsruhe Institute of Technology (KIT) from September 2011 to June 2014.

I declare that I have done this work by myself, no other reagents, equipment and methods were used other than those described in the thesis.

Chaolie Huang,

Karlsruhe, June 2014

Acknowledgements

Index

Abbreviations

(v/v)	Volume per volume
(w/v)	Weight per volume
ADAM	A Disintegrin And Metalloprotease
AP	Alkaline phosphatase
AP2	Activator Protein 2
BCIP	5-bromo-4-chloro-3'-indolyphosphat
BMP	Bone Morphogenetic Protein
bp	Base pairs
BSA	Bovine Serum Albumin
CAMs	Cell adhesion molecules
CBD	Catenin binding domain
Cdc42	Cell Division Cycle 42, small GTPase
CNC	Cranial neural crest
CoMO	Control morpholino oligonucleotide
ConA	Concanavalin A
C-cadherin	Placental cadherin homolog in *Xenopus*, also known as EP-cadherin
DAPI	4,6 Diamidino-2-phenylindoldihydrochloride
DEPC	Diethylpyrocarbonate
DN E-cadMu	Extracellular domain mutated E-cadMu
EC	Extracellular cadherin (repeat)
E-cadherin	Epithelial cadherin
E-cad MO	E-cadherin morpholino
E-cadMu	Morpholino binding site mutated E-cadherin rescue construct
E-cadMu ΔC	Cytoplamic domain deleted E-cadMu
E.coli	*Escherichia coli*
EMT	Epithelial to mesenchymal transition

FCS	Fetal calf serum
FGF	Fibroblast Growth Factor
H2B GFP	Histone 2B green fluorescence protein
HAV	Histidine-Alanine-Valine, homophilic binding site of cadherins
ISH	*in situ* hybridization
mbGFP	Membrane bound GFP
mbCherry	Membrane bound Cherry
MBSH	Modified Barth's saline with Hepes
LB	Luria Bertani Medium
M-cadherin	Muscle Cadherin
MEM	Modified Eagle's Medium
MO	Morpholino oligonucleotide
NBT	Nitro-blue tetrazolium chloride
NC	Neural crest
N-cadherin	Neural cadherin
N-cad MO	N-cadherin morpholino oligonucleotide
ODC	Ornithine Decarboxylase
PAPC	Paraxial Protocadherin
P-cadherin	Placental cadherin
PCP	Planar cell polarity
PCR	Polymerase Chain Reaction
PCNS	Protocadherin in Neural Crest and Somites
(A)PBS	(Amphibian) Phosphate buffered saline
PVDF	Polyvinyl-difluorid
PFA	Paraformaldehyde
QAV	Glutamine-Alamine-Valine, homophilic binding site of cadherins
Rac	Ras-related C3 botulinum toxin substrate
RhoA	Ras homolog gene family member A

Rpm	Rotations per minute
RT	Room temperature
RT-qPCR	Quantitative real-time PCR
Sdf-1	Stromal cell-derived factor-1
SDS-PAGE	Sodium dodecyl sulphate-polyacrylamide gel electrophoresis
SOC	Super Optimal Broth with Glucose
TEMD	N,N,N',N'-Tetramethylethylendiamine
TM	Transmembrane domain
Trp2	Tyrosinase-related protein-2
Wnt	Wingless/INT-related
WT	Wild type
XB-cadherin	Placental cadherin homolog in *Xenopus*, also known as U-cadherin

1   Introduction

In the development of a multicellular organism, an essential element in regulating tissue morphogenesis is the initial formation, dynamic rearrangement and constant maintenance of cell-cell contacts, as mediated mainly by cell adhesion molecules (CAMs). As several classes of molecules can mediate cell adhesion, cadherins appear to be the major adhesion molecules. Cadherin mediated cell adhesion not only allows cells in tissue to recognize each other forming coherent functional structures, but also drive many cellular behaviours such as cell sorting and directional cell migration, which makes them a very interesting subjects in the context of developmental biology.

1.1   Cadherins

The research of cadherins starts in early 1980s, when Jacob and co-workers first described E-cadherin (uvomorulin), and its role in blastomeres compaction of an early developing mouse embryo (Hyafil et al., 1981; Peyrieras et al., 1983). Until now, over a hundred different cadherin family members have been identified in mammals (Hulpiau and van Roy, 2009). In invertebrates, cadherins in *Drosophila* and *Caenorhabditis elegans* have also been studied (Oda et al., 1994; Sano et al., 1993). Cadherins are best known for their function in establishing cell-cell contacts, the *zonola adherens*, that leads to apical-basolateral cell polarity in epithelia (Takeichi, 1995). However, cadherins are also necessary for cell proliferation and for signalling in cell differentiation (Geiger and Ayalon, 1992; Wollner and Nelson, 1992). Moreover, cadherins are required in many processes during tissue morphogenesis, tissue organization and collective cell migration (Becker et al., 2012; Takeichi, 1995). Disturbed cadherin functions are often associated with congenital defects in organogenesis, metastasis and tumour invasion in cancer (Berx and van Roy, 2009; El-Amraoui and Petit, 2010; Thompson and Price, 2002).

Cadherins are a group of transmembrane glykoproteins mediating calcium dependent homophilic cell-cell adhesion. Based on their structure and function, the cadherin superfamily can be divided into four major groups: classical cadherins (type I and type II), protocadherins, desmosomal and atypical cadherins. Cadherins are comprised of three domains, an extracellular domain, a hydrophobic transmembrane (TM) domain and a highly conserved cytoplasmic domain Fig (1.1)

(Takeichi, 1990). The extracellular domain of cadherins consists of consecutive extracellular cadherin (EC) repeats. Each EC repeat contains about 110 amino acids and forms an immunoglobulin-like fold consisting of seven β-strands that are arranged as two opposed β-sheets. The connections between successive EC domains are rigidified by coordination of Ca^{2+} ions, which is mediated by conserved amino acids in all cadherins (Boggon et al., 2002; Nagar et al., 1996; Pokutta et al., 1994). The binding of calcium is essential for the proper function of cadherins. Removal of calcium abolishes the adhesive function of cadherins and renders them vulnerable against proteases. The cytoplasmic regions of cadherins are less conserved, except for some binding motifs shared within specific cadherin families. For instance, there are two catenin-binding motifs in classical cadherins, which bind the armadillo proteins β-catenin and p120 (Fig1.1) (Takeichi, 1990).
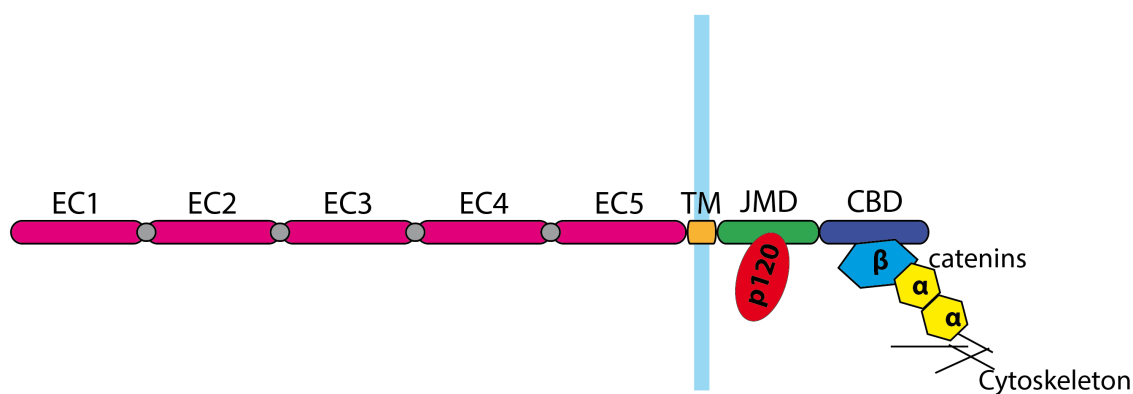
Fig1.1 Schematic structure of a classical cadherin. The extracellular domain consists of five cadherin repeats (EC1-5) bridged by calcium ions (grey), whereas the transmembran domain (TM) anchors the protein within membrane. The cytoplasmic domain contains a juxtamembrane domain (JMD) that binds p120, and a catenin binding domain (CBD) for β-catenin binding. The cytoplasmic domain is further anchored to the cytoskeleton via β-catenin and α-catenin.

Cadherins form cluster via dimerization with other cadherins, which can occur in *cis*-orientation (between molecules from the same cell) or in *trans*-orientation (between molecules from different cells). In *trans*-orientation, cadherins are oriented in an opposing direction, interacting their EC1 repeats by strand swapping. Strand swapping describes the replacement of one β-strand with the strand of the other in opposite EC1 domains. Critical for the interaction are the side chains of conserved tryptophan residues, which fit into a hydrophobic pocket on the EC1 domain of the binding partner (Boggon et al., 2002; Harrison et al., 2011; Häussinger et al., 2004; Patel et al., 2006). Type I cadherins and desmosomal cadherins have one tryptophan residue, tryptophan-2

(Trp2), in the N-terminal of the first EC repeat (EC1), whereas type II cadherins have two conserved tryptophans (Trp2 and Trp4) (Patel et al., 2006). The hydrophobic pocket is formed by a HAV motif (type I cadherins) or QAV motif (type II cadherins) containing a highly conserved alanine residue (Ala80) (Blaschuk et al., 1990; Nose et al., 1990). Mutations in the tryptophan residue or in the HAV (QAV) motif leads to loss of cadherins adhesion function (Niessen et al., 2011; Patel et al., 2006). Adhesions between cadherins are further strengthened by *cis*-interation of cadherin molecules. In a *cis*-interaction, the EC1 domain of one cadherin is non-symmetrically interacting with the EC2 domain of a partner cadherin, with additional contributions from the EC2-3 linker and the apex of the EC3. On contrary to the *trans*-interaction, the *cis*- interaction orients partner cadherins in parallel. Since each cadherin ectodomain can simultaneously engage in two *cis*-interactions with their EC1 and EC2/3 region, the *cis*- interface arranges cadherins into linear arrays (Harrison et al., 2011). When the *cis*- interaction is ablated, cell adhesion can still occurs but the extent of cadherin accumulation at cell-cell contact regions is diminished, and the resulting junctions are unstable (Harrison et al., 2011).

The mechanisms of cadherin clustering are controversial. Many experiments suggest that catenins and their interaction with the cytoskeleton are required for cadherins to be clustered into adherens junctions (Chu et al., 2004; Fujimori and Takeichi, 1993; Shewan et al., 2005; Yap et al., 1998). However, recent studies report that junction-like structure can be formed by extracellular domain of classical cadherins alone, which involves both strong homophilic *trans*-interactions and weaker lateral *cis*-interactions (Hong et al., 2010; Ozaki et al., 2010). Nonetheless, *in vivo* cadherin clustering requires interactions with the actin cytoskeleton. The binding of cadherins to the actin cytoskeleton is mediated by α- and β-catenin. β-catenin binds directly the conserved intracellular tail of cadherins and recruits α-catenin, which in turn, interacts with actin filaments (Drees et al., 2005; Yonemura, 2011). Coupling cadherins to the cytoskeleton provides an anchorage to contractile actomyosin networks, which exert physical forces that are responsible for cell-cell contact remodelling during development. Furthermore, the intracellular adhesion complex regulates the membrane organization of cadherins and influences the stability and mobility of cadherin clusters through the mechanosensing activity of cadherins (Cavey et al., 2008; Kametani and Takeichi, 2007; Liu et al., 2010; Martin et al., 2010; Martin et al., 2009; Mège et al., 2006; Smutny et al., 2010). Cadherins at cell-cell contacts respond to increased stiffness of the substrate by enhanced clustering (Ladoux et al., 2009). Shear forces applied on the E-cadherin-coated bead and E-cadherin expressed cell can increase stiffness at cadherin junctions, confirming the E-cadherin complex functions as a mechanosensor (le Duc et al., 2010). Furthermore, cadherin mediated mechanical sensing is coordinated to drive coherent

changes. In *Drosophila*, the lateral ectoderm migrates toward the dorsal midline and encloses the more dorsal amnioserosa. Studies have shown that the contractions of amnioserosa cells are required for this process and are coordinated with contractions of an actin cable spanning the entire leading edge of the lateral ectoderm (Solon et al., 2009). Mechanism of this coordination is thought to involve E-cadherin and integrins, which transmit tension between the lateral ectoderm and the amnioserosa (Gorfinkiel and Arias, 2007; Gorfinkiel et al., 2009).

Apart from the interaction with cytoskeleton, p120 is another regulator of cadherin stability. Binding of p120 to the juxtamembrane domain (JMD) of the cadherin cytoplasmic tail stabilizes cadherin localization at the cell surface, and induces cadherin clustering resulting in the formation of AJs (Anastasiadis and Reynolds, 2000; Xiao et al., 2007). Dissociation of p120 from the cadherin complex leads to endocytic internalization of cadherins (Davis et al., 2003; Hoshino et al., 2005). Moreover, p120 binds to Rho GTPases (Magie et al., 2002) and its key effector Rho kinase (ROCK) (Smith et al., 2012), suggesting that components of the cadherin-catenin molecular complex may spatially coordinate Rho activity. GTPases are guanine nucleotide-binding proteins that regulate the cytoskeleton and influence many cellular processes including cell protrusion formation (Jaffe and Hall, 2005). Members of Rho GTPases family have been identified at cadherin mediated adhesion sites, and cadherin adhesion is able to active Rac signaling at contact sites (Kitt and Nelson, 2011; Kovacs et al., 2002; Nakagawa et al., 2001; Noren et al., 2001; Yamada and Nelson, 2007). Guanine nucleotide exchange factor (GEF) catalyses GTP loading and activates Rho. Trio, a Rac GEF, is identified in a complex with M-cadherin and Rac and necessary for activation of Rac upon adhesive ligation of M-cadherin Cadherin at junctions (Charrasse et al., 2007). Trio also interacts with Cadherin-11 in *Xenopus* (Kashef et al., 2009).

1.2   Cadherins in collective cell migration

Collective cell migration is described as a coordinated migration of a cell population through cell-cell cooperation (Theveneau and Mayor, 2012a), which is observed during cell movement in morphogenesis, wound healing and cancer metastasis (Friedl and Gilmour, 2009; Rørth, 2009; Theveneau and Mayor, 2012b). In the context of morphogenesis alone, a number of collective migratory events are known to occur. In *Drosophila*, collective migration is employed during border cell migration (Montell, 2003). In vertebrates, collective migration is extensively studied in

gastrulation movement and neural crest migration (Alfandari et al., 2010; Bouwmeester et al., 1996; Friedl and Gilmour, 2009). Also, the key role for collective migration has been revealed in the development of sensory lateral line in zebrafish (Haas and Gilmour, 2006). During these processes, cadherin mediated cell-cell interactions play an essential role in the collectiveness of migratory cells.

The border cells in *Drosophila* embryos are a group of cells that undergoes collective migration. The border cells arise at the anterior pole of the egg chamber and migrate toward the posterior and then dorsal side of the oocyte, contributing to micropyle formation (Montell, 1994).The border cell cluster consists of border and polar cells (Montell, 2003), where the non-motile polar cells are surrounded by border cells. The cluster stays cohesive as they detach from the surrounding follicle cells and migrate posteriorly in between and along nurse cells. E-cadherin is required for border cell migration by engaging in two different ways. First, the expression of E-cadherin in border cells is essential for them to polarize. Second, E-cadherin expressed in both border cells and nurse cells establishes the contact, allowing the border cell cluster to migrate (Geisbrecht and Montell, 2002; Niewiadomska et al., 1999; Pacquelet and Rørth, 2005). It is suggested that the traction force generated by E-cadherin mediated adhesion may be responsible for cell movement (Niewiadomska et al., 1999).

Mechanoresponsive cadherin-catenin complex is also involved in collective cell migration of the head mesendoderm cells in *Xenopus* during convergent extention (CE). The leading edge cells of the head mesendoderm arise from deep endoderm cells at early gastrula stage, whereas the following cells behind the leading edge are involuted prechordal mesoderm cells. At mid-blastula, head mesendoderm cells polarize along the animal-vegetal axis and migrate directly as a cohesive sheet towards the blastocoel roof (Bouwmeester et al., 1996). It is shown that force induced polarized cell protrusion is C-cadherin dependent. Local tension on cadherin adhesions localizes plakoglobin and intermediate filament to the adhesion sites, which both are required for polarized protrusive behaviours. It is therefore proposed that tension on C-cadherin-mediated adhesion between migrating head mesendoderm cells induces polarized cell protrusions and directed migration (Weber et al., 2012). In contrast, the migration of mesoderm in zebrafish requires E-cadherin (Ulrich et al., 2005), where the germ layer progenitor cells rely on E-cadherin to undergo directional migration as cell groups (Arboleda-Estudillo et al., 2010).

E-cadherin-dependent cell polarization is also found in the wound healing. It is observed that the sensing of substrate stiffness and force transmission is coordinated by E-cadherin-based cell-cell contacts across tissues, inducing polarization of cytoskeleton and migration in the direction of the

wound in in the cells that are far from the wound edge (Ng et al., 2012). It is shown that E-cadherin adhesion induced cell polarization of cell migration to be actin-dependent (Desai et al., 2009), but the mechanism by which E-cadherin directs actomyosin-dependent cell polarization remains unclear. In epidermal wound closure, sprouting vessels and epithelial cancer, desmosomal cadherins, including desmoglein1, desmoglein 3 and desmosomes, are also involved in the cell-cell junction formations, yet their specific contribution to collective migration is unclear (Chidgey and Dawson, 2007; Khan et al., 2006; Moll et al., 1999).

Collective cell invasion in cancer and morphogenic movements exhibits striking resemblance, including not completely de-differentiated forms of rhabdomyosarcoma as well as well-differentiated carcinomas, melanoma and breast cancer (Friedl and Gilmour, 2009; Friedl et al., 1995; Hegerfeldt et al., 2002; Nabeshima et al., 1999). It is shown that the collective invasion of vulvar squamous cell carcinoma A431 cells is dependent on intact P- and E-cadherin mediated cell-cell contacts and p120 catenin (Macpherson et al., 2007). Nevertheless, the mechanism of how cohesiveness facilitates collective cell invasion *in vivo,* and the role of cadherins is still poorly understood.

1.3 Neural crest as model system for studying cadherin function in collective cell migration

Neural crest (NC) cells are embryonic mesenchymal cells exhibiting extensive collective migration during their development (Theveneau et al., 2010). Thus, they provide an excellent model for studying the molecular mechanisms of cadherins in collective cell migration *in vivo* and *in vitro*.

NC cells are a highly motile and pluripotent stem cell population that is characteristic for vertebrates. They arise at the neural plate border and give rise to a variety of derivatives such as craniofacial cartilage and bone structures, smooth muscle, peripheral and enteric neurons, glia and melanocytes (Kalcheim and Le Douarin, 1986; Wagner, 1990). Despite their ectodermal origin at the neural plate border, NC has the potential to give rise to cell types characteristic of more than one of the classical germ layers. Therefore, they are defined as the "the fourth germ layer" (Hall, 2000). Defects in migration, proliferation and differentiation of NC are usually associated with a variety of diseases such as Piebaldismus, DiGeorge-, and Waardenburg syndrome (Aubry and Morand, 1964; DiGeorge, 1968; Hall, 1979; Spritz, 1997; Waardenburg,

1951). Moreover, migrating NC cells display many similarities with metastasizing tumour cells in respect of their migration behaviours and involved molecules, and serve therefore as an optimal model system for investigating cell-cell interaction, communication, morphology and migration mechanisms (Gammill and Bronner-Fraser, 2003; Kulesa and Gammill, 2010).

The induction of the NC occurs in the ectodermal germ layer as a consequence of multiple instructive cues generated at the border between the presumptive neural plate and the epidermis (LaBonne and Bronner-Fraser, 1998). A dynamic interplay of BMP, Wnt, FGF and Notch signalling is responsible for the induction of the neural plate border (Milet and Monsoro-Burq, 2012) and subsequently contribute to the induction of early NC specifiers. In *Xenopus*, the onset of the expression of NC specifier genes occurs during mid- to late-gastrulation and the earliest expressed NC specifier genes include *Snail2* (*Slug*), *Snail, Sox8, Sox9, FoxD3, twist, Ets1, AP2, c-myc* and *Id* genes (LaBonne and Bronner-Fraser, 1999). *Snail1*, *Id3*, *Sox9*, and *Sox10* maintain the NC identity and control cell survival (Kee and Bronner-Fraser, 2005; Sonnenberg-Riethmacher et al., 2001). Furthermore, all these transcription factors act together to further refine the specification, and promote emigration of NC cells (LaBonne and Bronner-Fraser, 1999).

After their specification at the border of the neural plate, the NC population separates from the neighbouring neuroepithelium by delamination, which is believed to involve at least a partial epithelium-to-mesenchaymal transition (EMT) (Ahlstrom and Erickson, 2009; Alfandari et al., 2010). This is followed by extensive migration of NC cells throughout the embryo. In *Xenopus*, the cranial neural crest (CNC) cells migrate collectively as a cohesive cell sheet (Alfandari et al., 2003; Theveneau and Mayor, 2011), where the three segments (mandibular, hyoidal and branchial segments) of CNC migrate directly beneath the ectoderm in ventral direction toward the pharyngeal pouches (Sadaghiani and Thiébaud, 1987) (Fig1.2). The mandibular segment, which originates from the mesencephalon, moves ventrally to the optic vesicle, migrate around the eye vesicle, eventually invade the mandibular arch and contribute to the formation of the quadrate and Meckel's cartilage, as well as the ethmoidal-trabecular plate (Sadaghiani and Thiébaud, 1987). The hyoid segment originates from the anterior part of the rhombencephalon. They migrate downward over the mesoderm of the hyoid arch from the rostral part of the otic vesicle, finally into the hyoid arch and take part in the formation of the ceratohyal cartilage. The branchial segment of CNC originates from the posterior part of the rhombencephalon and migrates over the branchial region posterior to the otic vesicle. During migration, the branchial segment gradually subdivides into two - the anterior and posterior – subpopulations. These cells

form the branchial arches and differentiate into cartilages of the grills and connective tissues (Sadaghiani and Thiébaud, 1987; Theveneau and Mayor, 2011).
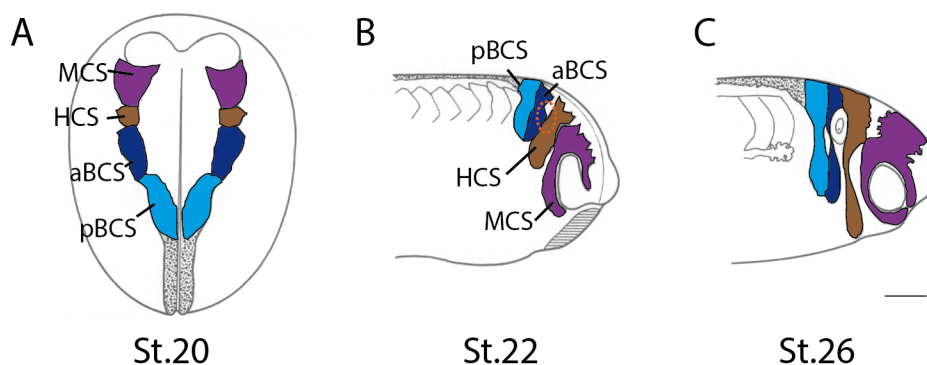
Fig1.2 Schematic representation of cranial neural crest (CNC) migration at different stages of *Xenopus* development. (A) At stage 20, the three segments of the CNC (MCS, HCS, BCS) are discernible after neural tube closure and start to emigrate. **(B)** At stage 22, MCS migrate ventrally around the eye; HCS descends downward towards the hyoid arch from the rostral part of the otic placode, whereas the BCS migrates over the branchial region posterior to the otic vesicle. The groove between HCS and BCS (orange dashed circle) is the otic placode. **(C)** At stage 26, the MCS surrounds the eye. The HCS has penetrated into the hyoid arch, and the BCS are located on the branchia region. MCS, mandibular crest segment (lily); HCS, hyoid crest segment; aBCS (brown), anterio branchial crest segment (dark blue); pBCS (light blue), posterior branchial crest segment. Modified from (Sadaghiani and Thiébaud, 1987). Scale bar = 50 µm.

During migration, NC cells interact with the neighbouring tissue and react to a variety of signals controlling their polarity and directionality, allowing them to colonize their differentiation regions. In fact, the directed migration of CNC cells is mediated by the cooperation of many different mechanisms. Recent studies reveal that the coordinated regulation of collective chemotaxis, co-attraction and contact inhibition of locomotion (CIL) is required for correct CNC migration (Carmona-Fontaine et al., 2008; Carmona-Fontaine et al., 2011; Theveneau et al., 2010; Theveneau et al., 2013). CIL is defined as "the stopping of the continual locomotion of a cell in the same direction after collision with another cell" (Abercrombie, 1979). CNC cells display CIL *in vivo* and *in vitro*, which is required for their directional migration (Carmona-Fontaine et al., 2008). However, to maintain the cohesive cluster of migrating CNC cells, the complement fragment C3a and its receptor C3aR mediated coattraction is required, which counterbalance the dispersion of cells caused by CIL (Carmona-Fontaine et al., 2011). Moreover, the chemokine Sdf1 serves as a chemoattractant for collective CNC cell migration *in vitro* and *in vivo*, promoting directional

migration by stabilizing contact-dependent cell polarity (Theveneau et al., 2010; Theveneau et al., 2013). Furthermore, a "chase-and-run" behaviour between CNC cells and placodal cells is recently proposed (Theveneau et al., 2013). In this model, Sdf-1 dependent chemotaxis attracts CNC cells towards placodal cells, which lie adjacent to the CNC tissue during migration. Once in contact, CIL between CNC cells and plalcodal cells inhibits the protrusion in placodal cells, where the symmetry of placodal tissue is broken inducing directional movement. The coattraction and repulsion movement is self-sustained due to chemotaxis and CIL, which promote persistent coordinated migration of both cell populations (Theveneau et al., 2013). Of all these mechanisms of CNC migration, cadherin mediated cell-cell adhesions are involved. However, the mechanisms of their involvement are not fully understood and require further elucidation.

1.4   Cadherins in *Xenopus* CNC migration

In the migration of CNC cells, a switch of cadherin expression is observed in mice and chicken during their EMT, which allow cells to lose their epithelial morphology, dissemble cell-cell junctions and obtain mesenchymal characters. During this process, classical type I cadherins, for instance E-cadherin and N-cadherin, are down-regulated, whereas the expression of mesenchymal type II cadherins like Cadherin-6B (*G. gallus*) and Cadherin-7 (*G. gallus*) increases (Nakagawa and Takeichi, 1995, 1998; Wheelock et al., 2008). In *Xenopus*, both the type I classical cadherin N-cadherin and the type II classical cadherin Cadherin-11, as well as the protocadherin PCNS are expressed in NC cells (Hadeball et al., 1998; Rangarajan et al., 2006; Theveneau et al., 2010).

N-cadherin expression is found in CNC cells during their migration, and both gain-and loss-of-function of N-cadherin inhibit CNC migration *in vivo* (Theveneau et al., 2010). *In vitro* studies demonstrate that functional blocking antibodies against N-cadherin prevent CIL and collective polarization of CNC cells toward a Sdf1 gradient (Theveneau et al., 2010). N-cadherin mediated CIL is responsible for the repulsion behaviour between CNC cells and placodal cells in the "chase-and-run" model of CNC migration. In this process, N-cadherin localizes at cell-cell contacts and inhibits protrusion formation of the placodal cells (Theveneau et al., 2013). Furthermore, N-cadherin is necessary for generating an asymmetric focal adhesion distribution relative to the contact site and therefore promotes directional migration (Theveneau et al., 2013).

Cadherin-11 is a type II cadherin expressed in migrating CNC cells in *Xenopus* (Hadeball et al., 1998). Overexpression and knockdown of Cadherin-11 inhibit CNC migration *in vivo* (Borchers et al., 2001; Kashef et al., 2009), indicating a defined level of Cadherin-11 mediated adhesion is required for cells to migrate. One of the regulators of Cadherin-11 mediated cell-cell adhesion is the metalloproteases ADAM13, which cleaves between the EC3 and EC4 in the extracellular domain of Cadherin-11 and modulates its adhesive function (McCusker et al., 2009). The cleavage product can bind the uncleaved Cadherin-11 via homophilic interaction, therefore promote or inhibit adhesion (McCusker and Alfandari, 2009). It is reported that Cadherin-11 mediated CIL between CNC cells is required for their migration (Becker et al., 2013). Additionally, Cadherin-11 binds to GEF Trio. The fact that constitutively active forms of RhoA, Rac and cdc42 functionally substitute for Cadherin-11 reveals a novel cadherin function of regulating protrusive activity in CNC cells (Kashef et al., 2009). Furthermore, it has been recently shown that Cadherin-11 is also involved in cell-substrate adhesion (Langhe et al., in revision).

Besides classical cadherins, the protocadherin PCNS is also expressed in *Xenopus* CNC (Rangarajan et al., 2006; Schneider et al., 2014). Knockdown of PCNC inhibits CNC migration *in vivo,* but the molecular mechanism still needs to be elucidated (Rangarajan et al., 2006). Reconstitution experiments show that another protocadherin PAPC, which shares 65% identical amino acids with PCNS, is able to compensate for the loss of PCNS (Schneider et al., 2014). In fact, overexpression of PAPC also leads to migration defects similar to knockdown of PCNS, indicating a possible role of PAPC in regulating CNC migration (Schneider et al., 2014).

2   Aim of the work

The goal of this work is to characterize the expression of different *Xenopus* cadherins and to investigate their function during CNC migration.

Up to the begin of this work, several cadherins have been described to be involved in CNC migration including the mesenchymal type II cadherin Cadherin-11, N-cadherin as classical type I cadherin, and the protocadherin PCNS (Hadeball et al., 1998; Rangarajan et al., 2006; Theveneau et al., 2010). However, a comparative expression analysis of these cadherins in CNC cells has not been performed so far.

To quantify the expression of the known cadherins and to identify possible novel cadherin subtypes expressed in CNC, quantitative real-time PCR with specific primers for Cadherin-11, N-cadherin, E-cadherin, XB-cadherin, C-cadherin, PCNS and PAPC should be performed. Since CNC migration involves a serial of dynamic changes in cell shape as well as adhesive properties, the CNC cells from different stages of CNC migration should be compared. Quantification of the relative expression level from premigratory (stage 17), emigrating (stage 20) and migratory (stage 23) CNC cells should demonstrate how the expression level of each cadherin subtype changes during migration. By comparing the obtained C_T values from CNC samples to a standard curve, the absolute copy number of each cadherin could be calculated, allowing a direct comparison of all expressed cadherins in the CNC tissue. Furthermore, the subcellular localization of these cadherin should be investigated through (1) ectopic expression of GFP tagged constructs and (2) immunofluorescence staining with specific antibodies on CNC explants.

Surprisingly, during this work, E-cadherin expression is found in CNC cells. Its localization and protein expression should be further illustrated via immunofluorescence staining on whole embryo sections and immunoblotting of embryo lysates. In order to understand the role of E-cadherin in CNC cells, loss-of-function experiments should be performed by morpholino injections. I*n situ* hybridization with CNC specific markers and transplantation experiments should demonstrate the loss of E-cadherin function on CNC migration *in vivo*. Furthermore, with CNC explants, the role of E-cadherin knockdown on cell morphology should be investigated. Moreover, reconstitution experiments with different E-cadherin deletion constructs as well as other cadherins should elucidate the specific function of E-cadherin in regulating CNC migration.

Finally, a possible redundant function between other cadherin subtypes in regard to CNC migration should also be examined by reconstitution experiments.

3   Materials

3.1   Antibodies

3.1.1   Primary antibodies

Name	Host	Dilution	Source
α-Digoxygenin-AP		1:3000	Roche Applied Science, Mannheim
α-HA (12CA5)	Mouse	1:400	Roche Applied Science, Mannheim
α-C-Cadherin (6B6)	Mouse	undiluted	DSHB Hybridoma Bank, USA
α-E-Cadherin (10H3)	Mouse	undiluted	DSHB Hybridoma Bank, USA
α-E-Cadherin (5D3)	Mouse	undiluted	DSHB Hybridoma Bank, USA
α-N-Cadherin (MNCD2)	Mouse	undiluted	DSHB Hybridoma Bank, USA
α-XB-Cadherin (6D5)	Mouse	undiluted	DSHB Hybridoma Bank, USA
α-Tubulin	Mouse	1:2000	Abcam, Cambridge, UK

Tab 3.1: Primary antibodies used in this work.

3.1.2   Secondary antibodies

Name	Description	Dilution	Source
GαM-Cy3	Cy^{IM}3-conjugated goat-anti-mouse IgG	1:400	Dianova GmbH, Hamburg
GαM-AP	Alkaline Phosphatase conjugated goat-anti-mouse IgG	1:2000	Dianova GmbH, Hamburg
GαR-AP	Alkaline Phosphatase conjugated goat-anti-rabbit IgG	1:2000	Dianova GmbH, Hamburg
GαM-POD	Peroxidase conjugated goat-anti-mouse IgG	1:5000	Dianova GmbH, Hamburg

NeutrAvidin-HRP	Pierce High Sensitivity NeutrAvidin-Horse radish peroxidase	1:1000	Thermo scientific, Germany

Tab 3.2: Secondary antibodies used in this work.

3.2 Bacteria strains

E.coli - JM-109 (Chemo- and Electrocompetant) (Promega, Mannheim)

Genotyp: *end*A1 *rec*A1 *gyr*A96 *thi hsd*R17 (r_k- m_k+) *rel*A1 *sup*E44 D(*lacpro*AB)

[F' *tra*D36 *pro*AB *lac*I$_q$ZDM15]

3.3 Chemicals and reagents

All other chemicals are purchased from the following companies: Applichem GmbH (Darmstadt), Fluka GmbH (Taufkirchen), Merck (Darmstadt), Carl Roth GmbH & Co. (Karlsruhe), Serva (Heidelberg) or Sigma-Aldrich (Taufkirchen).

- 2-log DNA Marker (New England Biolabs, Frankfurt)
- Con A Sepharose (Amersham Biosciences, Sweden)
- Complete, EDTA-free Protease Inhibitor Cocktail tablets (Roche Diagnostics GmbH, Mannheim)
- Phosphatase Inhibitor (Roche Diagnostics GmbH, Mannheim)
- DAPI (4,6 Diamidino-2-phenylindoldihydrochloride) (Merck KGaA, Darmstadt)
- Dextran-FITC (10,000 MW) (Invitrogen GmbH, Karlsruhe)
- Deoxyribonucleotide (Promega GmbH, Mannheim)
- DIG RNA Labeling Mix (Roche Diagnostics GmbH, Mannheim)
- DMSO (AppliChem, Darmstadt)
- Fetal calf serum (FCS) (GIBCO BRL Life Technology, UK)
- Horse serum (Invitrogen GmbH, Karlsruhe)

- iQ SYBR Green Supermix   (BioRad, Hercules, USA)
- Milk powder   (Heirler Cenovis GmbH, Radolfzell)
- Midori green advance   (Biozym Scientific GmbH, Oldendorf)
- NBT/BCIP Stock solution   (Roche Diagnostics GmbH, Mannheim)
- PageRulerTM Prestained Protein Ladder   (Fermentas, St.Leon-Rot)
- Penicillin/Streptomycin   (PAA Laboratories GmbH, Cölbe)
- RNAlater   (Ambion, Austin, USA)
- Sodium dodecyl sulfate (SDS)   (Serva, Heidelberg)

3.4   Enzymes

- GoTaq DNA-Polymerase   (Promega GmbH, Mannheim)
- *Pfu* Turbo DNA Polymerase   (Agilent Technologies, USA)
- Restriction Endonucleases   (Promega GmbH, Mannheim) (New England Biolabs, Frankfurt)
- SP6, T3, T7 RNA-Polymerase   (Roche Diagnostics GmbH, Mannheim)
- T4 DNA Ligase   (Promega GmbH, Mannheim)
- DNase I, RNase free   (Roche Diagnostics GmbH, Mannheim)
- MMLV Reverse Transcriptase   (Promega GmbH, Mannheim)

3.5   Kits

- Digoxygenin/Fluorescein RNA labeling Kit   (Roche Diagnostics GmbH, Mannheim)
- ECL Plus Westen Blotting   (Amersham GmbH, Freiburg)
- High Pure PCR Purification Kit   (Roche Diagnostics GmbH, Mannheim)
- High Pure Plasmid Isolation Kit   (Roche Diagnostics GmbH,

Mannheim)

- High Pure RNA Isolation Kit   (Roche Diagnostics GmbH,

  Mannheim)

- Homogenizer   (Invitrogen, USA)

- Nucleobond XtraMidi   (Macherey Nagel, Düren)

- mMESSAGE mMACHINE[TM]   (Ambion, Austin, USA)

- PureLink[TM] RNA Mini Kit   (Ambion, Austin, USA)

- BCA Protein Assay Kit   (Novagen/Merck, Darmstadt)

3.6   Morpholino-Oligonucleotide

All Morpholino oligonucleotides (MO) are synthesized by Gene Tools, LLC, USA. C-cadherin antisense oligodeoxynucleotide is synthesized by Sigma-Aldrich, Germany (Tab 3.3).

Name	Sequence
C-cadherin antisense oligodeoxynucleotide	5'-C*C*T* CTC CAG CTC CCT* A*C*G -3' (asterisks indicate phosphorothioate-modified residues) (Heasman et al.,1994b)
E-cadherin-MO	5'-AAC CAG GGC CTC TTC AAC CCC ATT G-3' (Nandadasa et al.,2009)
N-cadherin-MO	5'-GAA GGG CTC TTT CCG GCA CAT GGT G-3' (Nandadasa et al.,2009)
Xcadherin-11-MO	5'-CTT TCT TCA TTT TTG GTA GTG TTG T-3'
Control-MO	5'-CCT CTT ACC TCA GTT ACA ATT TAT A-3'

Tab 3.3: Morpholino oligonucleotides and antisense oligodeoxynucleotide used in this work.

3.7   Primers for PCR

All listed primers are synthesized by biomers.net GmbH, Ulm.

Name	Sequence
Emut_fwd	5'-CGA ATT CAA GGC CTA TGG GCC TCA AAC GAC CTT GGT TAC TTG GTG CTG TCG TGT TG-3'
Emut_rev	5'-CAG CAC CAA GTA ACC AAG GTC GTT TGA GGC CCA TAG GCC TTG AAT TCG AAT CGA-3'

Emu_MutHAV _fwd	5'-GAC AAT TAC GTT CTT TTT TCC CAT ATG GTG TCA TCA AAT GGG GCA AAT GTG G-3'
Emu_MutHAV_ rev	5'-CCA CAT TTG CCC CAT TTG ATG ACA CCA TAT GGG AAA AAA GAA CGT AAT TGT C-3'
Emu_MutTrp2_fwd	5'-GAA AAG ACA AAA AAG AGA CGC GGT GAT TCC ACC AAT CAT AG-3'
Emu_MutTrp2_rev	5'-CTA TGA TTG GTG GAA TCA CCG CGT CTC TTT TTT GTC TTT TC-3'
EmuTM_XhoI_fwd	5'-GAG CCT TTA CTA CCT CGA GAA GAT GAG ACT CGG G-3'
EmuTM_XhoI_rev	5'-CCC GAG TCT CAT CTT CTC GAG GTA GTA AAG GCT C-3'

Tab 3.4 Primers used in mutagenesis PCR for generating E-cadherin mutants.

Name	Sequence
Ecad_RT_fwd	5'-CGA CCT TTG GAC AGA GAA GC-3'
E-cadherin rev	5'-GCA CAG AGC CTT CAA AGA CC-3'
XB-cadherin_fwd	5'-TAT CCT TGC TGC TGC TCC TG-3'
XB-cadherin rev	5'-TCA CCT CCA CCT TCC TCT CC-3'
N-cadherin for	5'-CAG CAA CGA TGG CTT AGT GA-3'
N-cadherin rev	5'-ATT GTA ACG GAG ACG GTT GC-3'
Xcadherin-11 fwd	5'-TCG GAT ACT GTG GTC GGA AG-3'
Xcadherin-11 rev	5'-CAT CCT CTG GGT TGA TGC TG-3'
XPAPC_RT_fwd	5'-CCC AGT CGG TCT CTT CTT CTT TG-3'
XPAPC_RT_rev	5'-TTG CTG ATG CTG CTC TTG GTT AG-3'
PCNS_RT_fwd	5'-TGG AGA CCA GCA AAC AGA CA-3'
PCNS_RT_rev	5'-CAC TTA CAC TTC GGC ACA AA-3'
xTwist_fwd	5'-CTC AGT GAA GCG CAA CAA GA-3'
xTwist_rev	5'-CTC TGA CGC TCC CTG ACA TT-3'
xslug_fwd	5'-ACC TGC AGA CCC ATT CTG AT-3'
xslug__rev	5'-CAC AGC AAC CAG ATT CCT CAT-3'
xsnail_fwd	5'-GGC ACC AGT TAT TGC CTT TC-3'
xsnail_rev	5'-TGT TGT TCC ATC CAC CTG TC-3'

xbra_fwd	5'-TTC AGC CTG TCT GTC AAT GC-3'
xbra_rev	5'-TGA GAC ACT GGT GTG ATG GC-3'
ODC (57)_ fwd	5'-CAT TGC AGA GCC TGG GAG ATA-3'
ODC (57)_ rev	5'-TCC ACT TTG CTC ATT CAC CAT AAC-3'
ODC (62)_ fwd	5'-GCC ATT GTG AAG ACT CTC TCC ATT C-3'
ODC (62)_ rev	5'-TTC GGG TGA TTC CTT GCC AC-3'

Tab 3.5 Primers used in quantitative real-time PCR.

3.8   Constructs for RNA injection

Construct	Vector	Reference
E-cadherin full length	HA-pCS2+	Sang-Wook Cha, UK
E-cadherin full length Mu	HA-pCS2+	this work
E-cadherin DN	HA-pCS2+	this work
E-cadherin ΔC	HA-pCS2+	this work
GAP43-GFP	pCS2+	T. Bouwmeester, Heidelberg
GAP43-mCherry	pCS2+	B. Kraft, Karlsruhe
Histon2B-mCherry	pCS2+	R. Mayor, UK
Histon2B-GFP	pCS2+	R. Mayor, UK
N-cadherin full	pcDNA3.1	Nazan Kücükieylan, Ulm
XB-cadherin full length	pSP64T	Nazan Kücükieylan, Ulm
Xcad11 mutated	pcDNA3.1	A. Köhler, Karlsruhe

Tab 3.6 Constructs for generating mRNA used in embryonic injections.

3.9   Constructs for preparation of antisense RNA *in situ* probes

	Linearized	Transcribed	Reference
c-Myc	*ApaI*	*SP6*	R. David, Ulm
XAP-2	*HindIII*	*T7*	A. Borchers, Göttingen
Xeya-1	*BamHI*	*T7*	R. David, Ulm

XTwist	*XbaI*	*T7*	M. Sargen, UK

Tab 3.7 Constructs for synthesizing *in situ* hybridization probes

3.10 Solutions

All solutions are either autoclaved or used from sterile stock solutions and double-distilled water or DEPC-H2O. Sterile filtration (Ø 0,2 μm) is used for chemicals that cannot be autoclaved (e.g. Methanol, Triton X-100 or Tween 20).

- **Alcian Blue Solution:** 20 mg Alcian Blue in 15 ml Acetic Acid and 35 ml 100% (v/v) Ethanol
- **Ampicillin Stock solution (1000x):** Ampicillin 100 mg per ml of double-distilled water. Store at -20°C. Working concentration 1:1000 in LB Medium
- **APBS:** 2.7 mM KCl, 0.15 mM KH_2PO_4, 103 mM NaCl, 0.7 mM Na_2PO_4, pH 7.5
- **APS:** 10% (w/v) Ammonium persulfate in H_2O
- **Blocking Buffer for Immunostaining:** 1% (w/v) BSA in 1x PBS
- **Blocking Buffer for Western blot:** 5% Milk powder in TBST
- **Cysteine Solution:** 2% (w/v) L-Cysteine hydrochloride in 0.1x MBSH, adjust pH 8.2 with 10 M NaOH
- **Danilchik's Buffer:** 53 mM NaCl, 15 mM NaHCO3, 13.5 mM Na2CO3, 4.5 mM K-Gluconsaure, 5 mM Bicin, 1 mM CaCl2, 1 mM MgSO4, adjust pH 8.3 with 1 M HEPES buffer and sterile filtration (Note: Add CaCl2 and MgSO4 after adjusting pH and no autoclaving)
- **3% (w/v) BSA in Danilchik's Buffer**
- **DAPI Solution:** Stock solution 1 mg/ml in DMF, working concentration 1:1000 in blocking solution
- **DEPC-H2O:** Add 1 ml of Diethylpyrocarbonate in water, keep it shaking overnight and autoclave
- **Electrophoresis running buffer:** 25 mM Tris, 192 mM Glycin, 0,1% (w/v) SDS
- **Freezing medium (cell culture):** 40% medium + 40% heat inactivated FCS + 20% DMSO
- **G418 (cell culture):** 1 g in 10 ml DMEM High Glucose, sterile filtered and aliquot
- **HBS:** 10 mM HEPES, 150 mM NaCl, pH 7.5
- **Heat inactivated FCS:** heat FCS 30 minutes at 56°C

- *In situ* **Alkaline Phosphatase (AP Buffer):** 0.1 mM Tris-HCl pH 9.5, 0.05 mM MgCl2, 0.1 mM NaCl, 0.1% (v/v) Tween 20 in DEPC-H2O

- *In situ* **blocking solution:** 2% BMB in 1× MAB

- *In situ* **bleaching solution:** 0.5 x SSC, 5% (v/v) Formamide and 20% (v/v) Hydrogen Peroxide in 100% ethanol

- *In situ* **stain solution:** 1.5 µl NBT, 1.5 µl BCIP per ml AP Buffer

- *In situ* **hybridization buffer:** 50% (v/v) Formamide, 5x SSC, 2% Torula RNA (v/v), 0.1% (v/v) Heparin solution, 1x Denhardt's solution, 1 mg/ml Ribonucleic acid, 0.1% (v/v) Tween 20, 0.1% (w/v) CHAPS, 10 mM EDTA

- *in situ* **SSC (20%):** 300 mM Na-Citrat pH 7.0, 300 mM NaCl

- *in situ* **wash solution1:** 50% Formamid, 2x SSC, 0.1% Tween 20

- *in situ* **wash solution 2:** 25% Formamid, 2x SSC, 0.1% Tween 20

- *in situ* **wash solution 3:** 12.5% Formamid, 2x SSC, 0.1% Tween 20

- *in situ* **wash solution 4:** 2x SSC, 0.1% Tween 20

- *in situ* **wash solution 5:** 0.2x SSC, 0.1% Tween 20

- *in situ* **MAB (5×):** 0.5 M Maleic acid, 0.75 M NaCl, pH 7.5

- **LB-AMP-Agar Plates:** 1.5% (w/v) Select agar in LB medium and autoclave; after cooling to 55°C add 1 ml ampicillin stock solution per liter and pour into petri dish (Ø 9.4 cm), store cooled plates at 4°C

- **LB-AMP-Medium:** 1 ml Ampicillin solution per liter LB-Medium (1:1000)

- **LB (Lysogeny broth) Medium:** 10 g Tryptone, 5 g Yeast extract, 5 g NaCl, 1 liter water, adjust pH 7.5 with NaOH

- **Lysis Buffer:** 0.2 M NaOH, 1% SDS

- **MBSH (10x):** 880 mM NaCl, 24 mM NaHCO3, 100 mM KCl, 4 mM CaCl2, 3.3 mM Ca(NO3)2,100 mM HEPES, 8 mM MgSO4, pH 7.4

- **MEM (1x):** 100 mM MOPS pH 7.4, 2 mM EGTA, 1 mM MgSO4 diluted in DEPC-H2O

- **MEMFA:** 3.7% (v/v) formaldehyde in 1×MEM (Modified Eagle's Medium)

- **Mowiol:** 6.0 g Glycerin, 2.4 g Mowiol 4-88, 6.0 ml ddH$_2$O, 12.0 ml 0.2 M Tris-HCl (pH 8.5), 25 mg DABCO per ml solution

- **Neutralization Buffer:** 2.8 M Potassium acetate, adjust pH 5.1

- **Nile-Blue-Solution:** 0.5 M Na$_2$HPO$_4$, 0.5 M NaH$_2$PO$_4$, 0.1 g Nile Blue (Chloride) in 1 l H$_2$O

- **Orange G-Ladepuffer (5x):** 4 g Saccharose, 0.025 g Orange G in 10 ml H$_2$O

- **4% Paraformaldehyde in 1x PBS (100 ml):** Mix 4 g Paraformaldehyde with 80 ml pre-warmed (56°C) water. Add 1 M NaOH with constant stirring until solution becomes clear. Add 10 ml 10 x PBS and adjust pH 7.4 with conc. HCl at room temperature

- **PBS (10x):** 1.37 M NaCl, 27 mM KCl, 15 mM KH_2PO_4, 65 mM Na_2PO_4, pH 7.5

- **PBST:** 1x PBS, 0.1% (v/v) Tween 20

- **10x Phosphatase Inhibitor Solution:** Dissolve one PhosSTOP tablet in 1 ml millipore water

- **10x Protease Inhibitor Solution:** Dissolve one complete mini EDTA-free tablet in 1 ml of millipore water

- **PTW:** 20x PBS, 0.1% (v/v) Tween 20

- **Resuspension Buffer:** 50 mM Tris-HCL (pH 8.0), 10 mM EDTA (pH 8.0), 100 µg/ml RNase A

- **SDS load buffer (5x):** 0.5 M Tris-HCl (pH 6.8), 10 % (w/v) SDS, 20 % (v/v) Glycerin, 5 % (v/v) β-Mercaptopropandiol, 0.1 % (w/v) Bromophenol blue

- **SDS load buffer (10x):** 1% (w/v) SDS, 250 mM Tris, 1.92 M Glycin

- **SOB-Medium:** 20% (w/v) Bacto tryptone, 0.5% (w/v) yeast extract, 0.05% (w/v) NaCl, 0.25% (w/v) $MgCl_2$, pH7.0, sterilize by autoclaving

- **SOC-Medium:** 20 mM $MgCl_2$, 20 mM $MgSO_4$, 20 mM Glucose in SOB-Medium

- **Start Buffer (FPLC):** 10 mM HEPES, 150 mM NaCl, 10 mM Imidazol, pH 7.5

- **20x SSC:** 3 M NaCl, 300 mM Na-Citrate pH 7.0

- **TAE (50x):** 2 M Tris-Base, 1 M Acetic acid, 0.1 M EDTA, pH 8.3

- **TBS (10x):** 25 mM Tris-HCl pH 7.4, 137 mM NaCl, 5 mM KCl, 0.7 mM $CaCl_2$, 0.5 mM $MgCl_2$

- **TBST:** 1x TBS, 0.1% Tween 20

- **Transfer Buffer:** 25 mM Tris, 192 mM Glycin, 10% (v/v) Methanol

3.11 Devices

- Binocular microscope
  - Leica L2   (Leica Microsystem, Bensheim)
  - Leica KL 200 LED   (Leica Microsystem, Bensheim)
  - Leica S6E   (Leica Microsystem, Bensheim)
- Centrifuges

- o Biofuge fresco   (Kendro, Langenselbold)
- o Eppendorf Table centrifuge   (Eppendorf AG, Hamburg)
- o Heraeus® Fresco   (Thermo Fisher Scientific Inc., USA)
- o Hettich Universal 32 R with swing rotor   (Andreas Hettich GmbH & Co. KG, Tuttlingen)
- o Multifuge® 3 S-R   (Kendro, Langenselbold)
- Electroporator, Micropulser   (Bio-Rad, Munich)
- Flatbed-Gel electrophoresis chambers   (Amersham, Freiburg)
- Fluorescence binocular microscope
  - o Leica MZ10   (Leica Microsystem, Bensheim)
  - o Leica HZ FLIII   (Leica Microsystem, Bensheim)
  - o Software Openlab 5.5.0   (Openlab, Heidelberg)
  - o Digital camera Retiga Exi   (QImaging, Burnaby, Canada)
  - o Cold light source KL 1500 LCD   (Leica Microsystem, Bensheim)
- Fluorescence microscope
  - o Spinning disc (Axio Observer.Z1)   (C. Zeiss AG, Germany)
  - o Laser (405 nm, 488 nm and 568 nm)   (C. Zeiss AG, Germany)
  - o Objectives (5x, 10x, 25x, 40x, 63x)   (C. Zeiss AG, Germany)
  - o Camera AxioCam MRm   (C. Zeiss AG, Germany)
  - o Software AxioVision 4.8.2.0   (C. Zeiss AG, Germany)
- Fluorescence microscope DMIRE2   (Leica microsystem, Bensheim)
- Gel Documentation Systems
  - o Gel Max   (Intas, Göttingen)
  - o Diana II   (Raytest, Straubenhardt)
- iCycler (PCR)   (Bio-Rad Laboratories Inc.,USA)
- Incubator APT LineSerieBD/ED/FD   (Binder, Tuttlingen)
- Magnetic Stirrer MR 2000   (Heidolph, Schwabach)
- Microflow 2- Sterile cabinet   (NUNC, Thermo Fisher Scientific, USA)
- Micropipette Puller Model P-97   (Sautter Instruments, USA)

- Microinjection System   (H. Saur Laborbedarf, Reutlingen)

  - Cold light source, Fiber Optic Light Source EK-1   (Euromex)

  - Diaphragm pump MZ2   (Vacuubrand)

  - Pneumatic Picopump PV 820

  - Sterio microscope MIC 1630 ZS   (Euromex)

- Microvolume Spectrometer COLIBRI   (Titertek Berthold, Pforzheim)

- Orbital Shaker   (Thermo Fisher Scientific, USA)

- PAGE apparatus, Mini Protean II and Blot apparatus, Mini Trans Blot   (Bio-Rad, Munich)

- pH-Meter   (WTW, Weilheim)

- Photometer   (Eppendorf, Hamburg)

- Thermomixer compact   (Eppendorf, Hamburg)

- UV-Lamp   (Bioblock Scientific, Illkirch, FR)

- Vortex machine   (Heidolph, Schwabach)

- Water bath WB12   (Memmert, Schwabach)

4 Methods

4.1 Developmental biology methods

4.1.1 Keeping of *Xenopus laevis*

Separated by gender, 10-13 adult *Xenopus laevis* are kept in 50 liter aquarium tanks with water temperature between 18-20 degrees. The water in the aquarium system is sterilized by a bacterial filter and UV-radiation. A day-night rhythm is achieved by automated illumination, giving 14 hours daylight each day. The diet consists of compound feeds and additionally chopped beef heart once a week. After laying eggs, female frogs are kept in 3% (w/v) NaCl overnight to prevent infection and allow their skin to regenerate. On the next day they will be transferred back to the aquarium tanks.

4.1.2 Induction of egg deposition

Female frogs need to be pre-injected with Human Chronic Gonadotropin (HCG) hormone to induce egg deposition. HCG induces oocyte maturation, which is obtained from urine of pregnant women and provided as lyophilized powder. For 300 kilo units, 100 ml of 0.5% NaCl is added for reconstitution and stored at -20°C. An injection with 600 units of HCG subcutaneously induces egg deposition after 14-16 hours. If eggs are required after 20-22 hours, 100 units of the HCG is injected first, and another 600 units of HCG is injected 6-8 hours before desired egg deposition. *Xenopus* females are squeezed subsequently every hour and for maximum four batches. The skin of the frogs should remain moist permanently to prevent skin irritation. Eggs are collected in a petri dish for fertilization. After giving eggs, the females are kept in salted water (30 g sea salt in 10 l water) overnight, allowing better regeneration of their skins and preventing possible infections. Frogs injected with hormone will rest at least three months until next hormone injection.

4.1.3   Testis extraction and *in vitro* fertilization

To obtain testis, the male frog is first anesthetized by 0.25% (w/v) amino benzoic acid ethyl ester solution for at least 30 minutes. The cervical spine will be cut followed by the separation of the connecting nerves. First, a small cut is made at the bottom left of abdominal region, which cut through the skin and abdominal wall. Along the small cut, a midline incision through the abdominal wall is performed to open the abdominal cavity and expose the organs. The testis are pale yellow and located beneath the kidney. The dissected testis are stored in 1x MBSH buffer at 4°C for approximately five days.

To fertilize the eggs, a small piece of testis is macerated in one ml of 1x MBSH buffer. 100 µl of the testis solution and 900 µl of sterile water (1:10 dilution) are added on to eggs collected in a petri dish for about one hour. The success of fertilization can be determined by the upward turning of the pigmented animal pole.

4.1.4   Jelly removal and Nile-Blue staining of albino embryos

Fertilized embryos are incubated in 2% (w/v) Cysteine solution (pH 8.2) to remove the jelly and then washed three times with 0.1x MBSH buffer once they are separable from each other.

The albino embryos can be stained for one hour with Nile-Blue solution after the treatment with cysteine, so that the blastomeres are more distinguishable. Stained embryos are washed one time again and kept in 0.1x MBSH.

4.1.5   Microinjection

DNA, RNA and antisense morpholino oligonucleotides are transferred within the embryos through microinjection using a very fine glass capillary. The glass capillary is prepared by a micropipette puller. The very thin tip of the capillary is then used as a needle for injection. Pumped by nitrogen gas or air, a defined volume of injection can be applied. Before each injection, the needle is calibrated on a standard calibration grid. Size of the droplet is adjusted until it fits right inside a square on the calibration grid, which corresponds to a droplet with a

diameter of 205 µm, equivalent to an injection volume of 4 nl. Fertilized embryos are then transferred on an agarose dish having wells with similar size of the embryos.

Depending on the experiments, embryos are injected at two- or sixteen-cell stage. Along with the desired constructs, a fluorescence tracer is normally added to the injection solution enabling a verification of the injected area. Commonly used fluorescence tracers are mRNA of membrane bound GFP (mbGFP) or membrane bound cherry (mbcherry) and Histone2B GFP (H2B GFP) or Histone2B cherry (H2B cherry), which marks either the cell membrane or nucleus. 500 pg of RNA is generally applied to generate strong fluorescence signal. Dextrans coupled with fluorescein-isothiocyanate (FITC) are also used as tracers for injected cells. Dextrans, hydrophilic polysaccharides synthesized by *Leuconostoc* bacteria, have the advantages of good water solubility, low toxicity and high stability. Dextran Fluorescein (Fluoro-emerald) used in this work is injected at a concentration of 2 mg/ml.

The left-right body axis of *X. laevis* is determined by the first cell division, an injection in one blastomere at stage 2 (two-cell stage) leads to manipulation of one side of the embryo, where the other side of the embryo serves as a control side of wild type. For experiments that require merely cell-labelling with fluorescence tracer, embryos are injected at stages 2, for instance labelling of neural crest cells to perform immunostaining. However, most experiments in this work, where Morpholino oligonucleotids or mRNAs are introduced into the embryo, the animal dorsal blastomere D1.2 at stage 5 (sixteen-cell) stage is injected to target specifically the cranial neural crest cells ((Nieuwkoop and Faber, 1967) (Fig 4.1).

| 16-cell injection | Stage 17 | Stage 26 |
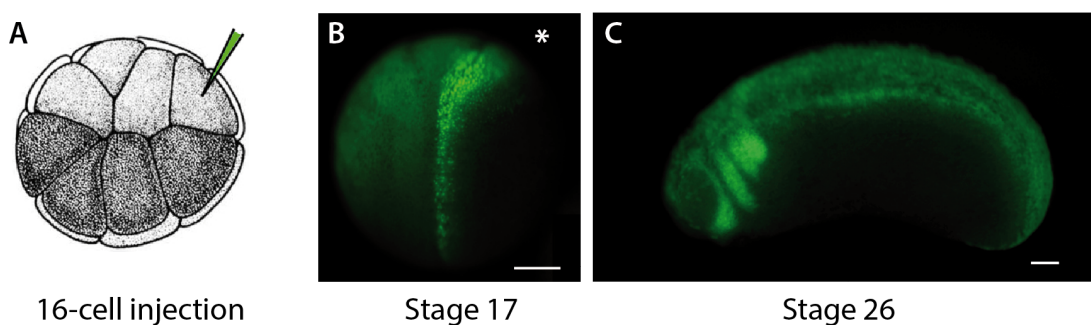
Fig 4.1 Microinjection of *X. laevis* embryos. (A) Scheme of a stage 5 (16-cell stage) *X. laevis* embryo according to Nieuwkoop and Faber, 1967. The animal dorsal blastomere D1.2 is injected. **(B)** Dorsal view of a mbGFP injected embryo at stage 17. Embryos that show strong fluorescence signal on one side of the embryo and particularly in cranial neural crest region are sorted at stage 17 for explantation. **(C)** Lateral view of a mbGFP injected embryo at stage 26. Embryo is left side injected. Embryos for *in situ* hybridization are sorted and fixed at this stage. * Indicates injected site. Scale bar: 100 µm

4.1.6   Embryo caring and fixation

Injected embryos are kept at a temperature between 14°C - 21°C in 0.1% (v/v) MBSH as culture medium. Higher temperature speed up the development of embryos with higher risk of low survival rate. Fresh medium is changed twice everyday and dead embryos are removed. The developmental stages are determined according to Nieuwkoop and Faber (1967).

Once the embryos have reached the desired stage, they are fixed applying different methods. For embryos that will proceed to *in situ* hybridization or cartilage staining, the culture medium is removed and embryos are incubated in MEMFA solution for one hour at room temperature. Embryos will then be washed and stored in 100% (v/v) Ethanol at -20°C. For protein and RNA extraction, embryos are collected and lysed directly, or they can be shock frozen in fluid nitrogen after removing medium and stored at -80°C. Another possibility to store embryo tissue is by directly submerging them into RNAlater.

4.1.7   Gene suppression by antisense morpholino knockdown

To study the function of a specific gene, the method of gene knockout is widely used. Due to the fact that *Xenopus laevis* has a tetraploid genome therefore the complete knockout of a specific gene is not possible. However, a downregulation of a specific target gene can be achieved by appling the antisense technology .

In this work, antisense morpholino oligonucleotides (MO) are used to downregulate specific target genes. In DNA molecules, the bases are bound to a desoxyribose ring. MOs are chemically modified nucleic acid analogs, where the bases are bound to a heterocyclic morpholino ring instead of a desoxyribose or ribose ring. In addition they are linked via phosphorodiamidate groups, which unlike phosphodiester in DNA, are not charged (Fig 4.2). For characterizing of a particular target gene in *X. laevis*, the embryos are injected with a specific MO that binds complementary to the endogenous mRNA. The MOs are normally designed to bind the 5'UTR or to the start code of the target mRNA. The binding of the MO forms a double strand with the mRNA, which does not allow ribosome to bind anymore. Therefore the translation of this mRNA is blocked. The concentration of the MO is diluted with each cell division, but the MO molecules do not degrade since they are not recognizable by endogenous nuclease. But

even with the constant existence of the MO, not every endogenous mRNA can be bound; it is therefore called a knockdown instead of a knockout.
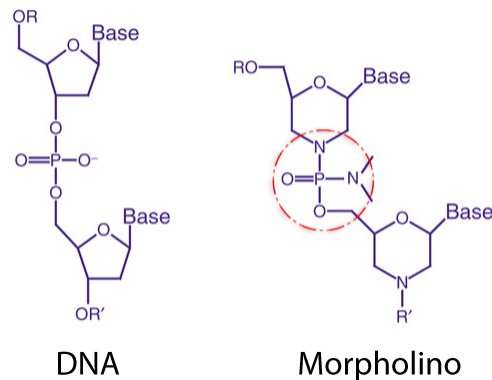
DNA   Morpholino

Fig 4.2 Difference in chemical structure of DNA and morpholino. (A) DNA nucleotide is consisted of a heterocytic base and a deoxyribose ring, linked through negatively charged phosphates. **(B)** The base of a morpholino nucleotide is connected to a morpholine ring through a phosphorodiamidate group (red circle). Modified from (Corey and Abrams, 2001).

The chemically modified structure of MOs has many advantages: the binding of MO to target RNA is very efficient and shows little tendency in additional non-specific base pairing. Rescue experiments with mRNA can often (partially) restore the wild type phenotype to the embryo and verify the specificity of a MO. Since MOs are linked through uncharged phosphorodiamidate backbone, they are not recognized by cellular proteins like nucleases, therefore display a high degree of stability in the embryo.

4.1.8   Whole mount *in situ* hybridization (ISH)

Whole mount *in situ* hybridization is a technique used to localize the expression of particular mRNAs in a whole embryo, which is based on the hybridization of a labelled antisense RNA probe with an endogenous target sequence of the mRNA. This method allows analysis of the temporal and spatial pattern of transcripts from a certain gene *in vivo*. The probe consists of a complementary sequence to the target gene, which is generated via *in vitro* transcription of a linearized plasmid DNA. Probes can be labelled with digoxigenin (DIG) or fluorescein that is covalently attached with the C5 of the uridinbase. Labelled probes are detected by an antibody/enzyme-conjugate, for example anti-DIG-AP. Alkaline phosphatase (AP) is able to

convert the substrate nitro blue tetrazolium (NBT) and 5-bromo-4-chloro-3-indolyl-phosphate (BICP) to a purple precipitate. BICP alone as substrate instead create a blue precipitate which can be combined in double in situ hybridization when expression of two genes need to be showed in parallel. The ISH protocol used in this work is slightly modified from (Harland, 1991).

Embryos are fixed in desired stages and transferred in 5 ml glass tubes. To obtain proper staining, pigmented embryos are bleached in the bleaching solution (containing hydrogen peroxide) for 30-60 minutes to remove the pigment in the epidermis. After a 30 minutes fixation in MEMFA the embryos are washed one time with 100% ethanol and rehydrated with 75%, 50% and 25% (v/v) ethanol incubation for 5 minutes each. Then, embryos are washed two times with PTW, which also permeabilize the embryos. Four hours pre-hybridization at 65°C with hybridization buffer, which contains ribonuclease acid, avoids unspecific binding of the probe. The probe is incubated for five minutes at 85°C to remove possible secondary structures. Hybridization with the probe at 65°C takes place overnight. The probe is recycled on the next day and stored until next use at -20°C. The remaining probe is washed off during successive incubation with washing solution 1, 2, 3, 4 for 10 minutes each, and in the end with washing solution 5 for 30 minutes at 65°C. The washing solutions contain a gradient of formamide, 20x SSC and 0.1% Tween. The embryos are washed twice with PTW and then with 1x MAB, with five minutes interval between each wash. In order to block unspecific binding sites, embryos are incubated in 1x MAB-2%BMB solution for two hours at RT. The embryos are incubated with anti-Digoxgenin-AP (1:2000) in 1x MAB-2% BMB blocking solution for four hours at RT. For washing, embryos are then transferred into 50 ml falcons containing 1x MAB solution and put overnight on a shaker at 4°C. On the next day the embryos are rinsed once with 1x MAB solution before two times five-minutes incubation with alkaline phosphatase buffer.

The staining solution is prepared by adding 1.5 µl NBT and 1.5 µl BCIP to every 1 ml of AP buffer. The AP that has been coupled to the antibody converts the substrate NBT/BCIP to a blue, hardly soluble precipitate (formazan). Staining can be carried out at RT or at 4°C, the latter takes longer time but gives less background. The staining is regularly checked and fresh staining solution should be changed if solution gets darker. Once the staining is reached to the desired level, the reaction is stopped by brief washing with water. Distaining with 100% methanol removes unspecific colour binding resulting in a better contrast of the specific staining. After a decreasing methanol series the embryos are fixed in MEMFA and stored for long time period in 1x MEM at 4°C.

4.1.9   Explantation of cranial neural crest (CNC) cells

For culturing and observing cranial neural crest cells *in vitro* under the microscope, glass chamber slides are used. The slides are coated with fibronectin (50 µg/ml) for one hour at RT. Afterwards the surface is washed three times with Danilchick's buffer and the same solution is used to fill the chamber.

Embryos at stage 17 are sorted under the fluorescence binocular according to the injected tracer at desired stage. The vitellin-membrane of the embryo is carefully removed with tweezers. For cell morphology study and immunostaining on CNC cells, the neural crest is explanted at stage 17. Embryos are transferred to a 2% agarose-coated petri dish filled with Danilchick's buffer. A grave similar to the size of the embryos is made so that the embryos are placed stably during explanting. An eyebrow knife and an eyelash knife are used to dissect embryos. Eyebrows or eyelashes are inserted into the needle of a syringe and fixed with nail polish.

During explantation, one hand with the eyebrow knife is used to hold the embryo in position, while the other hand with the eyelash knife can make cuts. To remove the epidermis on the injected site, one cut is first made parallel to the neural fold along neural plate border. The second cut is made with an angle of 45° to the first cut and the epidermis is carefully lifted. The cranial neural crest cells are gray shimmering cells that can be found directly beneath the epidermis tissue. These cells are carefully scraped without the underlying mesoderm and cut into smaller pieces if needed. Later, cells are transferred using a 10 µl pipette tip which has been blocked with 3% (w/v) BSA to prevent cells from sticking to it. After placing the neural crest cells onto fibronectin-coated chamber slides, the cells are allowed to adhere for one to two hours before microscopy is performed.

Neural crest explants for protein and RNA extraction are collected additionally at stage 20 and stage 23. At stage 20 the neural crest is becoming conspicuous as three segments (mandibular, hyoid and branchial crest segment) and starting to migrate rostrally under the optic versicle. These three segments are carefully dissected. At stage 23 the neural crest segments have migrated laterally and have become more distinguishable from the underlying tissue. The branchial crest segment is dividing into two portions (the anterior and posterior portion) and the epithelial placodes are located between the hyoid and branchial crest segments. To dissect neural crest at this stage, the whole segments together with epithelial placoderms are first separated from the rest of the embryo, and then the segments are carefully scratched from the attached epithelia placodes.

4.1.10   Immunostaining of neural crest cells

Two to three hours after plating the dissected neural crest cells on a fibronectin coated dish the cell cluster is well spread and the cells at edge of the explant are mostly monolayer. The cells can be then fixed with 4% paraformaldehyde in 1x PBS for 10-15 minutes. By one briefly incubation with non-ionic surfactant 0.5% Triton-X 100 in 1x PBS (0.5% PBST) the cells are permeabilized. After washing twice with 0.1% Triton-X 100 in 1x PBS (0.1% PBST), cells are blocked with 1% BSA in 1x PBS solution for 30 minutes. After washing once with 1x PBS the neural crest cells are incubated with the primary antibody overnight at 4°C (dilutions of used antibodies in this work are listed in Table 4.1).

Name	Host	Dilution
5D3 (E-cadherin)	Mouse	Undiluted cell culture supernatant
10H3 (E-cadherin)	Mouse	Undiluted cell culture supernatant
MNCD2 (N-cadherin)	Mouse	Undiluted cell culture supernatant
6D5 (XB-cadherin)	Mouse	Undiluted cell culture supernatant
Cy3 (anti-Mouse)	Goat	1:400

Table 4.1 Primary and secondary antibodies used for immunostaining for CNC explants along with their dilutions.

On the next day the primary antibody is removed and cells are washed with 0.1% PBST for three times. The neural crest cells are again blocked with 1% BSA in 1x PBS for 30 minutes. The secondary antibody is normally coupled with fluorescent dyes, which needs to be kept in dark to prevent bleaching of the fluorophore. Incubation with the secondary antibody is carried out for one hour at RT. The unbound antibody is removed by three times washing with PBST. Nuclei of the cells can be stained with DAPI (4',6-diamidino-2-phenylindole) for three minutes at RT. DAPI aggregates in the minor groove of DNA to form a fluorescent complex with dsDNA. Finally, the neural crest cells are washed thrice with 1x PBS and covered with 1x PBS. By storage at 4°C, the cells can be preserved for a period of time as long as they are constantly covered with PBS.

4.1.11 Transplantation of cranial neural crest cells

Transplantation is a method to analyze the migration behaviour of neural crest cells *in vivo*. Donor (or acceptor) embryos are injected with constructs along with fluorescence tracer and cultured until stage 17. Transplantation is carried out in 1% MBSH solution or Danichick's buffer. Neural crest cells from donor embryo is dissected (same like explantation, see 4.1.9) and laid to side, where at the same region in an acceptor embryo (normally non-injected wild type embryo) the neural crest is removed and discarded. However, the epidermis on the acceptor embryo needs to be cut in a way, so it can be flipped open to expose the underlying neural crest but still attached to the rest of the epidermis. This is essential, so the incision can be closed properly after transplantation and embryos can heal better. After removing the neural crest tissue from the acceptor embryo, the donor neural crest is immediately placed in the acceptor embryo and the epidermis is being covered on the newly placed neural crest (Fig 4.3 A).
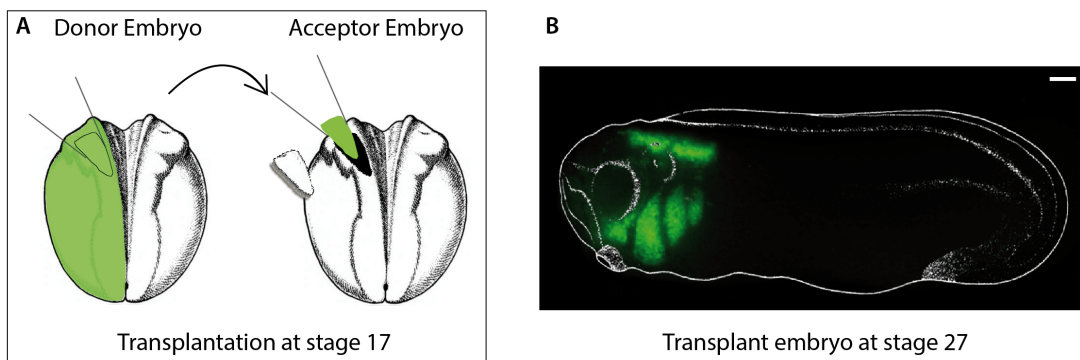
Fig 4.3 Transplantation of the embryo. (A) Scheme of a Donor- and Acceptor- embryo at stage 17. The neural crest of an H2B-GFP-injected embryo is transplanted into a wild type embryo. **(B)** Lateral view of a transplanted embryo at stage 27.

Transplanted embryos are left in 1% MBSH to heal for one hour until the incision in the epidermis is visibly closed. Embryos are then carefully transferred to 0.1% MBSH and cultured at 14°C or 16°C. On the next day when the transplanted embryos reach stage 28 the migration of the neural crest cells can be analyzed under the fluorescence binocular (Fig 4.3 B).

4.1.12   Frozen cryosection

The embryos are fixed in MEMFA for one hour at RT and stored in 100% ethanol. To prepare the embryos for embedding, they are rehydrated with successive incubation in 75%, 50% and 25% ethanol and washed with a solution of 0.1 M Tris-HCl (pH 7.4) and 0.1 M NaCl for 5 minutes each. Incubation with a medium of 15% (w/v) cold-water-fish gelatine and 15% (w/v) saccharose (solved in ddH$_2$O) at RT takes overnight. An the next day, the embryos are transferred to another medium with 25% (w/v) cold-water-fish gelatine and 15% (w/v) saccharose (solved in ddH$_2$O) and incubated at RT again overnight. After these equilibration steps the embryos are ready to be embedded and can be stored at 4°C.

Embryos are embedded in a medium with 20% (w/v) cold-water-fish gelatine and 15% (w/v) saccharose (solved in ddH$_2$O). The medium is poured in an aluminium form, which is pre-freezed by placing it on dry ice. After about five to ten minutes, embryos can be putted upon the frozen medium and more medium is added to cover embryos. Two to three embryos can be embedded in the same medium block inside the form. In order to place the embryos extended in parallel orientation, a toothpick can be used to adjust the position of the embryos, before the medium start to become hard. The block is left on dry ice about one hour for hardening. The block can be removed from the aluminium form and glued on to a holder. The embryos are normally sectioned with a thickness of 8-12 µm with a microtome. The sections are collected using a toothpick. The slides that used for collecting cyrosections are specially coated and positively charged on one side of the slide, which allows the sections to smoothly attach and adhere. The slides are slightly warmed and placed directly next to the sections. Sections are attached onto the pre-warmed glass automatically. Cryosections can be kept at -80°C.

4.1.13   Immunostaining on Cryosections

To perform immunostaining on cryosections, the section-slides are first dried at room temperature for one hour. After washing once with aceton, the sections are dried for 10 minutes and then rehydrated in APBS solution. To prevent unspecific binding, the sections are blocked for one hour at 4°C in 10% (w/v) FCS in APBS. The primary antibody (Tab 4.2) is incubated on the sections overnight at 4°C. On the next day, sections are washed five times with APBS and incubated with the secondary antibody for two hours at RT. After washing three times with

APBS, the sections can be incubated two minutes with DAPI solution for nuclei staining. Finally, the slides are covered with Mowiol and stored in the dark at RT.

Name	Host	Dilution
5D3 (E-cadherin)	Mouse	Undiluted cell culture supernatant
Cy3 (anti-Mouse)	Goat	1:400

Table 4.2 Primary and secondary antibody used for immunostaining of cryosections along with their dilutions.

4.1.14 Cartilage staining

To analyze neural crest derivatives in later development stage, one can stain the cranial cartilage of fixed embryos, permitting the examination of cartilage formation. Injected embryos are cultured in 0.1% MBSH till stage 45 and sedated with MS2222 before fixed in MEMFA for two hours. Fixed embryos are then dehydrated and stored in 100% (v/v) Ethanol.

Cartilage is a connective tissue that is rich in proteoglycans. Alcian blue is a group of polyvalent basic dyes that stains acid mucosubstances and acetic mucins located on the cartilage. By forming salt linkages with the acid groups of acid mucopolysaccharides, a dark blue staining can be achieved when the embryos are incubated in alcian blue solution for three nights. Embryos are then washed three times for 15 minutes in 95% (v/v) ethanol and rehydrated stepwise in decendant ethanol (100%, 75%, 50%, 25% (v/v) ethanal in 2% potassium hydroxide (KOH)). In order to increase the stability of the cartilage structure, embryos are incubated in ascendant glycerin solution (one-hour incubation in 20% (v/v), 40% (v/v), 60% (v/v) glycerin in 2% (v/v) KOH) and transferred overnight in 80% (v/v) glycerin in 2% (v/v) KOH. In the same solution are the embryos stored for long period.

To better identify the structure of the cartilage, epidermis, eyes and the rest of the body are carefully removed using tweezers. The cartilage can be photographed under a binocular and stored in 80% (v/v) glycerin in 2% (v/v) KOH.

4.2 Molecular biological methods

4.2.1 Preparation of chemo-competent *E. coli* bacteria

The ability for bacteria cells to take up extracellular DNA (competence for transformation) is induced by chemical methods using divalent cations (for example magnesium), which neutralize the unfavourable interaction between both negatives charged DNA molecules and components of the bacterial cell membrane. The permeability of membrane is thereby altered. Bacteria from the *E.coli* strain JM109 are spread on an antibiotic-free LB agar plate and incubated overnight at 37°C. On next day, a single colony is picked and seeded into 5 ml LB medium for overnight culture at 37°C with 225 rpm. 0.5 ml of the overnight culture is diluted in 50 ml of LB medium containing 20 mM MgSO$_4$. The bacteria cells are incubated in a 500 ml Erlenmeyer flask until the culture reaches an OD$_{600}$ of 0.4-0.6. Afterwards the bacterial culture is cooled on ice for five minutes and centrifuged at 4°C with 4500 × g. Cell pellets are resuspended in 5 ml of ice-cold TFB2 buffer and incubated on ice for 30 minutes. Each 100 µl of the bacterial suspension are aliquoted and stored at -80°C.

4.2.2 Transformation of chemo-competent *E. coli* bacteria

Chemically induced competence followed by transformation is a commonly used technique to introduce plasmids or other foreign DNA materials into *Escherichia coli*. For transformation 1 µg plasmid of interest is gently mixed with 100 µl of chemo-competent JM109 bacteria cells and incubated on ice for 30 minutes. The reaction mixture is then exposed to a 45 seconds heat-shock at 42°C. After another 5-minutes incubation on ice, 900 µl of SOC medium is added into the solution. The mixture is then shaken at 37°C with 225 rpm for one hour. To reduce the volume for plating, the mixture of cells and plasmid is centrifuged for five minutes at 2000 rpm and 800 µl of supernatant is discarded. The cell pellet is resuspended in the remaining SOC medium and plated on a LB/ampicillin plate. Finally, the plates are incubated overnight at 37°C.

4.2.3 Isolation of bacterial plasmid DNA in the small and medium scale

For isolation small scale DNA the "High Pure Plasmid Isolation Kit" from Roche and for medium scale the "NucleoBond Xtra Midi Plasmid DNA purification" from Machery-Nagel is used. The procedure is carried out according to the kit instructions.

On a small scale, a transformed colony of *E. coli* bacteria is picked and cultured in a 3 ml-LB/ampicilin medium overnight at 37°C with 225 rpm. On next day the bacteria culture is pelleted for 5 min at 13000 rpm. Pellets are resuspended in 250 µl suspension buffer containing RNase. The resuspended pellets are lysed by adding 250 µl lysis buffer containing sodium dodecylsulfate, which causes the rupture of bacterial cells. After gently inventing the tubes three to five times, 350 µl chilled binding buffer is added to the lysed solution. The solution is gently mixed and incubated on ice for 5 minutes. The high salt content in binding buffer leads to precipitation of bacterial proteins, chromosomal DNA and cell debris. However, smaller and circular plasmid DNA molecules stay in solution. A 10-minutes centrifugation at 13000 rpm separates the precipitate from the supernatant containing plasmid DNA. The supernatant is then transferred on to a filter column, by which the plasmid DNA is adsorbed on the membrane. The membrane is subsequently washed with 500 µl and 700 µl washing buffer containing 95% (v/v) ethanol. This washing step eliminates nuclease activity and removes salts, which would otherwise suppress the elution. Finally, the plasmid DNA is eluted with 50 µl elution buffer.

On medium scale, a transformed colony of *E. coli* bacteria is added in 100 ml of LB-ampicillin medium and shaken at 37°C with 225 rpm overnight. Resuspension, lysis and neutralization are done in the same manner like small-scale isolation, but with larger volumes. To separate the supernatant, the precipitated cell-mix is filtered firstly through a clearing column and subsequently binding column, on which DNA is absorbed. The column is washed with endotoxin removal buffer and washing buffer containing 95% (v/v) ethanol. Finally the plasmid DNA is eluted with 500 µl of nuclease-free water.

4.2.4   Precipitation and purification of nucleic acids

To precipitate nucleic acids, 10 µl 3 M sodium acetate, 5 µl EDTA (0.5 M, pH 8.0) and 250 µl 100% (v/v) ethanol is added to each 100 µl nucleic acid sample. The mixture is incubated at -20°C for a minimum of 20 minutes. Precipitated nucleic acids is then pelleted by centrifuging at 13000 rpm for 15 minutes at 4°C. To remove salt and alcohol residues the pellet is washed with 70% (v/v) ethanol once and dried at RT. The pelleted nucleic acids are then dissolved in double distilled water and stored at -20°C (DNA) or -80°C (RNA).

Optionally, nucleic acids can be cleaned via gel filtration columns with an affinity matrix, which gives relatively lower nucleic acid yield but purer products. In this work, *in vitro* synthesized

mRNA and RNA probe for *in situ* hybridization is purified through the "ProbeQuant G50 Micro Columns". G50 Micro column is a gel filtration column, which contains sephadex. This is a cross-linked dextran gel that is manufactured in a bead form and used to separate low and high molecular weight molecules. The degree of cross-linking can be varied to adjust the fractionation properties of the gel. Here the sephadex column is used to remove the small molecules like digested or unincorporated nucleotides from the transcription and labelling reactions. Procedure is carried out according to manufacturer's instructions.

4.2.5   Determining the concentration of DNA and RNA

The concentration of nucleic acid can be determined by measuring the optical density at 260 nm after the following formula:

$$C \ [\mu g/ml] = A_{260} \times V \times F$$

In formula, A_{260} stands for absorbance at $\lambda = 260$, V = dilution factor and F = multiplication factor.

The concentration is calculated by multiplying the optical density 260 with the dilution and the specific multiplication factor. The multiplication factor for single-stranded DNA, double-stranded DNA and RNA is 33, 50 and 40 respectively. Nucleic acids and proteins have absorbance maxima at 260 and 280 nm respectively. The ratio of absorbance at 260 and 280nm ($A_{260/280}$) is commonly used as a measure of purity in both nucleic acid and protein extractions. A ratio of 1.8 is accepted as pure for DNA and a ratio of 2.0 is pure for RNA.

4.2.6   Restriction of DNA

Restriction endonucleases are found in many different species of bacteria. Their original biological function is to recognize and digest foreign DNA (e.g. DNA of an infecting virus) but they are now commonly used as tools in engineering DNA. The DNA sequence those nucleases recognize is usually palindromic, either with overhanging sticky or blunt ends. A reaction mixture is typically consists of 20 µl with 1 µg DNA, one unit of restriction endonuclease and 1/10 volume of 10x reaction buffer. The digestion of DNA takes at least 1-2 hours, incubating at the optimum reaction temperature indicated by the enzyme manufacturer.

4.2.7   Analysis by flatbed gel electrophoresis

Nucleic acids are negative charged because of their phosphate backbone. This enables their separation in an agarose gel by applying an electric field. The speed, at which the nucleic acids migrate through the gel, is inversely proportional to the logarithm of their size. Smaller molecules migrate faster and reach longer distance than larger ones through the agarose gel.

For an analysis gel, 1% (w/v) agarose is dissolved in 1x TAE buffer and midori green is added and mixed properly. It is then poured in gel-stack and a comb is fitted carefully. Nucleotide acid samples are analysed by running them through the gel applied with voltage of 90 to 120 volts. The 2-log DNA marker is used to show the size of standard nucleic acid fragments, by which the size of the samples can be compared. 2 µl loading buffer (Orange G) is added to the sample and loaded into wells on gel. Midori green intercalates with DNA base pairs and results in an excitation at λ=254 nm or λ=312 nm when beamed UV light.

4.2.8   DNA extraction from Gel

DNA fragments are separated by gel electrophoresis. The desired DNA fragments can be carved with a scalpel. The extraction of DNA is carried out using the "High Pure PCR Product Purification Kit" from Roche. Guanidine thiocyanate in the binding buffer denatures the DNA. Filtering the sample through filter tubes allows the DNA to bind on glass fiber fleece layers in the tube. The binding membrane is washed with 500 µl and 200 µl washing buffer containing 95% (v/v) ethanol. Finally, the DNA is eluted with nuclease free water.

4.2.9   *In vitro* transcription

For synthesizing RNA from linearized DNA, the "mMessage mMachine Transcription Kit" (Ambion, USA) is used. Different RNA polymerases (SP6, T7 or T3 polymerase) can be used according to the polymerase binding sites on plasmid DNA. Linearized DNA is mixed with 2x NTP/CAP (ribonucleotides), which add a 7-methyl guanosine cap structure at the 5' end of newly synthesized RNA. Capped RNA mimics most eukaryotic mRNAs found *in vivo* and is therefore protected from degrading by RNases. The reaction mix contains 6 µl linearized DNA, 10 µl NTP/CAP, 2 µl of 10x reaction buffer and 2 µl of RNA polymerase. The mix is incubated at 37°C

for at least two hours. To digest the DNA template after transcription, 1 µl of DNase is added to the mixture and incubated again at 37°C for 15 minutes. The nucleotide residues are removed by using "ProbeQuant G50 Micro Columns" or precipitation method. Nucleotide probes for *in situ* hybridization are synthesized with the "Digoxygenin/fluorescein RNA-labelling kit" from Roche. 20 µl reaction mixture contains 1 µg linearized-DNA, 2 µl RNA polymerase, 2 µl 10x digoxigenin or fluorescein-labelling mix and transcription buffer, same steps are followed as *in vitro* transcription. The quality of the mRNA or the RNA probe can be examined by gel electrophoresis. mRNA should be stored at -80°C while the RNA probe can be kept in -20°C.

4.2.10   Amplification of specific DNA fragments by PCR

The polymerase chain reaction (PCR) is an *in vitro* method to amplify DNA fragments. This technique is based on using the ability of DNA polymerase to repeatedly synthesize new strand of DNA complementary to the offered template strand. The method relies on thermal cycling, which enables the repeated heating and cooling of reaction for DNA replication. Besides the DNA template, other main components in PCR reaction are primers, short pieces of single–stranded oligonucleotides that are complementary to the target sequence, and DNA polymerase that synthesize new strands of DNA complementary to the target sequence. The first step in the PCR process is denaturation, where the dsDNA is heated at 95°C and splitten into ssDNA. At the second step of annealing, primers bind to the ssDNA providing 3'-OH group for DNA polymerase. The temperature of annealing is dependent on the length and GC/AT ratio of primers, which is normally around 50°C to 60°C. In the elongation step at 72°C, new dNTPs are added to the 3'-OH end of the primers by DNA polymerase. In this way a new complementary DNA strand is synthesized, which will be denaturated in the next cycle and use as template. This process is repeated and the amount of DNA is increased exponentially. The thermostabile *Taq* polymerase from *Thermus aquaticus* is wildly used in PCR reactions, whereas for longer sequence *Phusion* polymerase (from *Pyrococcus furiosus*) with 3'-5' exonuclease proof-reading activity provides higher fidelity.

A PCR sample mixture consists of following components:

5 µl   5× GoTaq Buffer

5 - 50 ng   DNA Template

1 µl	dNTPs (10 mM)
125 ng	Primer forward
125 ng	Primer reverse
0.5 – 1 µl	*Taq*-Polymerase
X µl	H$_2$O
Add to 50 µl	

A standard PCR program consists of following steps using a thermo cycler:

Cycles	Time	Temperature	Description
1x	5 min	95°C	Denaturation
30-33x	30 sec	95°C	Denaturation
	30 sec	50-60°C	Annealing
	30 sec	72°C	Elongation
1x	10 min	72°C	Elongation
1x	∞	4°C	

Table 4.3 Program for standard PCR.

4.2.11   Mutagenesis PCR

Mutagenesis is used to purposely change the genetic sequence. Analysis of the subsequent changes in the gene product elucidates the impact of mutation and therefore the functional effect of certain part of the gene. Mutagenesis applied in this work is site-directed mutagenesis that introduces mutations at a defined site. Changes to sequence can be made using PCR by simply including the desired change in one of the PCR primers. The changes can be base substitutions, additions, or deletions. The primers are designed to include the desired change. As the primers are extended in the PCR, the resulting amplification product incorporates the mutation, replacing the original sequence.

To ensure the efficiency of primer annealing, the mutagenesis primer should be in between 25-45 base pairs with a melting temperature over 78°C and GC content over 40%. PCR sample

mixture consists of 50 µl of total volume. It includes 5 µl reaction buffer (10x), 5-50 ng dsDNA, 125 ng of forward and reverse primer, 1 µl dNTPs, 1 µl DNA polymerase enzyme and distilled water to make up volume. A typical mutagenesis PCR program is showed in Table 4.4.

After reaction, 1 µl of DpnI restriction endonuclease is added in the mixture that cleaves methylated DNA. This does not affect the PCR product (newly synthesized mutated DNA) but remove template DNA. The incubation with DpnI is carried out at 37°C for one hour. Afterwards transformation in *E. coli* is performed and samples are analysed by sequencing.

Cycles	Time	Temperature	Description
1x	30 sec	95°C	Denaturation
16 x	30 sec	95°C	Denaturation
	1 min	55°C	Annealing
	2 min/kb	68°C	Elongation
1x	10 min	68°C	Elongation
1x	∞	4°C	

Tabel 4.4 Program for mutagenesis PCR.

4.2.12 Quantitative real-time PCR

4.2.12.1 Introduction

The real-time reverse transcription polymerase chain reaction (RT-qPCR) is an *in vitro* method for amplifying defined sequences of RNA in biological samples (Rappolee et al., 1988) and it is one of the most sensitive and the most flexible quantification methods for detection of mRNA (Bustin, 2000). RT-qPCR applies essentially the same principle of a PCR reaction, by which the nucleic acid present in a complex sample can be specifically amplified in a cyclic process. Benefits of this procedure over conventional methods for measuring RNA include its sensitivity, large dynamic range as well as accurate quantification. Especially for detection of low-abundance mRNA, which often obtained from limited tissue samples, RT-qPCR is the method of choice for its high sensitivity and comparatively easy setup. The results of real-time PCR can either be qualitative (presence or absence of a gene) or quantitative (number of copies of DNA). Conventional PCR, however, can be only semi-quantitative. Therefore, quantitative real-time

PCR (RT-qPCR) is generally the method of choice for quantitating differences in gene expression levels.

4.2.12.2   Real-time monitoring of PCR reaction

In a conventional PCR, the amplified product, or amplicon, is detected by an end-point analysis of running the product on an agarose gel after the reaction has finished. RT-PCR in contrast, allows the accumulation of the amplified product to be detected and measured during the reaction progresses. The detection is therefore in "real time". Real-time detection of PCR products is made possible by including in the reaction a fluorescent dye that reports the increase in the amount of DNA with a proportional increase in a fluorescent signal. The fluorescent dyes employed for this purpose include DNA-binding dyes and fluorescently labelled sequence-specific primers or probes. The fluorescent dye SYBR Green I used in this work is a DNA-binding dye that non-specifically and preferentially binds to double-stranded DNA (dsDNA). SYBR Green I exhibits little fluorescence when it is free in solution, but its fluorescence increases up to 1,000-fold when it binds dsDNA (Bio-Rad applications guide, 2006). Therefore, the overall fluorescent signal is proportional to the amount of present dsDNA, and increases when the amplified products accumulate. Specialized thermal cycler equipped with a fluorescence detection laser is used to monitor the change of fluorescence during amplification. The measured fluorescence reflects the amount of amplified product in each cycle.

4.2.12.3   PCR amplification

In an amplification plot of PCR reaction (Fig 4.4), the cycle number of PCR reaction is shown on the x-axis, and the fluorescence from the amplification reaction, which is proportional to the amount of amplified product in the tube, is shown on the y-axis. PCR amplification goes through two phases, an exponential phase followed by a non-exponential plateau phase. During the exponential phase, the amount of product molecules doubles in each cycle. However, as the reaction proceeds and the PCR products increase, efficiency of amplification reaction is gradually compromised due to the availability of nucleotides and activity of the enzyme. At this point, the reaction slows and enters the plateau phase (cycles 28-40 in Fig 4.4). Hence, end-point PCR measurements tell us very few about the initial amounts of target molecules that were

present in the samples. The real-time quantitative assay measures the increase in fluorescence during the exponential phase. Initially, fluorescence signal remains at background levels and increases in fluorescence are not detectable. As the product accumulates exponentially, enough products are eventually amplified to yield a detectable fluorescent signal. The cycle number at which fluorescence first rises above background fluorescence is called the threshold cycle, or C_T. The C_T value is measured in the exponential phase when reagents are not limited, this parameter can be used to accurately calculate the initial amount of template present in the reaction.
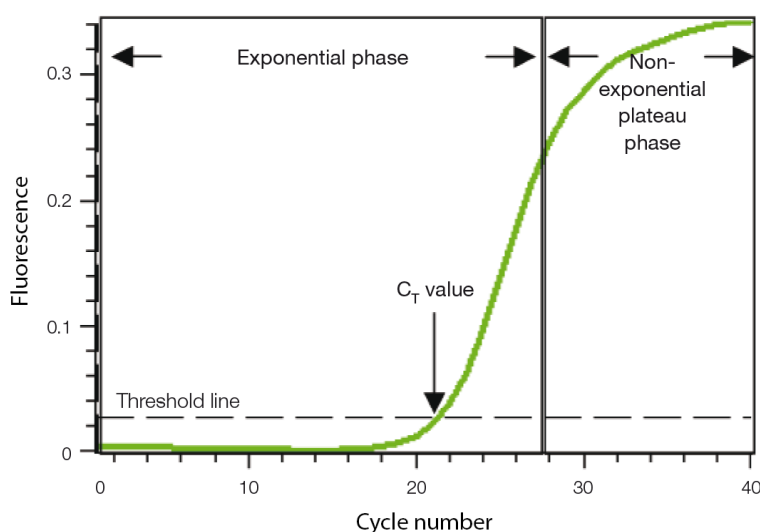
Fig 4.4 Amplification plot of a PCR reaction (modified from Bio-Rad applications guide, 2006): The PCR cycle number is plotted on the x-axis, and the measured fluorescence is shown on the y-axis. The amplification plot shows two phases, an exponential phase followed by a nonexponential plateau phase. The real-time PCR monitor the amount of PCR product and measure the C_T value during the exponential phase.

Because the C_T value of a reaction is determined by the amount of template present at the beginning of the amplification reaction, the larger amount of template there is present at the start of the reaction, the fewer amplification cycles it will be required to reach the threshold cycle. Thus, the reaction will have a lower C_T. In contrast, if a small amount of template is present at the beginning of the reaction, more amplification cycles will be need for accumulating enough products to give a fluorescent signal above background. The reaction will therefore have a high C_T. C_T value and its relationship to the template molecules form the basis for quantitative real-time PCR assay.

4.2.12.4   Overview of real-time PCR workflow

In this work, the real-time PCR is performed to detect genes of interest in *X. laevis* CNC explants as well as in whole embryos. Specific primers are designed to amplify a certain region of the target gene. Primers are firstly validated in test PCR reactions containing template and SYBR Green I reaction mix. Template used in the validation PCR reactions contains genes of interest and the specificity of the primers is verified through different assays. At the same time, the optimal annealing temperature and working concentration of the primers is chosen. Additionally, primers are checked for possible cross-reactions to gens with similar sequences. In the next step, RNAs from target tissue (CNC explants and whole embryos) are extracted and reverse transcripted to cDNA. Real-time PCR reactions are run on cDNA samples to quantify the initial amount of template in the test samples. Obtained data is used for relative quantification as well as for absolute quantification. For absolute quantification, standard curves based on plasmid DNA (containing exclusive gene of interest in full length) are constructed. In order to determine the number of cells in a CNC explant, nucleus staining is performed on the monolayer CNC explants and the average number of cells in CNC explants is used to calculate the absolute copy number of genes in one cell. Fig 4.5 summarizes the workflow of real-time quantification experiments performed on CNC cells, whereas details for every step are described in the paragraphs below.

C. Primer design, validation, reaction optimization

E. Relative quantification (fold change)

A. Sample collection → **B.** RNA extraction and cDNA synthesis → **D.** Quantitative real-time PCR

F. Absolute quantification (copy number)

St.17

St.20

St.23

90 CNC explants collected for each test sample

1. Serial dilution of plasmid DNA as templates for construction of standard curve

Plasmid with target gene sequence

Tube1 1:10 Tube2 1:10 Tube3 1:100 Tube4 1:1000 Tube10 1:1000000000

2. The regression line from the dilution curve is used to determine the copy number of the CNC test samples

Threshold cycle C_T

Test sample

Log starting quantity, copy number

3. Calclulate number of CNC cells in test samples

Count cell number of a CNC explant

4. Determine number of copies / CNC cell

Fig 4.5 Workflow of real-time quantification of CNC cells. (A, B) To detect and quantify expression of target genes in *X. laevis* CNC cells, real-time quantification is performed using RNAs extracted from *Xenopus* CNC cells in different stages. cDNAs are synthesized from the RNAs are amplified in the real-time assays. **(C)** The primers for real-time amplification are designed and verified through different assays including melting-curve analysis, where the optimal working condition of each primer pair is determined. **(D)** Real-time PCR is performed using verified primers and the obtained C_T values from test samples are analysed for relative **(E)** and absolute quantification **(F, 1-4)**. Standard curve for specific target gene is constructed using serial dilutions of plasmid DNA to determine the quantity of starting template DNA. The number of cells in test samples is calculated by counting cell number of a CNC explant. C_T, threshold cycle.

4.2.12.5 Design and optimization of reactions

When using SYBR Green I as DNA-binding dye for real-time PCR, a pair of PCR primers that amplifies the specific region within the target gene of interest is required. For choosing a target sequence and designing specific primers, the web-based program Primer3 (http://bioinfo.ut.ee/primer3-0.4.0/) is used for primer design. Since shorter amplicons are typically amplified with higher efficiency, the amplicon is designed to be 100-200 bp. An amplicon of at least 75 bp can be easier to distinguish it from primer-dimers that might form. The amplicon as well as the primers should have a GC content of 50-60%. The primers are normally 15-20 bp in length, with a melting temperature (T_m) between 55-65°C. Gs and Cs are placed on ends of primers. The specificity of primers is verified using the Basic Local Alignment Search Tool (http://blast.ncbi.nlm.nih.gov/Blast.cgi/). Synthesized primers are purified by HPLC. Newly designed primers need to be validated for their specificity and reaction efficiency. Optimized reactions should be specific and exhibit good amplification efficiency over a broad dynamic range. To determine the performance of the assay, the optimal annealing temperature has to be identified. An efficient way to assess the optimal annealing temperature is to use a thermal cycler capable of a temperature gradient, which allows a range of annealing temperatures being tested simultaneously. A range of temperature above and below the calculated T_m of the primers should be tested. An optimal annealing temperature is chosen from the gradient where the reaction gives the lowest C_T value and dilutions of template have evenly spaced difference of C_T values. The standard working concentration of primers is 0.25 µM, however, the optimal working concentration has to be experimentally determined individually for each primer pair.

The main drawback of the DNA-binding dyes is their lack of specificity, since they bind to any dsDNA (Deprez et al., 2002). As a consequence, the presence of nonspecific products (e.g. primer dimers) in the real-time PCR reaction may contribute to the overall fluorescence and affect the accuracy of the quantification (Wilhelm and Pingoud, 2003). Therefore, it is necessary to check the specificity of the assay by analysing the reaction product. A melting-curve analysis can be use to identify different reaction products including nonspecific products such as primer dimers (Ririe et al., 1997). After completing amplification reaction, a melt curve is generated by increasing the temperature in small increments and monitoring the fluorescent signal in the process. As dsDNA denatures when it reached its melting temperature, the fluorescent signal decreases (Fig 4.6). The negative first derivative of the change in fluorescent signal is plotted against the temperature, which gives a characteristic peak at the amplicon's melting temperature (T_m, at which 50% of the base pairs of a DNA duplex are separated). Different fragments with

different melting temperature therefore appear as separate peaks (Ririe et al., 1997). An optimized reaction should have a single peak in the melting-curve analysis, corresponding to a single band of the expected size on agarose gel. Sequencing of the amplification product can also be an additional way to verify the specificity of the primers.
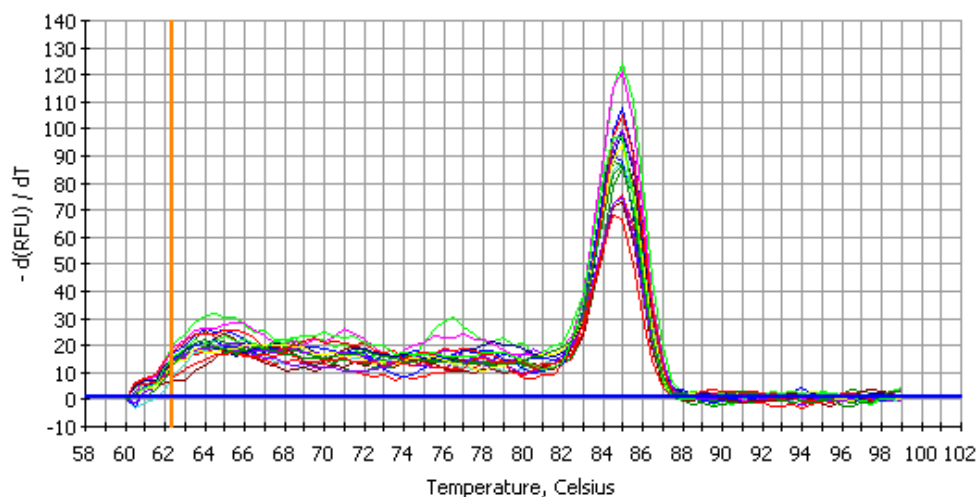
Fig 4.6 Example of melting-curve analysis to confirm the specificity of PCR amplification. The melting process of dsDNA causes a sharp reduction in the fluorescence signal around the melting temperature (T_m) of the PCR product, resulting in a clear peak in the melting curve. The negative derivative of the change in fluorescence is plotted as a function of temperature (-d(RFU)/dT). Assayed samples are a serial dilution series from a plasmid containing the sequence of Cadherin-11.

The efficiency, reproducibility, and the detectable range of the assay can be determined by constructing a standard curve using serial dilutions of a template. In this work, both plasmid DNA containing target sequence and cDNA from *X. laevis* embryo are used to construct the standard curve and verify the efficiency of the assay. Both templates give similar results. The cDNA is synthesized from a RNA mix of wild type embryos in different development stages, where the target gene is expressed. Serial dilution series are made from the cDNA template to cover all potential template concentrations that may be encountered during the study. Standard curves generated by plasmid DNA are described in detail in 4.2.13.10. For each dilution a standard qPCR protocol is performed in triplicate for all primer pairs to be used in the experiment.

The standard curve is constructed by plotting the logarithm (log) of the starting quantity of the template (or dilution factor in case of unknown quantity) against the C_T values obtained during amplification of each dilution. The equation of the linear regression line, along with the correlation coefficient (R^2), can then be used to evaluate whether the qPCR assay is optimized.

Ideally, if the amount of DNA molecules doubles with each amplification cycle, the dilution series will produce amplification curves that are evenly spaced. The spacing of the fluorescence curves is determined by the equation 2^n = dilution factor, where n is the number of cycles between curves at the fluorescence threshold. For example, with a 10-fold serial dilution of DNA, 2^n = 10. Therefore, n = 3.32, which means, the C_T values of the curves should be separated by 3.32 cycles. Evenly spaced amplification curves produce a linear standard curve.

The R^2 value of a standard curve represents how well the experimental data fit the regression line, which implies, how linear the data are. Linearity gives a measure of the viability in assay replicates and whether the amplification efficiency is the same for different starting template copy numbers. If the observed C_T values between replicates have significant difference, this will lower the R^2 value. R^2 value is greater than 0.980 for all quantitative PCR reactions in this work (Fig 4.7).
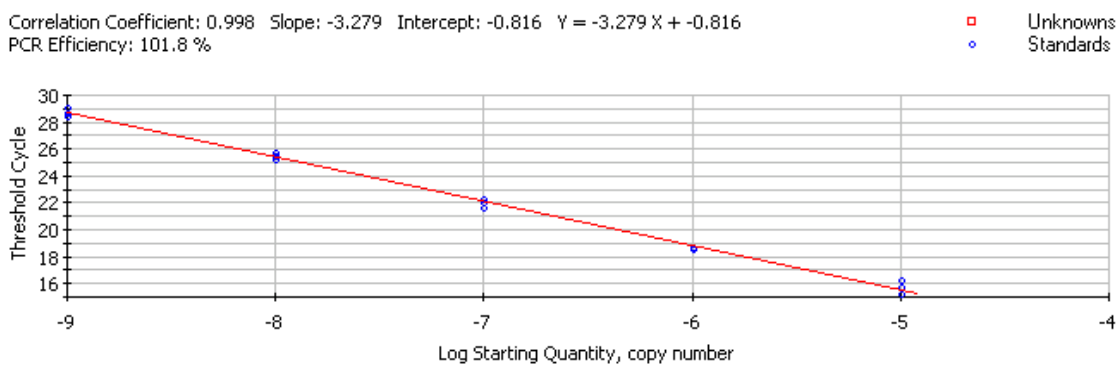
Fig 4.7 A standard curve is generated to assess reaction optimization. A standard curve is generated using a 10-fold dilution of a standard amplified in the real-time PCR system. Each dilution is assayed in triplicate (blue cycles). The C_T value is plotted against the log of the starting quantity of the template for each dilution. The equation for the regression line and the correlation coefficient (R^2) are shown above the graph. The calculated amplification efficiency is 101.8%. Blue cycles: Triplicates of 10-fold dilutions from the standard. Red line: The regression line that can be used to determine the starting quantity of test sample from the experimental C_T values.

Efficiency of the amplification (E) is calculated from the slope of the standard curve using the following equation (Rasmussen et al., 2001):

$$E = 10^{-1/slope}$$

If the PCR product doubles perfectly during each cycle of amplification, there is a 2-fold increase in the number of copies, in which case the reaction efficiency is 2. One can calculate from the equation above that the optimal slope of the standard curve will be -3.32, which shares the same

absolute value as the ideal spacing of the fluorescent curves. The amplification efficiency can also presented as a percentage, which is the percentage of template that is amplified in each cycle.

$$\%\text{Efficiency} = (\text{E-1}){\times}100\%$$

For an ideal reaction,

$$\%\text{Efficiency} = (\text{2-1}) \times 100\% = 100\%$$

An efficiency close to 100% is an indicator of sensible and reproducible assay. In practice, an efficiency of 90%-110% is considered acceptable, which represents the slope between -3.1 and -3.6 of the standard curve. All PCR reactions in this assay are optimized to fit to this criteria.

4.2.12.6 RNA extraction from whole embryo and from CNC explants

RNA extraction is carried out using two sets of RNA isolation kits depending on the abundance of the source material. The total RNA from whole embryos can be achieved using the "High Pure RNA Isolation Kit" from Roche. Embryos collected at desired stages are immediately proceed to lysis or shock frozen by liquid nitrogen and stored at -80°C. Embryos are first homogenized in 1x PBS with a cannula (diameter 0.40 mm). By adding the lysis/binding buffer containing a chaotropic salt (guandine HCl) and a detergent, the embryos are lysed while simultaneously RNases are inactivated. The lysate is applied to the filter tube, where nucleic acids bind to the glass fiber fleece. After centrifuging, the DNA is digested with DNase I directly on the filter for 30 Minutes at RT. Brief wash-and-spin steps remove the digested DNA fragments and other contaminating substances. The purified RNA is then eluted in 30 µl low-salt elution buffer.

CNC explants for RNA extraction are dissected and submerged directly in RNAlater for storage. RNAlater solution is an aqueous tissue storage reagent that rapidly permeates tissues to stabilize and protect cellular RNA. For quantification in the real-time PCR, approximately 90 CNC explants are collected for each test sample. To isolate RNA from CNC explants in the RNAlater solution, "TRIzol®Plus RNA Purification Kit" from Invitrogen and "PureLink TM RNA Mini Kit" from Ambion is used. To every 20 CNC explants 500 µl TRIzol®Reagent is added and the tissue is homogenized with a cannula. TRIzol®Reagent is a monophasic solution of phenol, guanidine isothiocyanate with strong lysis capability, while maintaining the integrity of the RNA and inhibiting the RNase activity during sample homogenization and lysis. Next, the lysate is

transferred to the homogenizer and incubated at RT for five minutes before centrifuged at 12,000 x g for two minutes at 25°C. Incubation with TRIzol®Reagent and centrifugation ensures a complete dissociation of nucleoprotein complexes. After the homogenizer is removed, 60 µl chloroform is added to each 500 µl Trizol lysat and the mixture is shaken vigorously by hand for 15 seconds. This is then incubated at RT for two to three minutes and centrifuged at 12,000 x g for 15 minutes at 4°C. The addition of chloroform, followed by centrifugation, separates the solution into an upper aqueous phase containing RNA and a lower phenol-containing organic phase. The colourless upper phase is transferred to fresh RNA-free tube, followed by ethanol addition and centrifugation. The sample is then transferred to the PureLinkTM RNA Mini Kit Spin Cartridge containing a clear silica-based membrane to which the RNA binds during purification. After centrifugation at 12,000 x g for 15 seconds the flow-through is discarded. This step is repeated until the entire sample has been processed. Up to 700 µl of the sample can be pooled on to the same spin cartridge. The spin cartridge (containing the RNA bound) is washed with 350 µl wash buffer I containing guanidine isothiocyanate and centrifuged at 12,000 x g for 15 seconds at RT. The flow-through is discarded and the spin cartridge is inserted in to new collection tube. Digestion with DNase is carried out according to "On-column PureLink DNase Treatment protocol" and the PureLink DNase mixture is set up as following:

Components	Volume per Reaction
10 x DNase I Reaction Buffer	8 µl
Resuspended DNase (3U/µl)	10 µl
RNase free water	62 µl
Total volume	80 µl

80 µl of PureLink DNase mixture is added onto the surface and incubated for 15 minutes at RT. Afterwards the spin cartridge is washed again with wash buffer I and centrifuged at 12,000 x g for 15 seconds at RT. After inserting the spin cadrige into new collection tube, 500 µl wash buffer containing ethanol is added and centrifuged down, which ends the DNase treatment. The same washing step is repeated one more time and centrifuged again to dry the membrane. To elute the RNA, 30 µl RNase-free water is added to the center of spin cartridge and incubated at RT for one minute. The Spin Cartridge with the Recovery Tube is centrifuged for two minutes at 13,000 x g at RT and the purified RNA is collected in the Recovery Tube. The concentration of the total RNA is determined by a photometer and the RNA is stored at -80°C.

4.2.12.7 cDNA template synthesis (reverse transcription)

For quantification of gene expression by RT-qPCR, the RNA is first transcribed into cDNA in a reaction using the enzyme reverse transcriptase. An aliquot of the resulting cDNA can then be used as a template for multiple qPCR reactions.

In a 10 µl reaction tube 150 ng RNA mixed with 2 µl oligo (dT) primers is first heated five minutes at 70°C to melt potential secondary structure within the template. After cooling to 4°C, 10 µl Transcriptions Mix from 4 µl 5x Puffer, 1 µl dNTPs, 0.5 µl Reverse Transcriptase from Moloney murine leukemia virus (MMLV) und 4.5 µl water is added. The mixture is incubated at 25°C for five minutes and then at 42°C for one hour. As control for DNA contamination, a similar reaction mixture only lacking of the reverse transcriptase is carried out in parallel.

For cDNA synthesis from RNAs with low concentration, the "iScript^{TM}cDNA Synthesis Kit" is applied. iScript is a modified MMLV-derived reverse transcriptase preblended with a RNase inhibitor. A blend of oligo (dT) and random hexamer primers is also present in the reaction mix, which minimizes the total volume for other components in the reaction besides the template. The RNA template can therefore be filled up to 16 µl in a 20 µl reaction mix. The reaction setup is described below:

Components	Volume per Reaction
5 x iScript reaction mix	4 µl
Nuclease-free water	x µl
Total RNA 150 ng	x µl
Total volume	20 µl

The complete reaction mix is incubated successively for five minutes at 25°C, 30 minutes at 42°C and five minutes at 85°C. After cooling to 4°C, the cDNA can be used for qPCR reactions.

To evaluate possible contamination from genomic DNA, a minus-reverse transcriptase ("-RT") control is included for each RNA preparation. The "-RT" control is a mock reverse transcription containing all the RT-PCR reagents except the reverse transcriptase. "-RT" control sample is assessed together with other test samples in the real-time amplification next.

4.2.12.8 Real-time PCR measurements

The expression of the target genes and the reference gene Ornithine decarboxylase (ODC) (see relative quantification in 4.2.12.10) are assessed in RT-qPCR assay. The preformulated real-time PCR master mixes "iQ^{TM}SYBR Green Supermix" consist of reaction buffer, DNA polymerase, dNTPs and SYBR Green I dye. A standard SYBR Green I qPCR reaction contains the following components:

Components	Volume per Reaction
iQ^{TM}SYBR Green Supermix	10 µl
Primer mix	1 µl
cDNA	2 µl
Nuclease-free water	7 µl
Total volume	20 µl

For test sample containing target genes, triplets are run for each assay. Duplets of no template control (NTC) is included in every assay to exclude unspecific amplification reactions through primers or solution contamination. "-RT" control sample is amplified under the same condition as test samples. If a "-RT" control sample has a C_T value 10-15 cycles higher than an RT test sample, then the "-RT" control sample contained approximately more than 1000-fold less target sequence (assuming 100% efficiency, 1 C_T ≈ 2-fold difference in initial template amount). This means, less than 0.1% of the amplification product in the RT sample is attributable to the genomic DNA template. In this case it is determined that the genomic DNA is sufficiently negligible compared to the amplification of the cDNA sequence.

The cycling program used is shown below:

Cycles	Time	Temperature
3x	30 sec	95°C
1x	5 min	95°C
36 x	30 sec 30 sec 30 sec	95°C 56 - 62°C (optimal temperature for each primer pair) 72°C

80x	10 sec	60°C
1x	∞	4°C

Table 4.5 Cycling protocol for RT-qPCR.

4.2.12.9 Data analysis

As mentioned in introduction (4.2.12.1), real-time PCR is a method for determining the amount of nucleic acid in a sample. The acquired data through RT-qPCR need to be transformed to a form that is biologically meaningful. For example, one is interested in finding out: 1) the number of certain molecules in a cell, or 2) the fold change of a certain mRNA in an equivalent amount of CNC cells in stage 17 vs. in stage 23. The analysis methods that address these two questions are known as absolute quantification and relative quantification. The result of absolute quantification is the quantity of nucleic acid (copy number) in a given amount of sample (in a cell or in 1 μg of RNA) (see 4.2.12.11). The analysis of relative quantification however, results a ratio: the relative amount (fold change) of a transcript for equivalent amounts of test and control sample.

4.2.12.10 Relative quantification of gene expression

For a relative quantification, the quantities obtained from the qPCR experiment are normalized to the expression level of a reference gene. A reference gene is one whose expression level is constant across all test samples, which in our case is the Ornithine decarboxylase (ODC). The advantage of normalizing the expression of the target gene to that of a reference gene is that it compensates for any difference in the amount of sample tissue. If the levels of ODC mRNA expression is identical in all test samples, one can extract RNA from an approximately equivalent number of cells from all samples without determining the exact number of cells. The level of the target gene mRNA and the ODC mRNA in the test samples are then determined by a RT-qPCR assay. The relative expression of the target gene in different development stages is calculated by taking the ratio of the ODC-normalized target gene expression.

When comparing multiple samples using relative quantification, one sample is usually chosen as the calibrator (also known as the control sample), and the expression of target gene in all other samples is referred as an increase or decrease relative to the calibrator. In this work, the expression level of cadherin in stage 17, 20 and 23 are analyzed. Therefore, the CNC sample at

stage 17 (stage of pre-migratory CNC) is chosen as the calibrator and the CNC sample from later stages as test samples. The expression level of cadherin in stage 20 and stage 23 is always compared to the cadherin expression at stage 17.

To determine the relative expression of a target gene in the test samples and calibrator sample using reference gene as the normalizer, the expression levels of both target and reference gene need to be determined using RT-qPCR. After the C_T values are measured, the $2^{-\Delta\Delta C_T}$ method (Livak and Schmittgen, 2001) is used to determine the expression level of the target gene in the test sample relative to the calibrator sample. The $2^{-\Delta\Delta C_T}$ method assumes that both target and reference gene have similar and near 100% amplification efficiencies, which is verified in the primer validation and experiment optimization steps. The relative difference in the expression level of the target gene in different samples is determined through following steps:

First, the C_T value of the target gene is normalized to that of the reference gene (ref), for both test samples and calibrator sample:

$$\Delta C_{T(test)} = C_{T(target,test)} - C_{T(ref,test)}$$

$$\Delta C_{T(calibrator)} = C_{T(target,calibrator)} - C_{T(ref,calibrator)}$$

Second, the ΔC_T of the test sample is normalized to the ΔC_T of the calibrator:

$$\Delta\Delta C_T = \Delta C_{T(test)} - \Delta C_{T(calibrator)}$$

Finally, the expression ratio is calculated:

$$2^{-\Delta\Delta C_T} = \text{Normalized expression ratio}$$

The obtained result is the fold change (increase or decrease) of the target gene in the test sample relative to the calibrator sample and is normalized to the expression of a reference gene, in this work the expression of the ODC gene.

4.2.12.11 Absolute quantification of gene expression

The absolute quantification is achieved by comparing the C_T values of the test samples to a standard curve (Yu et al., 2005). The end result is a quantitative description of a single sample, which does not depend on the property of other samples. The absolute quantification is used, when one is interested in finding out the intrinsic property of a given sample. This method is also

useful, when the copy numbers of several target genes are compared. In other words, the amplification efficiencies of different target genes are independent and the quantification does not require similar amplification efficiencies or similar sizes of the amplification products. In this work, the absolute quantification is therefore chosen to determine the copy numbers of different cadherins in CNC explants.

In the absolute quantification, the quantity (in this work the copy number) of the unknown sample is interpolated from a range of standards of known quantity. To construct a standard curve, a template with known concentration is required. For this purpose, plasmid DNA containing target gene sequence (cDNA sequence of the target gene cloned in an expression vector) is used as template (Tab 4.6). Dilution of the plasmid is then performed and these dilutions serve as standards for constructing the standard curve. The range of template concentrations used for the standard curve encompasses the entire range of template concentration of the test samples to ensure that results from the test samples are within the linear dynamic range of the quantification assay.

Plasmid	Concentration	Plasmid size
Cadherin-11 in pcDNA3.1	1000 ng/ul	7842 bp
N-cadherin in pcDNA3.1	700 ng/ul	7000 bp
E-cadherin full length in HA-pCS2+	694 ng/ul	6820 bp
XB-cadherin full length in pSP64T	756 ng/ul	6215 bp
PCNS in pCMV SPORT16	756 ng/ul	8007 bp
xPAPC FL in pCS2	600 ng/ul	7746 bp

Tab 4.6 DNA plasmids used in this work to generate standard curves for absolute quantification along with their sizes and concentrations.

If a sample contains exclusively known plasmid DNA, one can calculate the copy number of this plasmid in a given sample. The concentration of the plasmid is measured using a photometer and the corresponding copy number is calculated using the following equation (Whelan et al., 2003):

$$\text{DNA (copy)} = \frac{6.022 \times 10^{23} \left(\text{copy/mol}\right) \times \text{DNA amount (g)}}{\text{DNA length (bp)} \times 660 \text{ (g/mol/bp)}}$$

For example, to determine the quantity of cadherin-11 expression in CNC explants, plasmid containing cadherin-11 sequence (Cadherin-11 in pcDNA3.1) is used to prepare dilutions for a standard curve. The copy number in the plasmid stock solution is 1.2×10^{11} copies per µl and a 10-fold serial dilution series of the stock solution is set up. Diluted plasmid solutions that ranging from 1×10^{5} to 1×10^{10} copies/µl are used as template standards to construct the standard curves for cadherin-11, because this covers the entire range of cadherin-11 concentration in the CNC tissue sample.

C_T values in each dilution are measured in triplicate and the mean C_T value is used to determine the copy number of a sample in the equation above. The logarithms of the initial template copy numbers from the standards are plotted along the x-axis and their respective C_T values are plotted along the y-axis. Each standard curve is generated by a linear regression of the plotted points. The equation for the linear regression line [y = ax+b] is created automatically by the analysis software and showed alongside the curve. Based on the equation for the linear regression:

$$C_T = a(\log \text{quantity}) + b$$

$$\text{Quantity} = 10^{(\frac{C_T - b}{a})}$$

The copy numbers of individual assays (in our case CNC samples form different frogs) for test samples are determined using their mean C_T values obtained from individual triplicate samples. At least three independent standard curves are generated and a mean and a standard deviation of the individual assays is reported.

In order to define the amount of sample assayed in the RT-qPCR, the cell number of a CNC explant is determined. Wild type CNC cells are explanted at stage 17 (see 4.1.9) and DAPI staining (see 4.1.10) is performed on spread, monolayer CNC cells. With the help of the dark purple stained nuclei, the cell number of CNC explant is counted and the mean cell number of a CNC explant is used to calculate the number of cells in the test sample.

4.2.13   Sequence analysis

Sequencing is carried out by GATC Biotech AG and the sequence analysis is performed using the software ApE (version2.0.47 by M. Wayne Davis).

4.3 Protein biochemical methods

4.3.1 Protein extraction from embryos

Embryos or explants at desired stage are homogenized in a protein extraction mix (1x MBSH, 1% Triton X100, 10 x Protease inhibitor and 5 mM EDTA). The mixture is incubated on ice for 10 - 15 minutes and then centrifuged at 13000 rpm for 30 minutes at 4°C. Supernatant is transferred into a new tube.

4.3.2 Separation and purification of glycoproteins via ConA Sepharose 4B

ConcanavalinA (ConA) is a tetrameric metalloprotein obtained from Jack bean (*Canavalia ensiformis*). ConA binds molecules containing α-D-mannopyranosyl, α-D glucopyranosyl, and sterically related residues. Therefore, it is chosen to enrich cadherins in lysates. 60 µl of the ConA beads suspension are used for 300 µl protein lysate. ConA sepharose beads are stored in 20% Ethanol and need to be equilibrated with buffer before being added to the lysate. Thus 1 ml 1x MBSH + 1% Triton is added to the beads and this is centrifuged for three minutes at 3000 rpm. Supernatant is then discarded and beads are resuspended in 1x MBSH + 1% Triton. Equilibrated ConA beads are subsequently added to protein sample and the mixture is kept rotating overnight at 4°C. The next day, the sample is centrifuged at 3000 rpm for three minutes and supernatant is discarded. Beads are washed twice with 0.5 - 1ml 1x MBSH + 1% Triton and the supernatant is again discarded. Proteins are eluted from beads by adding SDS-PAGE sample buffer and boiled for five minutes at 95°C. Samples are then centrifuged for two minutes at maximum speed and loaded on a gel.

4.3.3 Separation of proteins via SDS-polyacrylamide gel

SDS-PAGE (Sodium dodecyl sulfate-polyacrylamide gel electrophoresis) is a method by which proteins can be separated depending on their sizes. SDS is an anionic detergent that gives negative charges to proteins and the amount of bound SDS is proportional to the size of the

protein. Therefore, the charge density is same for all proteins and the separation of proteins in the polyacrylamide gel depends solely on the sizes of the proteins. The matrix that is used to separate the proteins is made of polyacrylamide. It is a polymer formed from cross-linked acrylamide subunits. The polymerization of acrylamide requires additionally ammonium persulfate (APS) and TEMD (N, N, N', N'-tetramethyl-ethylenediamine), as source of free radicals and a stabilizer respectively. By adding bisacrylamide, the polymerization reaction creates a gel that allows smaller molecules travel faster than larger ones. The negatively charged proteins are loaded in the polyacrylamide gel and an electric field is applied. Negatively charged proteins are attracted towards the anode. Since the protein samples are denatured when being boiled at 95°C with SDS loading buffer containing β-mercaptoethanol, the proteins are present in a primary form. This means, the mobility of the SDS loaded proteins are only affected by their molecular weight.

The acrylamide concentration of the gel can be varied from 5% to 25%. Lower percentage gels that have larger pores are used for resolving larger proteins. For detection of cadherins, 8% separation gels are applied. A stacking gel with 5% acrylamide on top of the 8% separation gel allows all proteins assemble at the front of separating gel (Tab 4.7).

Components	8% separation gel (5ml)	5% stacking gel (1ml)
H$_2$O	2.3 ml	1.4 ml
30% Acryl-Bisacrylamide Mix	1.3 ml	0.33 ml
1.5 mM Tris/HCl, pH 8.8	1.3 ml	--
0.5 mM Tris/HCl, pH 6.8	--	0.25 ml
10% SDS	0.05 ml	0.02 ml
10% APS	0.05 ml	0.02 ml
TEMED	0.003 ml	0.002 ml

Table 4.7 Formula for preparation separation and stacking gel.

To prepare the gel, the mixture for separation gel is first poured between two glass plates in a gel caster with some space left for stacking gel. During polymerization of separation gel, water is filled upon the gel mixture to achieve a straight line of the separation gel. After approximately 30 minutes for polymerization, the water above the separation gel is removed and the mixture of stacking gel is added. A comb is fitted carefully between the glass plates to create sample wells.

After another 20-30 minutes the comb is removed and the polymerized gel can be subjected to gel electrophoresis.

After loading the sample wells, the polyacrylamide gel is placed in a chamber filled with SDS-PAGE running buffer and an electric field is applied across the gel. A voltage of 70 V is firstly applied. After about 10 minutes when all samples have run through the stacking gel and appear as a line in front of separation gel, the voltage is raised to 110 V for separation. After certain amount of time, protein samples migrate different distances based on their sizes. Smaller proteins travel further down the gel, while larger ones remain closer to the point of start. Gel that contains separated proteins can then be used for further processing, for example Western blot or Coomasie staining.

4.3.4   Western blot analysis

Western blot is an analytic technique used to detect specific proteins. In order to make protein samples accessible for antibody detection, they are transferred onto a polyvinyl difluoride (PVDF) or nitrocellulose membrane. These membranes bind proteins with high affinity. PVDF membrane requires activation with methanol. Equilibrated membrane and the gel containing separated protein samples are sandwiched between thick filter papers (three papers each at bottom and top), which are soaked in transfer buffer. An electric field is applied with an electric current of 0.05 amperes per gel. Blotting takes 60-90 minutes. After blotting, the membrane is incubated for 30 minutes with 5% skimmed milk powder in 1x TBST to block nonspecific antibody binding sites. The membrane is then incubated with primary antibody against the protein of interest overnight at 4°C. On next day the membrane is washed three times for ten minutes, each with 1x TBST, and incubated with secondary antibody at room temperature for two hours. Secondary antibody is coupled with either alkaline phosphatase (AP) or peroxidase (POD). After incubation with secondary antibody, the membrane is washed again with TBST three times. For detection of AP, the membrane is washed two more times for ten minutes with the AP buffer. The substrate NBT/BCIP (1.5 µl pro 1 ml AP buffer) is mixed in the AP buffer and 5 ml solution is used to detect one blot. Secondary antibody coupled with POD is detected via a chemiluminescence reaction, in which the enzyme catalyzes the oxidation of luminol present in the substrate solution. The substrate solution is prepared using "The enhanced chemiluminescence (ECL)" solution mixture of A and B from the kit "ECL Plus westen blotting" and added onto the membrane. A CCD camera documents the chemiluminescence.

5   Results

5.1   Characterization of *Xenopus* cadherin expression in cranial neural crest (CNC) cells

5.1.1   Quantification of cadherin transcripts in CNC cells and in whole embryos during CNC migration via real-time PCR

To understand the roles of different cadherins in collective CNC migration of *X. laevis*, the expression levels of E-cadherin, XB/C-cadherin, Cadherin-11, PAPC and PCNS in CNC cells from late neurula (stage 17, premigratory) to early tailbud stage (stage 23, migratory) are investigated. The quantification of cadherin mRNAs is carried out by quantitative real-time PCR (RT-qPCR). Two methods for quantifying expression level of multiple cadherins are deployed: (1) relative quantification: comparative C_T method, which transforms a difference in C_T values (between the test sample and the calibrator sample) to a fold change in expression level; and (2) absolute quantification: the absolute copy number (of the test samples) can be achieved by interpolation of obtained C_T value (of the test samples) to a standard curve.

5.1.1.1 XB-cadherin and C-cadherin are not distinguished in this assay

XB-cadherin (or U-cadherin) and C-cadherin (or EP-cadherin) are maternally expressed cadherins in *Xenopus* embryo (Choi et al., 1990; Levine et al., 1994; Muller et al., 1994). As these two cadherins have a sequence identity of almost 92% at the amino acid level, they are characterized as pseudoalleles based on the tetraploidy of the *Xenopus* genome (Kühl and Wedlich, 1996).

RT-qPCR amplification performed on CNC sample with XB-cadherin primer yields an amplicon, which shows a single peak with melting temperature at 82°C in melting-curve analysis (Fig 5.1 B). Meanwhile, the amplicon of C-cadherin primer has a melting temperature at 86°C (Fig 5.1 C). The estimated size of the amplification product from XB-cadherin primers and C-cadherin primers is 100 bp and 200 bp, respectively, which is confirmed in the gel electrophoresis analysis (Fig 5.1 A). Sequences of the amplification products correspond to the estimated binding

regions, which are verified through sequencing analysis. However, binding regions of XB-cadherin and C-cadherin primer show high homology in sequences, suggesting both primers are able to cross-react with the other gene with no or very less mismatches.
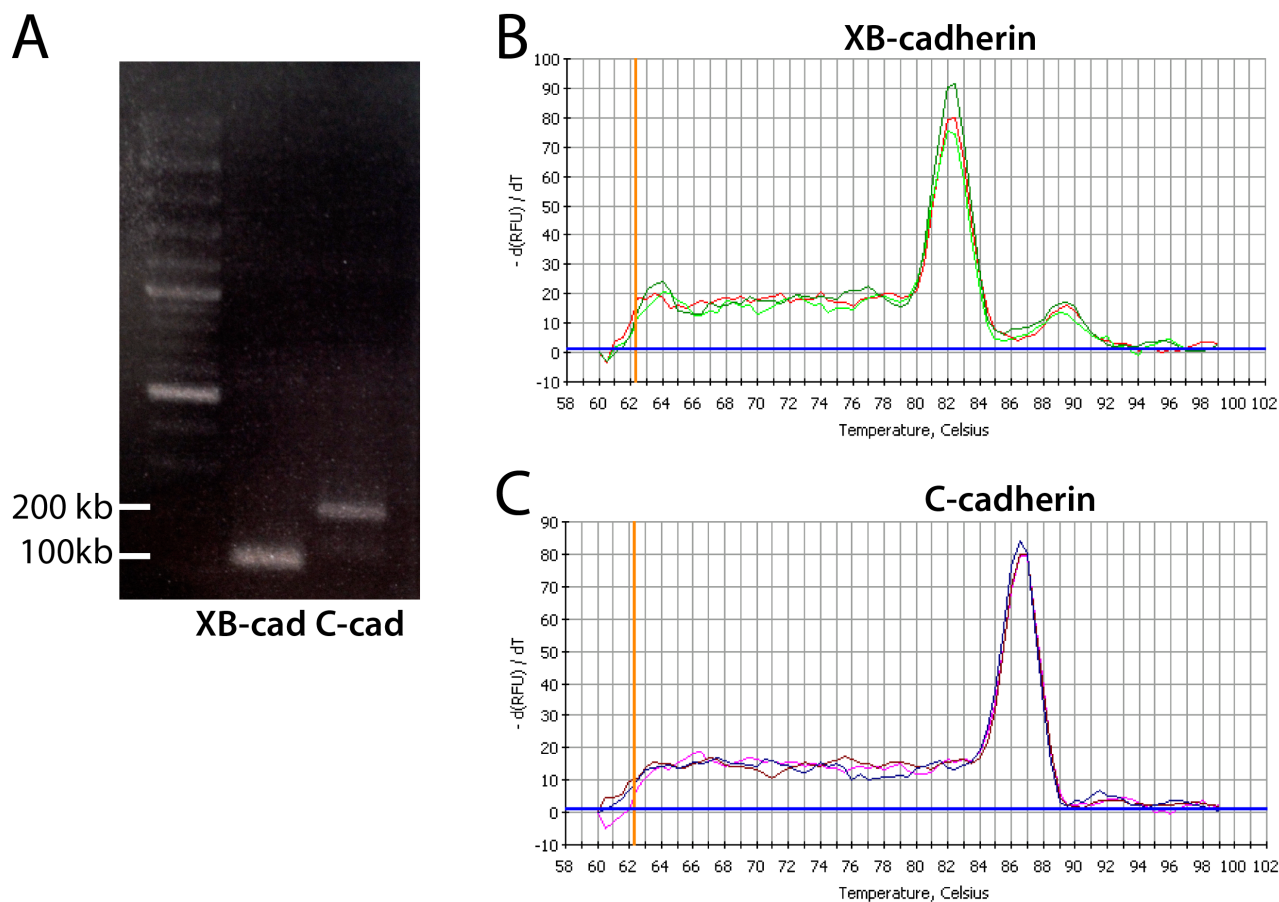
Fig5.1 Amplicons of XB-cadherin and C-cadherin primers via RT-qPCR. (A) cDNA from CNC cells amplified with XB-cadherin primer shows a 100 kb product in gel electrophoresis, whereas amplification with C-cadherin primer generates a 200 kb product. **(B)** Melting-curve analysis of the amplicon (triplets) amplified by XB-cadherin primer shows a single peak with melting temperature at 82°C. **(C)** Melting-curve (triplets) analysis of the amplicon amplified by C-cadherin primer shows a single peak with melting temperature at 86°C.

Although these two primers appear to generate distinct amplification products, it cannot rule out the possibility of cross-reaction. It is therefore concluded that the distinguishing of XB-cadherin from C-cadherin based on RT-qPCR amplification is not reliable. Based on the quantification level, it is speculated that the XB-cadherin primer possibly detects both XB-cadherin and C-cadherin transcripts. Thus, the quantitative results obtained with XB-cadherin primer are referred to as XB-and/or C-cadherin (XB/C-cadherin) in this work.

5.1.1.2 Confirmation of primer specificity

In RT-qPCR, six primer pairs are used to quantify the expression of N-cadherin, E-cadherin, XB/C-cadherin, Cadherin-11, PAPC and PCNS in CNC cells as well as in whole embryos. To ensure the specificity of the amplification product in the RT-qPCR assay, in addition to the primer validation mentioned previously in methods (4.2.12.5), cross reactivity of primers on non-templates DNA is also tested. Each RT-qPCR reaction is set up with a primer pair and a plasmid DNA as template, which does not contain the target sequence, in order to analyse the possibility of unspecific binding (Tab 5.1).

	N-cadherin primer	E-cadherin primer	Cadherin-11 primer	PAPC primer	PCNS primer	XB-cadherin primer
N-cadherin		32	32	30	34	--
E-cadherin	--		31	--	--	--
Cadherin-11	--	--		--	--	--
PAPC	32	--	30		--	--
PCNS	--	--	31	--		--
XB-cadherin	--	33	--	--	--	
C-cadherin	--	--	--	--	--	28

Tab 5.1 Cross-reaction analyses of different cadherin primers with non-template DNAs. The first row lists primers for detection of different cadherins and they are used for RT-qPCR reactions with each plasmid (first column) that contains the copy of another cadherin molecule. If an amplification product is detected, the C_T value is recorded. Slash indicates no amplification product.

For example, N-cadherin primer is used in RT-qPCR to amplify plasmid that containing sequence of E-cadherin, Cadherin-11, PAPC, PCNS and XB-cadherin, respectively. Due to the fact that SYBR Green I binds dsDNA unspecifically, any contamination in solutions or plasmid preparation can lead to a false positive product resulting in C_T value reading. This could explain some of the C_T reading in Tab 5.1. Additionally, samples of amplification products are sent for sequencing in case of relatively low C_T value ($C_T < 31$). Among sequenced samples, no specific amplification products are found by sequence analysis. Apart from primers for XB-cadherin, rest of the primers show no cross reactivity, in that no specific amplification products are detected in the RT-PCR with non-template DNA (indicated as slash in Tab 5.1).

5.1.1.3 Verification of CNC samples

CNC tissues from stage 17, 20 and 23, corresponding to premigratory, emigrating and migratory CNC cells respectively, are dissected for RT-qPCR. For comparison, whole embryos from the same developmental stages are also collected. Total RNAs are isolated from CNC tissue samples as well as from whole embryos, and cDNAs are synthesized from the extracted total RNAs respectively. cDNAs are diluted 1:4 and used as template for RT-qPCR. Quantitative real-time amplifications with several tissue specific markers are used to verify the identity of dissected CNC tissue in the samples. Relative quantification is performed by the $2^{-\Delta\Delta C_T}$ method (see 4.2.13.9a). The C_T values obtained from PCR are normalized to the expression of the reference gene, Ornithine decarboxylase (*ODC*). Since multiple marker genes are compared using relative quantification, the expression of *ODC* gene is also chosen as the calibrator. This means, the expression of *ODC* gene is set as 1 and the expression of all marker genes is referred as an expression ratio relative to the calibrator.

Neural crest specific transcription factors *twist*, *slug* (also known as *snail2*) and *snail*, which extensively expressed in neural crest cells (Hopwood et al., 1989; Locascio et al., 2002), are used here as marker for neural crest tissue. *twist* (Fig 5.2 A), *snail* (Fig 5.2 B) and *slug* (Fig 5.2 C) are present in high abundance in CNC samples through all three stages. In the same amount of RNA assessed in RT-qPCR, the expression of *twist* as well as that of *slug* is strongly enriched in CNC sample than in whole embryo samples (Fig 5.2 A, C), whereas the expression of *snail* does not show this kind of enrichment (Fig 5.2 B).

To ensure that CNC samples are obtained without contaminations from other tissue, samples are controlled with several other tissue markers. *Xbra* is used as a marker for general mesoderm tissue (Smith et al., 1991). As shown in Fig 5.2 D, the expressions of *xbra* are barely detectable in CNC samples throughout all stages. At stage 17, *xbra* expression equals roughly 0.1% of *snail* expression in the CNC sample. When compared to whole embryo samples, *xbra* expression in the CNC is about 10% of *xbra* expression in the whole embryo at 17 and 1% at stage 23 (Fig 5.2 D). This indicates that there is liminal mesoderm tissue present in the CNC sample. Since placodes are in close proximity to the CNC tissue, the presence of placodal tissue in CNC sample is being examined. The *Xenopus eya1* gene is expressed in placodes, somites as well as hypaxial muscle precursors and is therefore used here as a marker for placodes (David et al., 2001). As showed in Fig 5.2 E, the detected levels of *xeya1* in CNC samples are very low in comparison to CNC markers, with its expression matches about 1% of *snail* expression at stage 17. Additionally, in order to show that the placodal tissue stays intact after dissecting CNC, CNC

from one side of a wild type embryo is explanted and the embryo is left to heal. At stage 25, the embryo is fixed and *in situ* hybridization is carried out using *xeya1* as probe. The expression of *xeya1* on the side of CNC explantation is not impaired (Fig 5.2 F) indicating that only CNC are explanted. The *Xenopus* cytokeratin gene *xK81* (Type I cytoskeletal) is used here as a marker for epithelial ectoderm tissue (Jamrich et al., 1987). Similar to *xeya*1, the expressions of *xK81* in CNC samples reaches hardly 1% of *snail* expression at stage 17. These results indicate that the CNC samples consist mainly of CNC tissue.
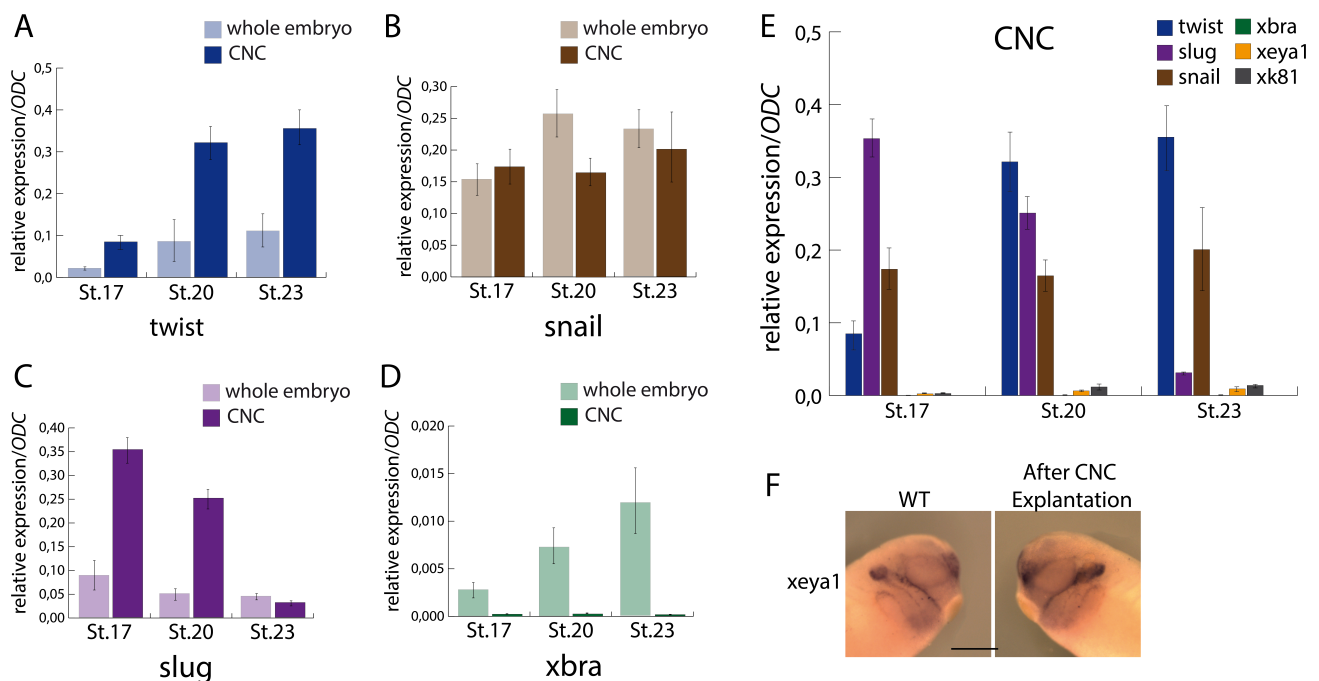
Fig 5.2 Verification of CNC tissue in RT-qPCR samples. RT-qPCR with different tissue marker genes are used to verify the identity of CNC tissue and control for other tissue contamination in PCR samples. CNC explants are dissected at the indicated stages. All values are normalized and calibrated to *ODC* expression (expression of *ODC* gene = 1). The bars indicate average and standard deviation of at least three independent experiments. The expression of CNC specific marker gene **(A)** *twist*, **(B)** *snail* and **(C)** *slug* are strong in CNC samples in comparison to whole embryo samples, whereas the expression levels of the mesoderm marker **(D)** *xbra* in the CNC samples are liminal. **(E)** The relative expression of the mesoderm marker *xbra*, placodal marker *xeya1* and epidermis marker *xk81* in comparison to CNC specific markers. **(F)** *In situ* hybridization for *xeya1* after CNC is removed. Scale bar = 200 µm

5.1.1.4 Relative quantification of cadherin expression in CNC cells during migration

To characterize the expression of different cadherins in CNC cells during their migration, RT-qPCR amplification is performed on CNC explants of stage 17, 20 and 23. After the C_T values are acquired, relative quantification is performed using $2^{-\Delta\Delta C_T}$ method. All C_T values are first normalized to the expression of *ODC* gene. To exhibit the change of expression levels, the expression level of each cadherin subtype at stage 17 is chosen as a calibrator (=1). The calculated ratio from a later stage sample is the fold change of expression level of this cadherin relative to stage 17 (Fig 5.3 A-F).
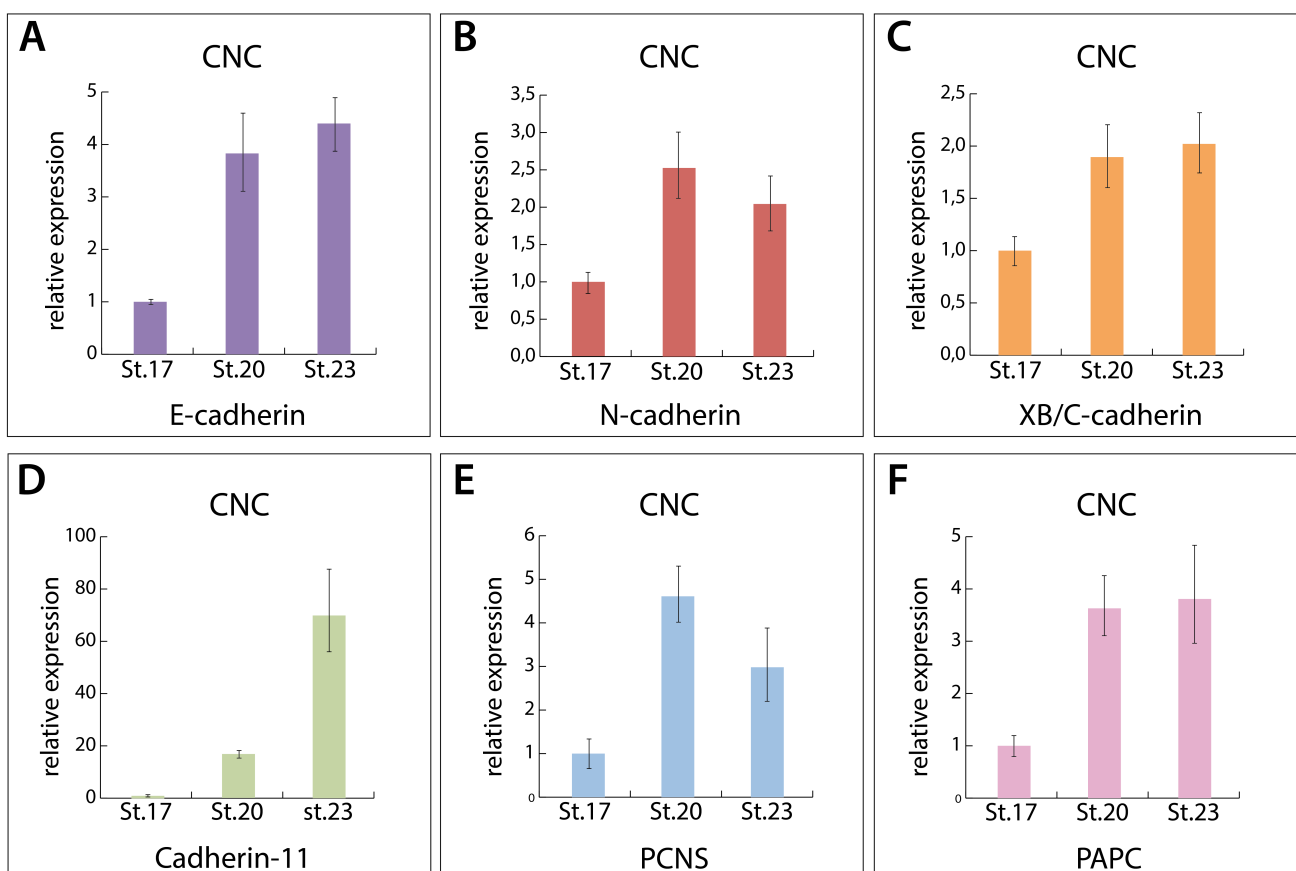
Fig 5.3 Relative expression of different cadherins in CNC cells during their migration. The expression level of **(A)** E-cadherin, **(B)** N-cadherin, **(C)** XB/C-cadherin, **(D)** Cadherin-11, **(E)** PCNS and **(F)** PAPC is shown as fold changes relative to stage 17. The expression of each cadherin at stage 17 is set as 1, and the expression ratio at stage 20 and stage 23 is the fold change relative to stage 17. At least three independent quantifications are performed and the bars indicate average values with standard deviations.

In CNC explants, transcripts of several classical cadherins as well as protocadherins are identified by RT-qPCR. Besides N-cadherin, Cadherin-11 and PCNS, which are known to be expressed in CNC (Hadeball et al., 1998; Rangarajan et al., 2006; Theveneau et al., 2010), the

expressions of E-cadherin, XB/C-cadherin and PAPC are for the first time described in the CNC cells. The expression of AXPC, however, is below the detection level (not shown). All detected cadherins show an increase of expression from stage 17 to stage 20, where CNC cells are beginning to emigrate. Among these cadherins, Cadherin-11 has a remarkably huge increase in its expression with 16 fold. As the CNC cell are migrating ventrally towards the pharyngeal pouches from stage 20 to stage 23, the expression levels of E-cadherin, XB/C-cadherin and PAPC increase slightly in a similar manner, whereas the expression of Cadherin-11 continue to rise immensely to a level that is about a 70-fold increase compared to stage 17. In contrast, the expression level of N-cadherin and PCNS decreases from stage 20 to stage 23.

5.1.1.5 Absolute quantification of cadherin expression during CNC migration

Since transcripts of multiple cadherins have been identified in the CNC cells, relative quantification (with each expression level of stage 17 as reference) fails to compare the expression level of one cadherin subtype against other. To further quantify the molecule number of each cadherin subtype in the CNC cells, an absolute quantification of RT-qPCR is applied. A plasmid DNA containing a specific cadherin cDNA sequence is used to construct the standard curve. As standards for RT-qPCR, a serial of 10-fold dilutions of this plasmid is made. And the obtained C_T values from these standards are used to generate the linear regression (see method). For each cadherin subtype, independent serial dilutions of the standards are assayed for at least three times, and the mean C_T values from each dilution are use for generating the standard curve. The RT-qPCR determined C_T values are plotted against the logarithm of the calculated initial copy numbers (Fig 5.4).

The absolute copy numbers of different cadherins in the CNC samples are then determined from the corresponding standard curves (Fig 5.4). To eliminate the loading difference in the initial template materials, the calculated copy numbers of each cadherin are normalized against the C_T values of the ODC gene.
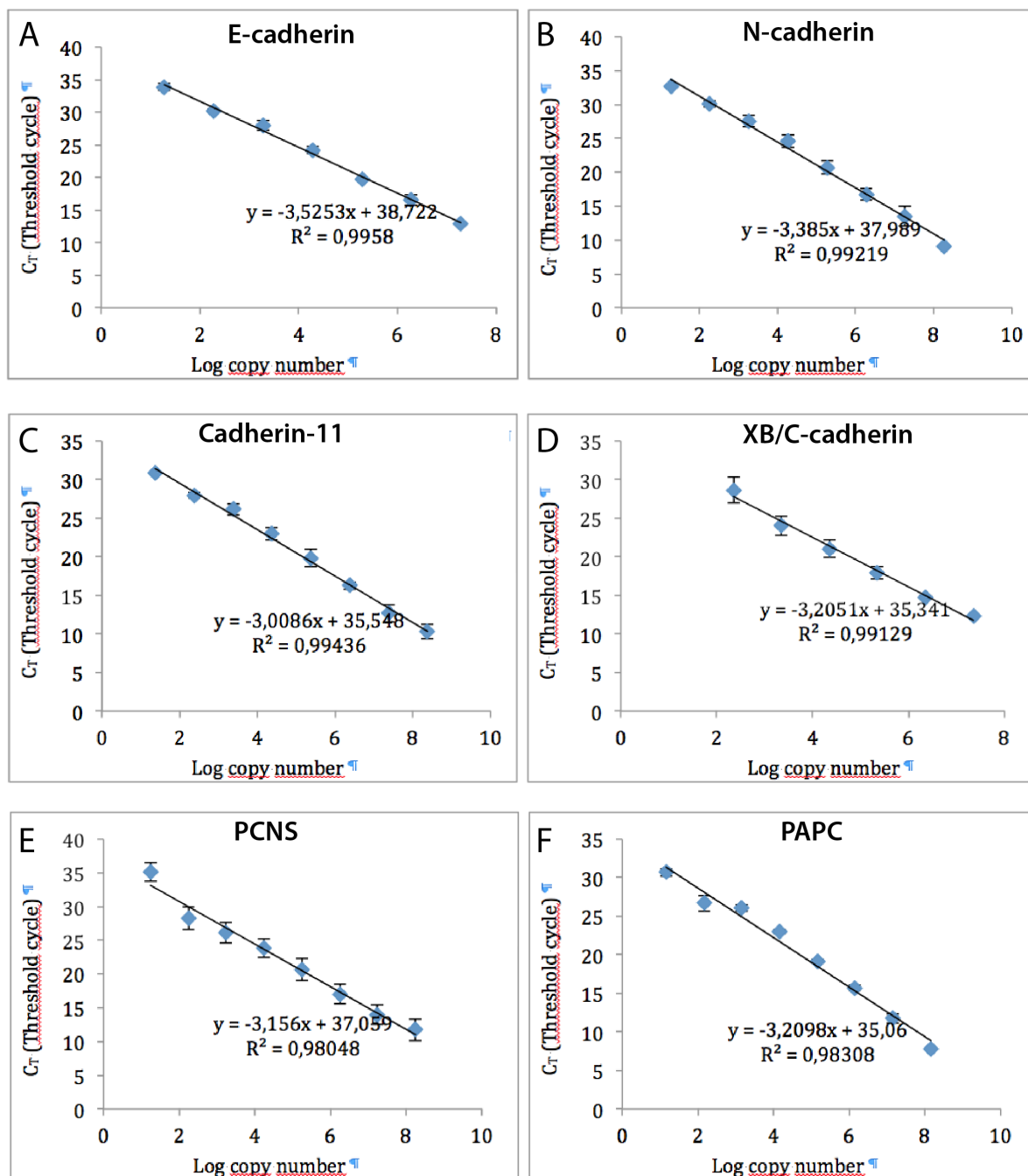
Fig 5.4 Standard curve for (A) E-cadherin, (B) N-cadherin, (C) Cadherin-11, (D) XB/C-cadherin, (E) PCNS and (F) PAPC. The standard curves are calculated with serial 10-fold dilutions of the plasmid DNA, ranging from 10 to 1×10^8 copies/µl. Each standard dilution is amplified by RT-qPCR using validated primers in triplicates. For each gene, the determined C_T values are plotted against the logarithm of their calculated initial copy numbers. Independent serial dilutions of the standards are repeated at least three times for each dilution and the mean value with standard deviation is shown. A standard curve is generated by linear regression through the points representing the mean values. The equation for the regression line and the correlation coefficient (R^2) are shown above the graph. The equation is used to determine the starting quantity of the test sample from the experimental C_T values.

Since the expression of the ODC gene has no significant change from stage 17 to stage 20 (data not shown), the mean C_T value of ODC gene is calculated based on all test samples, which represents the average amount of material that has been amplified through RT-qPCR. The difference between the C_T value of the ODC gene from individual test samples and the mean C_T value of ODC is determined and divided by each copy numbers of cadherins.

150 ng total RNA is originally used for cDNA synthesis. In order to calculate the exact amount of material used in RT-qPCR, it is assumed here that 150 ng of cDNA is obtained through reverse transcription. Total cDNA is then diluted 1:4, and 2 µl diluted cDNA is used as template for RT-qPCR. The dilution factor is calculated and the copy number per ng RNA of each cadherin is shown in Table 5.2 and Fig 5.5.

Name	Copy number per ng RNA					
	St.17		St.20		St.23	
	Whole	CNC	Whole	CNC	Whole	CNC
E-cadherin	1403	181	2721	607	1476	711
	± 579	± 8	± 1161	± 130	± 698	± 80
N-cadherin	139	275	662	513	545	526
	± 31	± 44	± 217	± 59	± 83	± 107
XB/C-cadherin	694	233	1291	719	468	785
	± 61	± 68	± 340	± 153	± 248	± 156
Cadherin-11	2.8	1	27	27	84	123
	± 1.8	± 0.4	± 3	± 25	± 19	± 36
PCNS	173	1375	464	1708	320	1027
	± 3	± 625	± 135	± 365	± 153	± 368
PAPC	54	20	198	60	172	61
	± 15	± 4	± 109	± 13	± 37	± 20

Tab 5.2 Copy numbers of cadherins in whole embryo and in CNC cells (/ng RNA).

The absolute quantification enables a quantitative comparison between each cadherin subtype in the CNC cells. The dominant cadherin expressed in the CNC cells during migration is the protocadherin PCNS. It is present with 1375 copies/ng RNA in premigratory CNC, later its expression increases to 1708 copies/ng RNA at emigration stage and finally decreases to 1027 copies/ng RNA in migratory CNC cells (Fig 5.5 E, Tab 5.2).
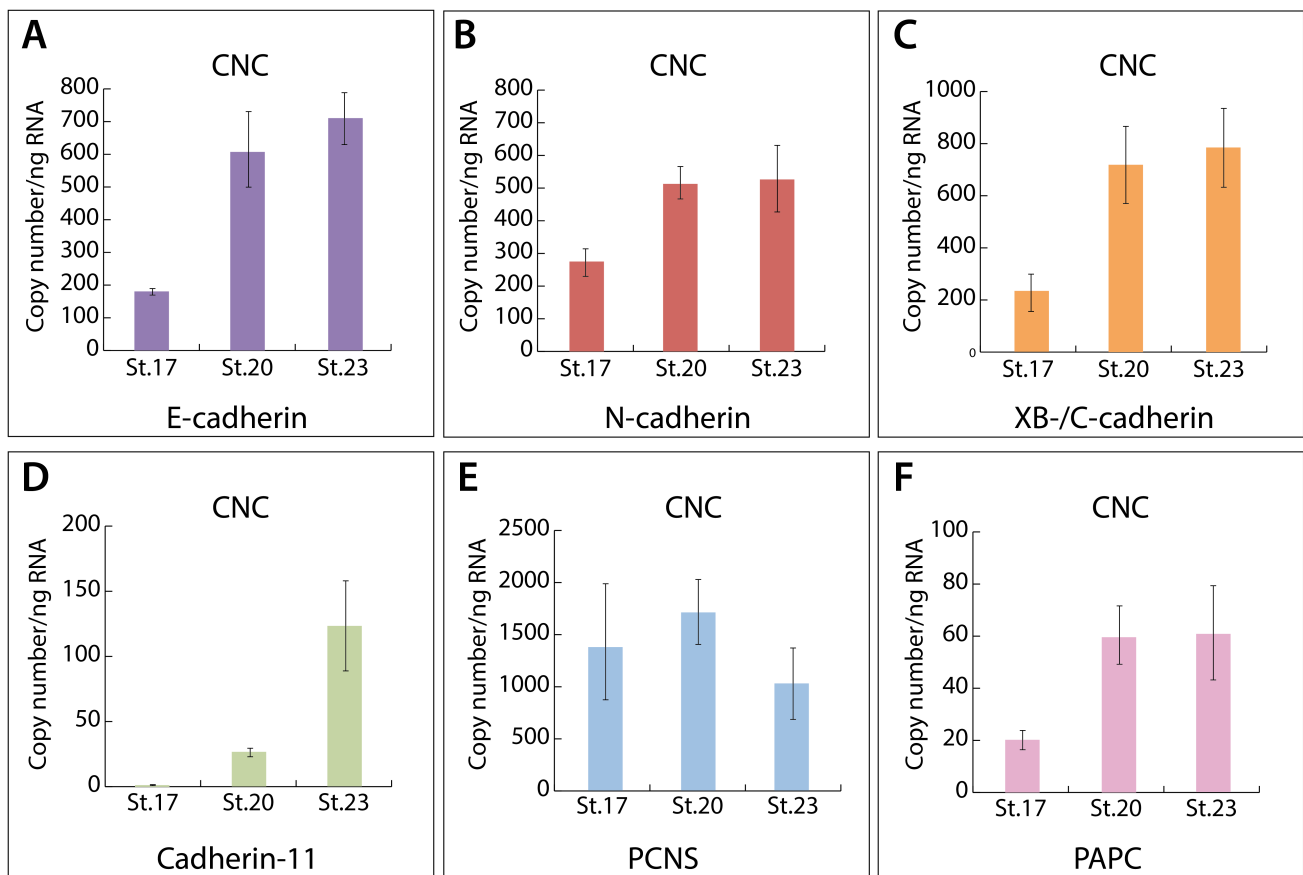
Fig 5.5 Copy numbers of (A) E-cadherin, (B) N-cadherin, (C) XB/C-cadherin, (D) Cadherin-11, (E) PCNS, (F) PAPC in CNC cells (per ng RNA). CNC explants are dissected at the indicated stages. Copy numbers of each cadherin in different stages during CNC migration are determined via absolute quantification and copy numbers per ng of RNA are plotted. At least three independent quantifications are performed and the bars indicate average values with standard deviations.

XB/C-cadherin is the second abundant cadherin expressed in CNC cells, with its copy number increases from 233 copies/ng to 719 copies/ng RNA at stage 20, and then continues its expression with 785 copies/ng RNA at stage 23 (Fig 5.5 C, Tab 5.2). Expression of E-cadherin begins from 181 copies/ng RNA at stage 17 to 607 copies/ng RNA at stage 20, and then increases again to 1476 copies/ng RNA at stage 23 (Fig 5.5 A, Tab 5.2). N-cadherin is also expressed stably in CNC cells, with 275 copies/ng RNA copies detected at stage 17, then 513 copies/ng RNA at stage 20 and finally 526 copies/ng RNA at stage 23 (Fig 5.5 B, Tab 5.2). Transcripts of Cadherin-11 and PAPC are present in relatively low abundance compared to other cadherins mentioned above. Nevertheless, consistent with the relative quantification data, the expression of Cadherin-11 rises most extravagantly among all cadherin subtypes during CNC migration from 1 copy/ng RNA at stage 17, 27 copies/ng RNA at stage20 to 123 copies/ng RNA at stage 23 (Fig 5.5 D, Tab 5.2). The expression of PAPC in CNC cells increases from stage 17

with 20 copies/ng RNA to 60 copies/ng RNA at stage 20, then constant with 61copies/ng RNA until stage 23 (Fig 5.5 F, Tab 5.2).

In order to further explicate the copy number of different cadherin subtypes on a single cell level, the number of cells within a CNC explant is determined by staining the nuclei of CNC explants with DAPI. The average cell number of a CNC explant is 573 ± 23 cells/explant. Assumed average 90 CNC explants are collected in the sample, same calculation of dilution factor is applied. It is determined then approximately 0.3 CNC explant is deployed as initial template in every PCR reaction mixture, which represents about 160 CNC cells. The copy number per CNC cell is then calculated by dividing the copy number of sample by 160. Here it is assumed that CNC explants from stage 20 and stage 23 have the same cell number as that from stage 17. The calculated copy numbers of each cadherin per cell are shown in Table 5.3 and Fig 5.6.

Name	Copy number per CNC cell		
	St.17	**St.20**	**St.23**
E-cadherin	4.2 ± 0.2	14.2 ± 3.0	16.7 ± 1.9
N-cadherin	6.4 ± 1.0	12.0 ± 1.4	12.3 ± 2.5
XB-cadherin	5.5 ± 1.6	16.9 ± 3.6	18.4 ± 3.7
Cadherin-11	0.03 ± 0.009	0.6 ± 0.08	2.9 ± 0.8
PCNS	32.2 ± 14.7	40.0 ± 8.6	24.1 ± 8.6
PAPC	0.5 ± 0.1	1.4 ± 0.3	1.4 ± 0.5

Tab 5.3 Copy numbers of cadherin transcripts per CNC cell.

With less than 15 copies/cell, E-cadherin, N-cadherin, PCNS and PAPC belong to the class of mRNAs, which comprises most mRNAs species in each cell, but expressed at a low level (5 to 15 molecules/cell for a typical mammalian cell) (Alberts B, 2002). PCNS with 24 copies/cell to 40 copies/cell (Fig 5.6, Tab 5.3) throughout migration phases can be categorized to the class of mRNAs, which present at an intermediate level (15 to 300 molecules per cell for a typical mammalian cell). To a lesser extent, XB/C-cadherin with respectively 17 copies/cell at stage 20 and 18 copies/cell at stage 23 can also be categorized to the mRNA class with intermediate abundance (Fig 5.6, Tab 5.3).
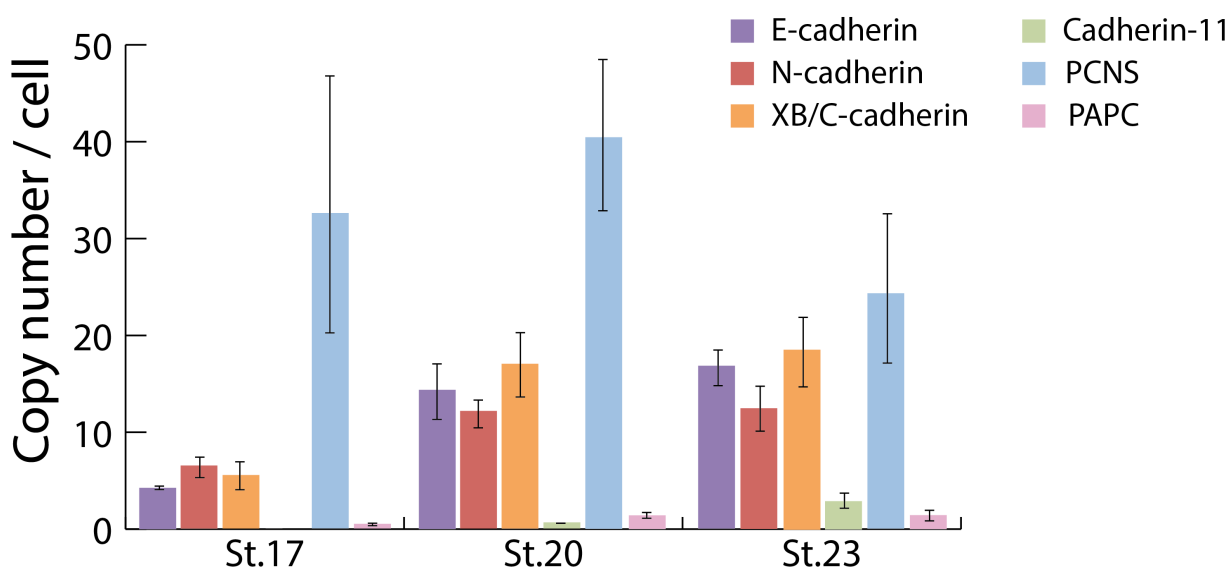
Fig 5.6 Copy number comparison of cadherin subtypes per CNC cell during their migration. CNC explants are dissected at the indicated stages. Copy numbers of each cadherin at different stages during CNC migration are determined via absolute quantification and copy numbers per CNC cell are plotted. At least three independent quantifications are performed and the bars indicate average values with standard deviations.

To better understand the abundance of the different cadherin subtypes in *Xenopus* cells in general, RT-qPCR assay is applied also for the quantification of cadherin molecules in whole embryo samples of same stages. Same amount of total RNA (150 pg) is used as initial template in PCR amplification and the gained C_T values are evaluated for absolute quantification in the same manner as for CNC cell samples. The calculated copy number of each cadherin subtype is shown in Table 5.2 and Figure 5.7.
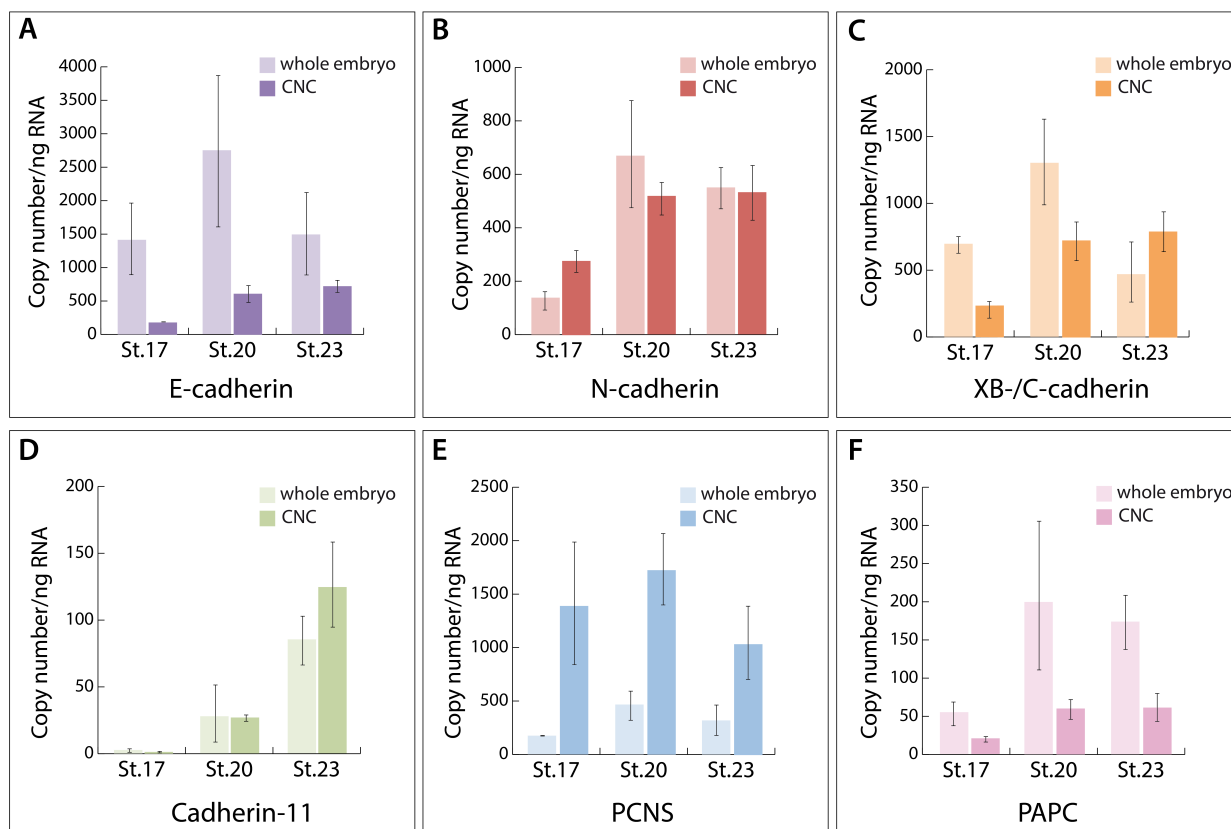
Fig 5.7 Comparison of cadherin expression in a whole embryo and in CNC cells. Whole embryo samples and CNC explants are collected at the indicated stages. The correlation between the two kinds of source materials is about one single embryo compared to roughly 22 CNC explants. Same amount of total RNA from a whole embryo and CNC explants is deployed for PCR amplification. Copy numbers of cadherins are determined via absolute quantification of RT-qPCR and copy numbers per ng of RNA are plotted. At least three independent quantifications are performed and the bars indicate average values with standard deviations.

It is noteworthy, that by applying the same amount of initial RNA in the RT-qPCR assay, the correlation between the two kinds of source materials is about one single embryo compared to roughly 22 CNC explants (calculated from the achieved average concentration of both materials). Taken that into consideration, the comparison of the whole embryo sample and the CNC sample elucidate further the enrichment of PCNS in CNC cells, where in case of E-cadherin and PAPC, the expression in the CNC cells represent a relative small portion compared to their expressions in other tissues. N-cadherin and XB/C-cadherin have relative abundant transcripts also in the whole embryo sample.The accumulation of Cadherin-11 in the whole embryo from stage 17 to stage 23 matches its pattern of increase in CNC cells.

5.1.2 Localization of endogenous cadherin in CNC cells

The quantification of cadherin transcripts in CNC cells via RT-qPCR establishes the mRNA expression levels of multiple cadherins. To further investigate the subcellular localizations of different cadherin subtypes, immunofluorescence staining are performed on CNC explants. The localizations of N-cadherin and Cadherin-11 are shown before using GFP tagged constructs, N-cadherin is localized at cell-cell contacts (Becker et al., 2012), whereas Cadherin-11 is additionally found in cell protrusions and in focal adhesions (Kashef et al., 2009; Langhe et al., in revision).

Localization showed with tagged cadherin constructs results in an overexpression situation and therefore do not necessarily represents the endogenous expression pattern of the cadherin. In this work, the subcellular localization of endogenous cadherins are demonstrated in the CNC explants using specific antibodies. To analyse the subcellular localization of cadherins, 500 pg mRNA of membrane bound GFP (mbGFP) are injected as lineage tracer in one blastomere at two-cell stage embryos. At stage 17, labelled CNC cells are explanted on fibronectin coated glass dishes, fixed and immunostained. The localization of endogenous cadherin is analysed by the spinning disk microscope.

Despite the high sequence homology of XB-cadherin and C-cadherin, the 6D5 monoclonal antibody detects specifically XB-cadherin (Muller et al., 1994), while the 6B6 antibody (Brieher and Gumbiner, 1994) is able to react with both C-cadherin and XB-cadherin. Using these two antibodies, XB-cadherin and C-cadherin are both detected in the CNC explants and their expressions are localized strongly at cell-cell contacts (Fig 5.8 A, B). N-cadherin is localized at cell-cell contacts in CNC explant (Fig 5.8 C), which consists with the localization shown by the N-cadherin-GFP construct (Becker et al., 2012). Likewise, E-cadherin is expressed at cell-cell contacts in CNC cells as well (Fig 5.8 D). The detection of endogenous cadherin proteins by immunofluorescence staining confirms the results of RT-qPCR that XB-cadherin, C-cadherin, N-cadherin and E-cadherin are expressed in CNC cells.
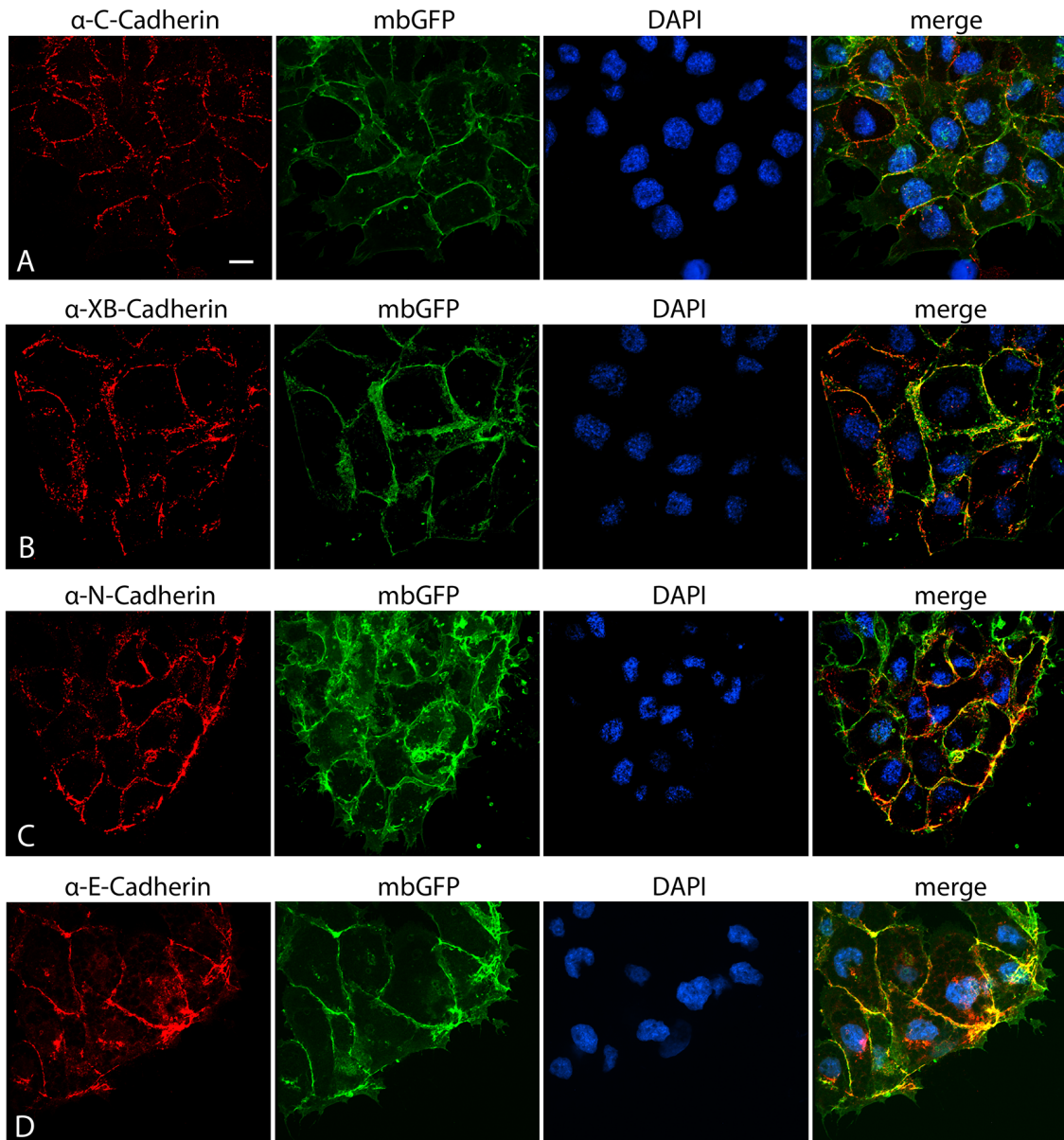
Fig 5.8 Immunostaining of cadherins in CNC cells. Immunostaining is performed on the CNC explants with primary antibody against **(A)** C-cadherin (6B6) (Brieher and Gumbiner, 1994) , **(B)** XB-cadherin (6D5) (Muller et al., 1994), **(C)** N-cadherin (MNCD2) (Theveneau et al., 2010), **(D)** E-cadherin (10H3) (Angres et al., 1991) and secondary antibody cy3. The second column shows the GFP marked membrane. The third column shows DAPI staining of nuclei. The fourth column shows merge pictures from the three channels. Scale bar = 10 μm

The endogenous localizations of PAPC and PCNC cannot be shown here due to lack of specific antibodies. Therefore, GFP tagged constructs are injected in the animal dorsal blasotomere at eight-cell stage. mRNA of membrane bound Cherry (mbCherry) is co-injected as lineage tracer. At stage 17, labelled CNC cells are explanted on fibronectin coated glass dishes. The localization of PAPC and PCNS is analysed by the spinning disk microscope.
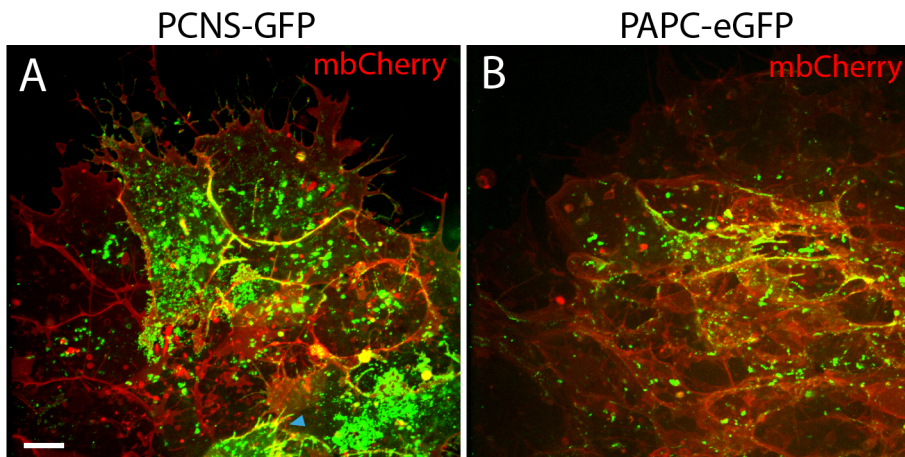
Fig 5.9 Localization of PCNS and PAPC in CNC cells. (A) PCNS is localized at cell-cell contacts, in vesicles and within cell protrusions (arrowhead), from (Becker et al., 2012) **(B)** PAPC is localized at cell-cell contacts and in vesicles. Embryo is injected respectively with PCNS-GFP and PAPC-eGFP and explanted at stage 17. Membrane bound cherry (mbCherry) is co-injected to label the membrane. Scale bar = 10 µm

PCNS is localized at cell-cell contacts, in cell protrusions and in intracellular vesicles (Fig 5.9 A). PAPC is observed also at cell-cell contacts and in vesicles (Fig 5.9 B).

5.2   Functional analysis of E-cadherin in *Xenopus* cranial neural crest cell migration

During the characterization of multiple cadherin subtypes in CNC cells, E-cadherin and the protocadherin PAPC are identified as two novel candidates that could be involved in the collective migration of CNC cells. The role of PAPC in regulating CNC migration is described in Schneider et al., 2014, while the function of E-cadherin in CNC cells is investigated in this work.

5.2.1   Heterogeneous E-cadherin expression in CNC subpopulations

Transcripts of E-cadherin are previously identified in CNC cells by RT-qPCR (Fig 5.3 A, Tab 5.2) and the subcellular localization of E-cadherin is demonstrated by immunofluorescence staining of CNC explants *in vitro* (Fig 5.8 D). To further verify the subcellular localization of E-cadherin in CNC cells *in vivo*, immunofluorescence staining for endogenous E-cadherin is performed on whole embryo cryosections (frozen section). To visualize CNC tissue in whole embryo sections

transplantation experiments are performed. Thereby, CNC cells are fluorescence labelled by injecting the donor embryo with 500 pg histone 2B GFP (H2B GFP) mRNA in one blastomere at two-cell stage. At stage 17, H2B GFP positive CNC cells are transplanted one-sided into another unlabelled, stage-matched, wild type host embryo (Fig 5.10 A). Transplanted embryos are left to heal properly and fixed at stage 27. Embedded whole embryos are subsequently tranverse sectioned (Fig 5.10 A) and immunofluorescence stained for E-cadherin using the monoclonal E-cadherin antibody 5D3 (Choi and Gumbiner, 1989). Images are taken by a spinning disk microscope.
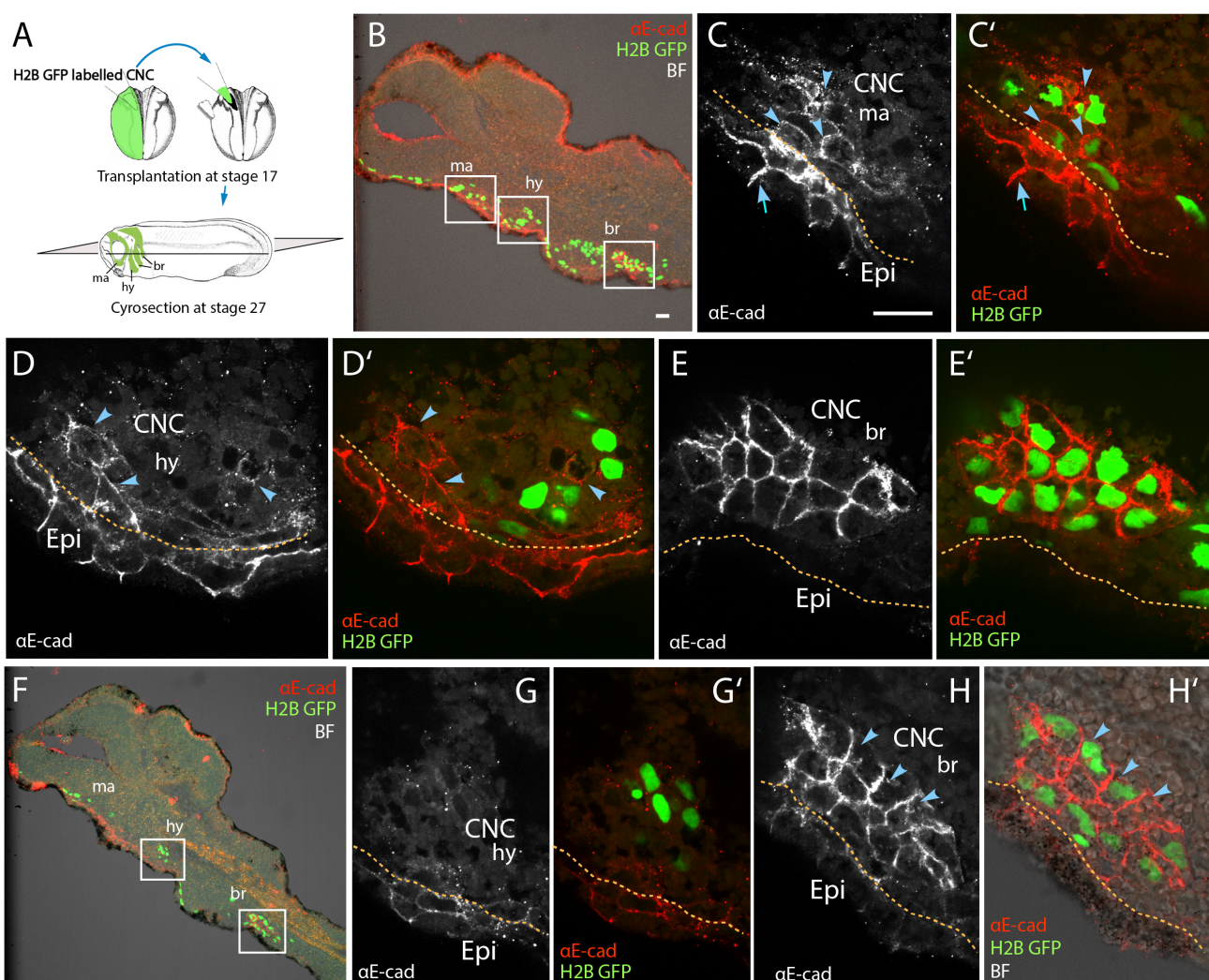
Fig5.10 E-cadherin is differently expressed in distinct CNC subpopulations. Immunofluorescence staining against E-cadherin 5D3 (Choi and Gumbiner, 1989) is performed on cryosections of whole embryos. Two transplanted embryos **(B, F)** with crop images are displayed **(A)** Schematics of the experimental approach for visualizing CNC cells in whole embryo sections: *Xenopus* embryo is injected with H2B GFP mRNA and the labelled CNC cells are transplanted into another unlabelled wild type host embryo. Transplanted embryos are fixed at stage 27 and transverse sectioned. **(B, F)** H2B GFP labelled CNC cells mark the mandibular (ma),

hyoid (hy) and branchial (br) CNC subpopulations in whole embryo section. Cropped image of mandibular **(C, C')**, hyoidal **(D, D'; G, G')** and branchial **(E, E'; H, H')** segment. Dashed orange lines indicate the boundary between epithelia (Epi) and CNC. Arrow shows E-cadherin staining in epithelia. Arrowhead indicates staining of E-cadherin in CNC. α-E-cad: anti-E-cadherin antibody (5D3); H2B GFP: CNC injected with H2B GFP mRNA; BF: bright field. Scale bar = 20 µm.

In Figure 5.10, two transplanted embryos (B and F) with crop images are displayed. Utilizing H2B GFP as lineage tracer, the CNC cells from donor embryos can be well distinguished from host tissue in the whole embryo sections (Fig 5.10 B, F). H2B GFP positive donor CNC cells are distributed in three subpopulations: mandibular, hyoid and branchial (anterior and posterior part), which are located directly adjacent to the epithelia (Fig 5.10 B, F). E-cadherin is localized in all CNC subpopulations (Fig 5.10 C, D, E, H arrowheads). Interestingly, the mandibular and hyoid subpopulations showed a relatively weak staining of E-cadherin (Fig 5.10 C, D, G arrowheads) compared to the posterior part of the branchial subpopulation, which exhibited a strong E-cadherin staining (Fig 5.10 E, E', H, H' arrowheads).

E-cadherin is localized predominantly at the cell-cell boundary, similar to the observation from immunofluorescence staining on CNC explants (Fig 5.8 D). The differential E-cadherin distribution in mandibular, hyoid and branchial arches suggests that different CNC subpopulations express E-cadherin in a heterogeneous manner.

5.2.2   E-cadherin expressing CNC cells could contribute to otic vesicle formation

It is generally accepted that the middle ear ossicles are CNC derivatives, and the branchial stream of CNC also contributes to the otic capsule formation, which surrounds and protects the inner ear (Gross and Hanken, 2008). Interestingly, it has also been shown in mice that the CNC contribute directly to the otic vesicle, which eventually forms the inner ear (Freyer et al., 2011).

Among the cryosections that are immunofluorescence stained for E-cadherin, it is observed that some populations of H2B GFP positive CNC cells arrange in a radial fashion, which probably corresponds to the invaginated otic vesicle at stage 27 (Fig 5.11 A-D).
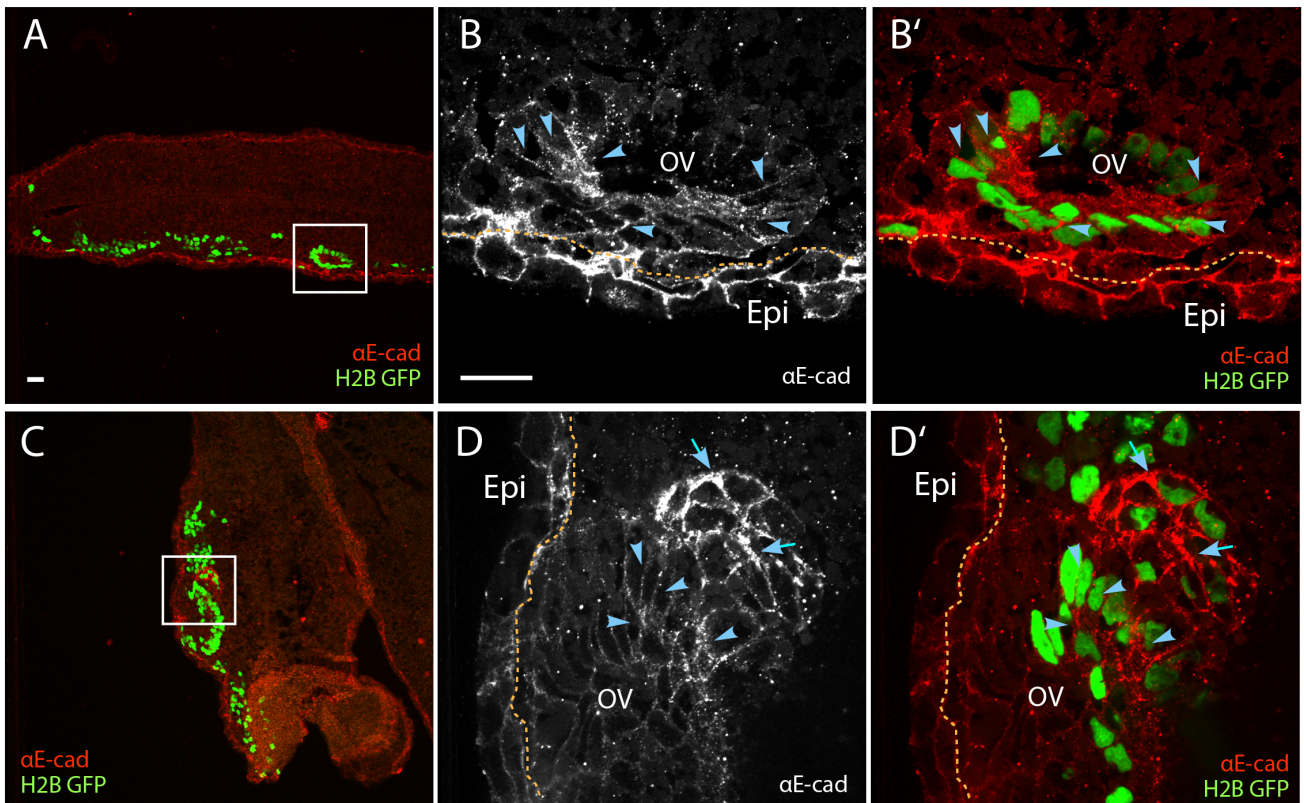
Fig5.11 E-cadherin expressing CNC cells contribute to the otic vesicle. Immunofluorescence staining against E-cadherin is performed on cryosections of whole embryos. **(A, C)** Transplanted whole embryo section shows H2B GFP labelled otic vesicle. **(B, B')** Cropped image of (A) shows E-cadherin staining of CNC cells located within the otic vesicle. (**D, D'**) Cropped image of (C) shows E-cadherin positive CNC located adjacent to the otic vesicle. Dashed orange lines indicate the boundaries of the epithelia (Epi). Arrow shows E-cadherin positive CNC cells outside the otic vesicle. Arrowhead shows staining of E-cadherin in the otic vesicle. OV: otic vesicle. α-E-cad: anti-E-cadherin antibody (5D3), H2B GFP: CNC injected with H2B GFP mRNA. Scale bar = 20 μm.

The otic vesicle is identifiable at this stage in sections as closed structure and has become detached from the epidermis (Fig 5.11 A, C). E-cadherin positive CNC population is observed to localize within the otic vesicle, indicating E-cadherin expressed CNC subpopulation could directly contribute to otic vesicle formation. Moreover, E-cadherin positive CNC cells are also found in close proximity but outside the otic vesicle structure (Fig 5.11 C, D arrows). This cell population could correspond to the sensory ganglion, which are located adjacent to the otic vesicle at this stage embryo (Quick and Serano, 2005).

5.2.3 E-cadherin protein is present in CNC throughout migration

To further verify the expression of E-cadherin during CNC migration on the protein level, immunoblotting for E-cadherin is performed with CNC explants. CNC explants are dissected from wild type embryos at stage 17, 20 and 23 respectively and the extracted proteins are enriched by ConA precipitation. Immunodetection is carried out with the E-cadherin specific antibody (5D3) (Choi and Gumbiner, 1989), whereas α-Tubulin is served as loading control. Protein samples applied for immunoblotting correspond to about 250 CNC explants for each stage. Endogenous E-cadherin is detected at estimated size (130 kDa) in CNC explants at stage 17, 20 and 23 (Fig 5.12).
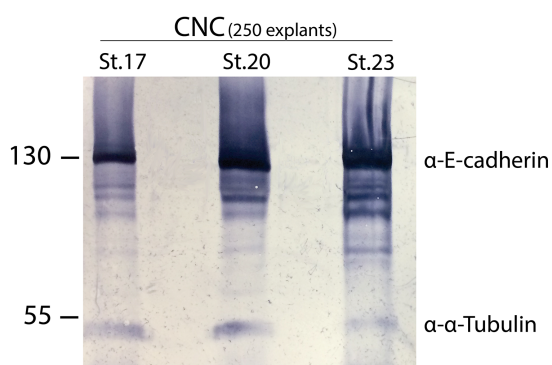
Fig5.12 Immunoblotting of endogenous E-cadherin expression in CNC explants. 250 CNC explants are dissected from wild type *Xenopus* embryos at indicated stages and cell lysates are prepared. Concanavalin A beads are used for enrichment of the protein samples and immunodetection is performed using E-cadherin antibody (5D3). Endogenous E-cadherin is detected in CNC explants in stage 17, 20 and 23. Immunodetection against α-Tubulin is served as loading control. PageRuler prestained protein ladder is used as marker.

5.2.4 Knockdown of E-cadherin blocks CNC migration *in vivo*

As E-cadherin is expressed throughout CNC migration, it is intriguing to investigate whether E-cadherin plays a role in mediating CNC migration. To examine this, loss-of-function analyses are conducted using an antisense morpholino oligonucleotide against E-cadherin (E-cad MO). Injections are performed in the dorsal animal blastomere D1.2 of 16-cell stage embryos (arrow in Fig 5.13 A) to target specifically the CNC tissue.
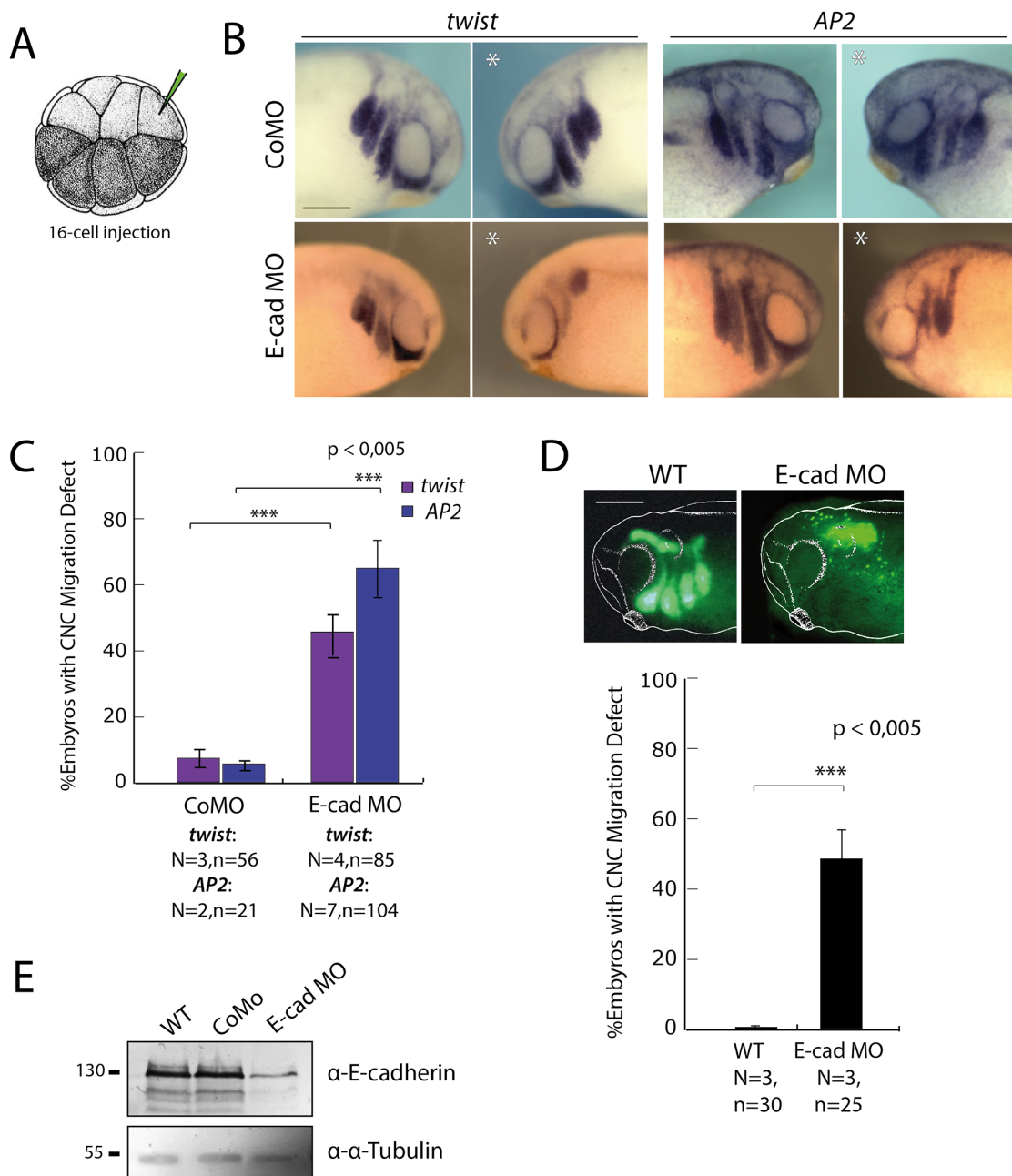
Fig5.13 E-cadherin knockdown blocks CNC migration *in vivo*. (A) Knockdown experiment is performed by injecting morpholino oligonucleotide against E-cadherin (E-cad MO) in the animal dorsal blastomere D1.2 in 16-cell stage embryos. **(B, C)** *In situ* hybridization for the CNC marker *twist* and *AP2* demonstrates migration defect caused by E-cadherin knockdown. Statistic of the *in situ* hybridization is shown in **(C)**. Bars indicate average percentage of embryos with CNC migration defect with standard deviations. * indicates the injected site. **(D)** Transplantation experiments of E-cadherin knockdown CNC cells into wild type host embryo. E-cad depleted CNC cells are unable to migrate ventrally into the pharyngeal pouches. **(E)** Efficiency test of E-cad MO by immunoblotting. Endogenous E-cadherin expression is significantly reduced in E-cad MO injected embryos, but not in wild type embryos or embryos injected with control morpholino (CoMO). PageRuler prestained protein ladder is used as marker. Significance in C and D is calculated by one-tailed test (Wissenschaftliche Arbeit, V. Knotz, 2013). Scale bar in B and D = 200 µm

8 ng E-cad MO is injected together with Dextran-FITC as lineage tracer. As control, a standard control morpholino oligonucleotide (CoMO) is used (Gene Tools and Phalanx Biotech Group). The MO injected embryos are cultured until stage 25 and sorted according to the injected site. *In situ* hybridization with the CNC marker *twist* and *AP2* as probe are carried out on fixed embryos. As shown in Fig 5.12 B, the injection of E-cad MO blocks significantly CNC migration *in vivo*. 46% (N=4, n=85) of the E-cad MO injected embryos exhibit migration defect shown by *twist* (Fig 5.13 C)*,* where the mandibular stream of CNC is able to migrate ventrally, but not the hyoid and branchial streams (Fig 5.13 B). Staining with *AP2* displays 66% (N=7, n=104) of the embryos with migration defect (Fig 5.13 C)*,* where the mandibular, hyoid, and branchial streams are partially fused and can only be observed in dorsal region of the embryo (Fig 5.13 B). Similarly, grafted E-cadherin knockdown CNC cells are unable to migrate into the pharyngeal pouches (Fig 5.13 D) in wild type host embryo.

The specificity of the E-cad MO is confirmed by immunoblotting. The E-cad MO and CoMO are injected in both blastomeres of a two-cell stage embryo. Embryos are lysed at stage 11 and proteins are extracted. Immunodetection is carried out against endogenous E-cadherin, using the E-cadherin antibody 5D3. Both, untreated wild type embryos and CoMO injected embryos display endogenous E-cadherin expression, whereas the E-cad MO injected embryos show significantly reduced E-cadherin expression (Fig 5.13 E).

CNC cells migrate ventrally to colonize the arches and contribute to the formation of facial skeletal structures and cartilages (Sadaghiani and Thiébaud, 1987). To evaluate the involvement of E-cadherin in regard to cartilage formation, E-cad MO is injected as described above in 16-cell stage embryos. Injected embryos are cultivated up to stage 47 and stained with Alcian Blue solution, which stains the cartilages. As control, CoMO is injected and the embryos are treated in the same manner as E-cad MO morphants.

The CNC cells of the mandibular arch give rise to the Merkel's cartilage (M) and the palatoquadrate cartilages (Q) that constitute the lower and upper jaw elements, respectively (Cerny et al., 2004; Lee et al., 2004). The CNC cells of the hyoid arch generate skeletal structures such as the stapes in the middle ear or structures involved in respiration and providing support for the tongue, for example the ceratohyal cartilage (C), and the branchial arches give rise to skeletal support for grills or throat structures (Fig 5.14 A) (Baltzinger et al., 2005). Injection of the E-cad MO results in a branchial arch phenotype, in that the E-cad MO injected side of the embryo displays size reduction of the grill cartilage (G). The formation of Merkel's and

palatoquadrate cartilage as well as the ceratohyal cartilage appears to be normal (Fig 5.14 B). No difference is observed on the CoMO injected side of the embryo.
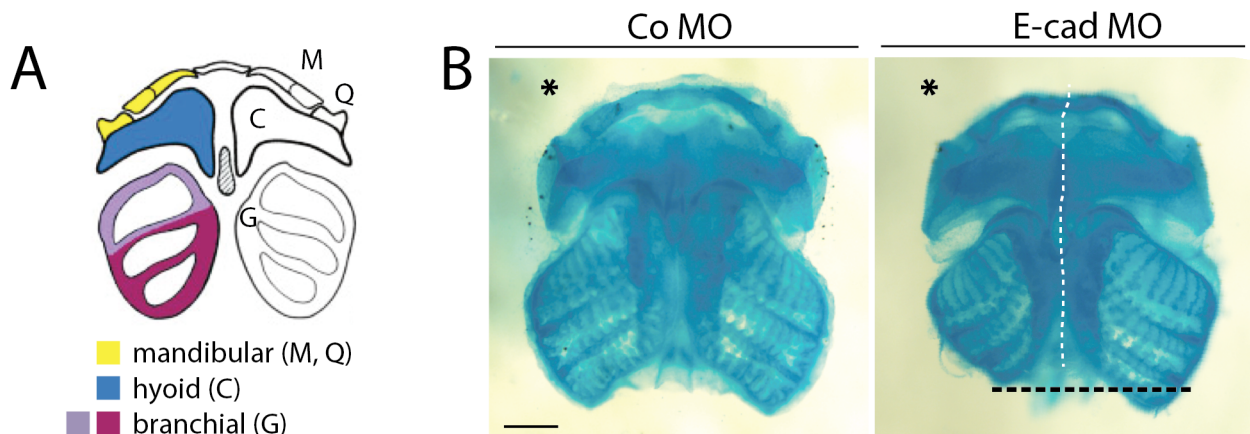
Fig5.14 E-cadherin knockdown leads to branchial specific cartilage defect. (A) Scheme of the *Xenopus* cartilage structure at stage 47 (ventral view), adopted from Baltzinger et al., 2005. M: Merkel's cartilage; Q: Palatoquadrate cartilage; C: Ceratohyal cartilage; G: Grill cartilage **(B)** Cartilage staining of CoMO and E-cad MO injected embryo at stage 47. Ventral view of the embryos are shown with * indicating the injected site. E-cad MO injected side of the embryo shows reduced branchial arch specific cartilage. White dashed line shows the middle line of the cartilage. Black dashed line indicates the reduced grill cartilage on E-cad Mo injected side. Scale bar = 350 μm.

5.2.5 E-cad MO caused CNC migration defects can be rescued by co-injection of an E-cadherin full-length rescue construct

To further demonstrate the specificity of E-cad MO causing the CNC migration defect, rescue experiments are carried out with an E-cadherin rescue construct where the MO binding site is mutated. The sequences of the MO binding sites from unmutated full length E-cadherin with a HA-tag (E-cadfl-HA), the mutated rescue construct E-cadherin-HA (E-cadMu-HA) and the E-cad MO are shown in Fig 5.15 A. The expression of E-cadMu-HA construct is examined by immunoblotting against the HA-tag. 500 pg mRNA of E-cadfl-HA is injected alone or together with 8 ng E-cad MO in both blastomeres of a two-cell stage embryo. mRNA of E-cadMu-HA is co-injected with E-cad MO in the same manner. Embryos are lysed at stage 11 and immunodetected for the HA-tag (Fig 5.15 B). The E-cadfl-HA is expressed at the estimated size (130kDa) and co-injection with E-cad MO diminishes the expression of E-cadfl-HA, since the translation of E-cadfl-HA is inhibited upon MO binding. However, the expression of the mutated rescue construct E-cadMu-HA is not affected by the co-injected E-cad MO. The E-cadMu-HA

construct (later as E-cadMu) is therefore used as full-length rescue construct for the following reconstitution experiments.

A

5'-CC ATG GGG TTG AAG AGG CCC TGG TT-3'   E-cadfl-HA
5'-CT ATG GGC CTC AAA CGA CCT TGG TT-3'   E-cadMu-HA
5'-AAC CAG GGC CTC TTC AAC CCC ATT G-3'   E-cad MO
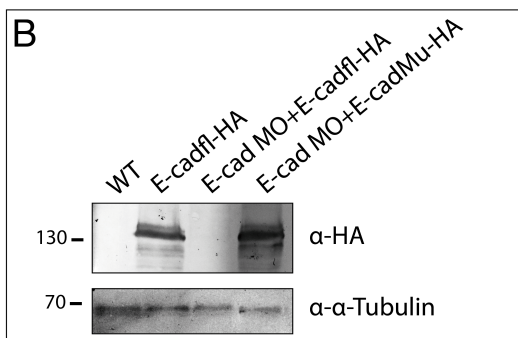
Fig5.15 Rescue construct of E-cadherin is expressed in the embryo and does not bind the E-cadherin morpholino. (A) The MO binding site sequence of the unmutated full length E-cadherin with a HA-tag (E-cadfl-HA), the MO binding site mutated E-cadherin rescue construct (E-cadMu-HA) and the E-cadherin morpholino (E-cad MO) is shown. Mutated nucleotides are indicated in red. **(B)** Expression of the E-cadherin rescue construct (E-cadMu) in embryos. Embryos are injected with mRNA of E-cadfl-HA, E-cadfl-HA along with E-cad MO and E-cadMu-HA along with E-cad MO, respectively. Immunodetection is performed on cell lysates against the HA-tag and α-Tubulin. WT: uninjected wild type embryos. Anti-α-Tubulin is served as loading control. PageRuler prestained protein ladder is used as marker.

First, different concentrations of the E-cadMu mRNA are co-injected with 8 ng E-cad MO in the dorsal animal blastomere in 16-cell stage embryos to titrate the rescue ability of this construct. Migration of CNC cells is analysed by *in situ* hybridization with *twist* on injected embryos at stage 25 (Fig 5.16 A).
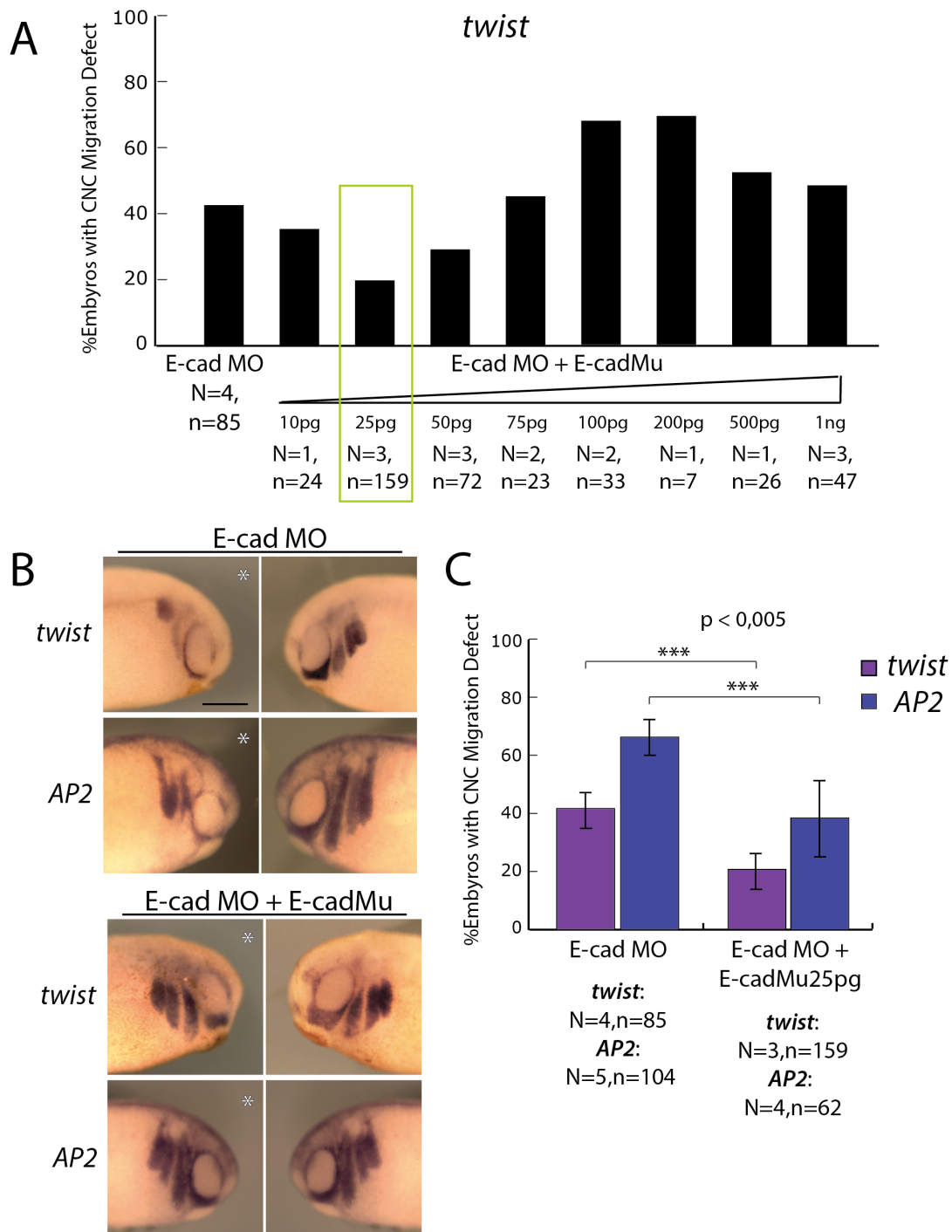
Fig5.16 Rescue experiments with the full-length E-cadherin rescue construct (E-cadMu). (A) Titration experiments for the effective dose of co-injected E-cadMu mRNA. Injection of E-cadMO as well as co-injection of E-cadMO and different concentrations of E-cadMu is carried out at 16-cell stage. Injected embryos are raised up until stage 25 and fixed for *in situ* hybridisation. *twist* is used as *in situ* probe and the bars indicate average percentage of embryos with CNC migration defect. * indicates the injected site. **(B, C)** Rescue experiments with 25 pg of E-cadMu mRNA are repeated and analysed by *in situ* hybridisation using both *twist* and *AP2* as probe. At least three independent experiments are performed and the average percentage is shown with standard deviations. Significance is calculated by one-tailed test (Wissenschaftliche Arbeit, V. Knotz, 2013). Scale bar = 200 μm.

As shown in Fig 5.16 A, of all mRNA concentration tested in the assay (concentration range from 10 pg to 1 ng), the best rescue effect is obtained with 25 pg of E-cadMu mRNA co-injected with 8 ng E-cad MO, which reduces the E-cad MO phenotype from 41% (N=4 n=85) CNC migration defect to 21% (N=3, n=159) (Fig 5.16 A, B).

Rescue experiments with 25 pg mRNA of E-cadMu are repeated following *in situ* hybridization using additionally the CNC marker *AP2* as probe. Co-injection of 25 pg E-cadMu mRNA along with E-cad MO restores the signal of *AP2* in mandibular, hyoid and branchial crest streams further in ventral region of the embryo (Fig 5.16 B), showing correct migration of CNC cells. And the frequency of phenotype is significantly reduced from 66% to 38% (N=4, n=62) (Fig 5.16 C). These results suggest that a rescue of the E-cadherin knockdown phenotype can be achieved by co-injecting of full-length E-cadherin rescue construct mRNA in a dose dependent manner. Notably, the observed rescue is a partial rescue of about 50% of the phenotype, which is statistically significant.

5.2.6   E-cadherin knockdown CNC cells fail to form cell protrusions *in vitro*

When CNC explants are dissected and plated on a fibronectin coated surface, wild type CNC cells adhere to the substrate surface and form cell protrusions in forms of filopodia and lamellipodia. Since the E-cadherin knockdown inhibit the migration of CNC cells *in vivo*, it is interesting to examine whether the cell morphology is influenced by the depletion of E-cadherin.

Therefore, *Xenopus* embryos are injected with 8 ng of E-cad MO in the dorsal animal D1.2 blastomere at 16-cell stage. 500 pg of each membrane bound cherry (mbcherry) and H2B GFP mRNAs are co-injected to visualize the cell membrane and nucleus, respectively. CNC cells are explanted at stage 17 and cultured on fibronectin for one hour. Cell morphology is then analysed by the spinning disk microscope.

Compared to wild type CNC or CoMO treated CNC cells, E-cadherin depleted cells generally do not survive well *in vitro*, as the cells at the edge of the explant dissociate and die within a few hours after dissection (Fig 5.17 B arrows), whereas wild type CNC or CoMO injected CNC cells have stable contacts towards other cells and stay as cell cluster for several hours. Moreover, E-cad depleted CNC cells display a more rounded morphology with significantly less protrusion formation (Fig 5.17 B arrowheads) compared to CoMO treated cells (Fig 5.17 A). Cell blebbings are additionally observed among E-cadherin knockdown cells (Movie1).
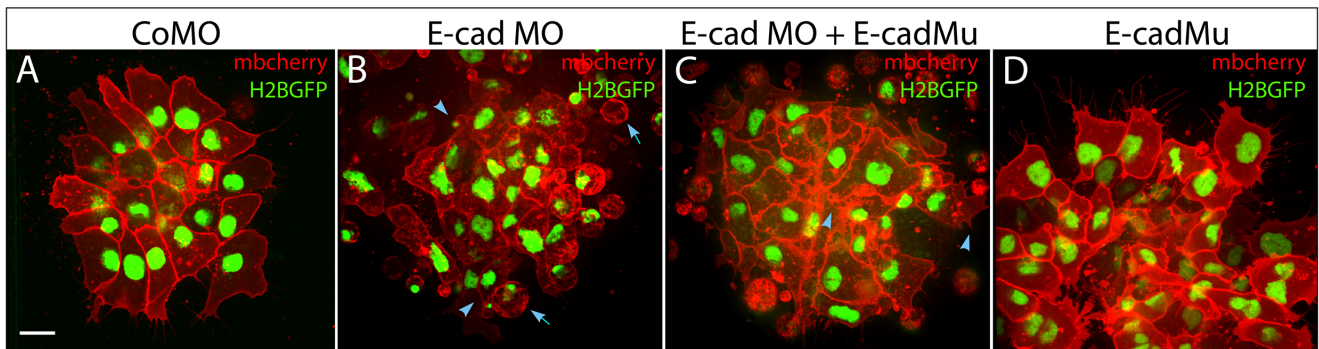
Fig5.17 E-cadherin knockdown alter protrusion formation in CNC cells *in vitro*. Embryos are injected with indicated constructs and the corresponding CNC explants are shown. **(A)** Injection of CoMO has no influence on CNC cell morphology. **(B)** E-cad knockdown CNC cells fail to form stable protrusions and show cell blebbing (arrow). Dead cells are often observed (arrows). **(C)** Protrusion formation (arrowhead) is restored by co-injecting 25 pg E-cadherin rescue construct (E-cadMu). **(D)** CNC cells injected with E-cadherin rescue construct (E-cadMu) alone display normal cell morphology. All constructs are injected at 16-cell stage along with membrane cherry (mbcherry) and H2B GFP mRNA as lineage tracer. Scale bar = 20 μm.

To test whether the change in cell morphology is specifically caused by the E-cadherin knockdown, the rescue experiment is conducted by co-injection of the full-length E-cadherin rescue construct (E-cadMu). Embryos are injected with 8 ng E-cad MO along with 25 pg E-cadMu mRNA, which is the same dose used in CNC migration rescue experiment *in vivo*. Compared to E-cadherin depleted cells (Fig 5.17 B), co-injection of E-cadMu rescued cell protrusion formation (Fig 5.17 C arrowheads, Movie 2). Expression of E-cadMu alone does not change the cell morphology (Fig 5.17 D).

5.2.7   The extracellular domain of E-cadherin is important for CNC migration *in vivo*

To identify which domain in the E-cadherin is necessary to mediate CNC migration, the rescue ability of different E-cadherin deletion mutants are tested. The extracellular domains (EC) of cadherins are important for the adhesive function of E-cadherin. A conserved tryptophan residue, Tryptophan (Trp2), forms a side chain that docks into a hydrophobic pocket in the partner EC1 domain (Harrison et al., 2011). The hydrophobic pocket is formed by a conserved His-Ala-Val (HAV) motif (Harrison et al., 2011). Compared to the full-length E-cadherin rescue construct (E-cadMu), a dominant negative form of E-cadherin rescue construct (DN E-cadMu) inhibits the homophilic binding of cadherins, by mutating both Trp2 and HAV motif in the EC1 domain. Therefore in DN E-cadMu, the Trp2 is replaced with alanine and the alanine residue in the HAV motif is replaced with methionine (Fig 5.18 B). To block the intracellular function of E-cadherin, a

cytoplasmic domain depleted form of E-cadherin (Ecad ΔC) is generated, by removing the juxtamembrane domain and the catenin-binding domain in E-cadherin (Fig 5.18 B).
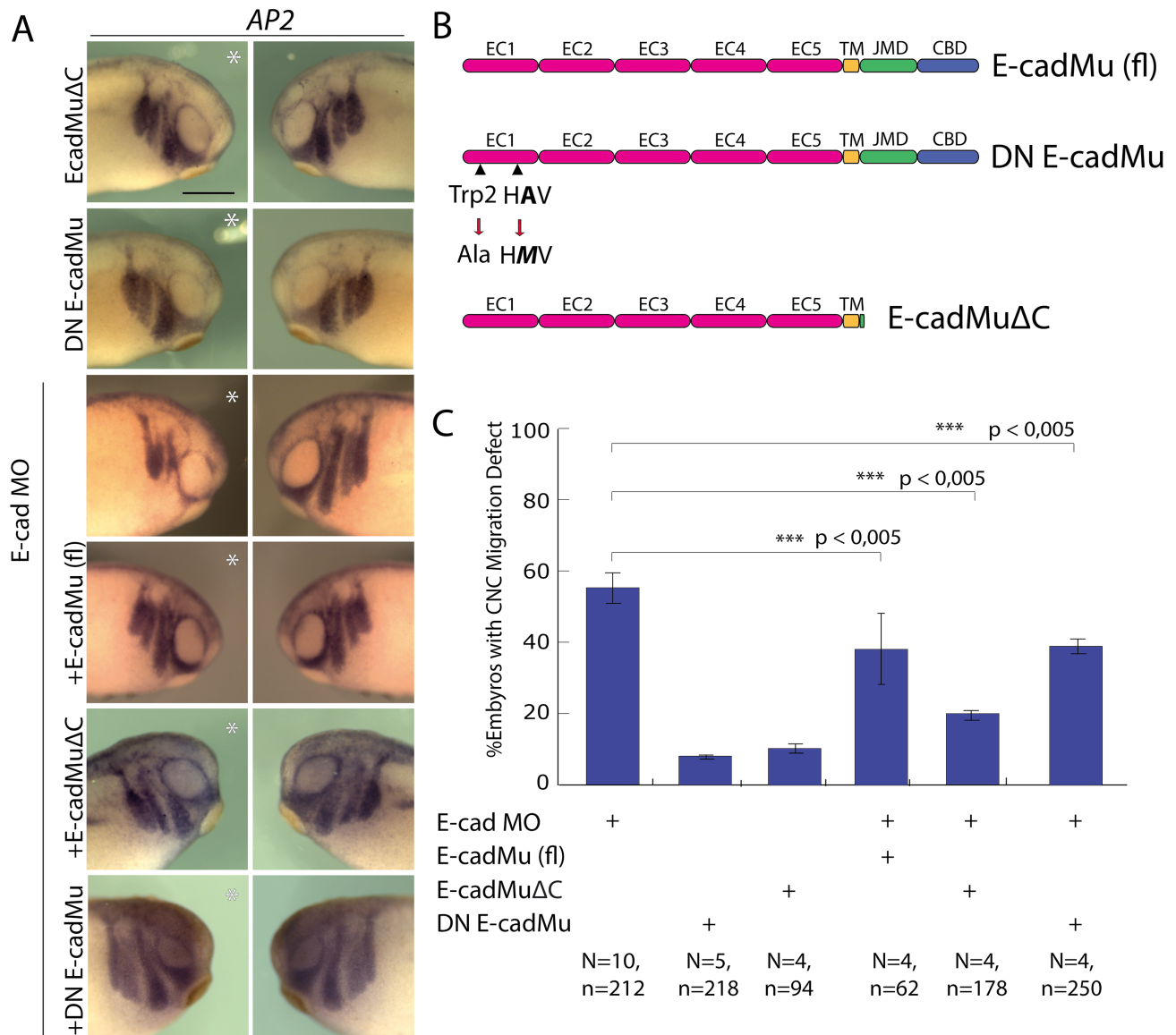
Fig5.18 The extracellular domain of E-cadherin can best reconstitute CNC migration *in vivo*.

(A) *In situ* hybridization with *AP2* as probe. Embryos are injected with indicated constructs and fixed at stage 25. Statistic of the *in situ* hybridisation is shown in **(C)**, bars indicate the percentage of embryos with migration defect. At least three independent experiments are performed and the average percentage is shown with standard deviations. * indicates the injected site. **(B)** Structures of E-cadMu (fl), DN E-cadMu and E-cadMuΔC. The Trp2 in EC1 domain is mutated to alanine, and the alanine in the HAV motif is replaced with methionine. The juxtamembrane domain and catenin-binding domain of E-cadMu is deleted in E-cadMuΔC. Significance is calculated by one-tailed test (Wissenschaftliche Arbeit, V. Knotz, 2013). Scale bar = 200 μm.

E-cad MO and E-cadherin mutants are injected in the animal dorsal blasotomere in 16-cell stage embryos. CNC migration is then investigated on injected embryos at stage 25 by *in situ* hybridisations using *AP2* as probe. Co-injection of 25 pg DN E-cadMu mRNA with 8 ng E-cad MO is able to restore the migration of three CNC streams (Fig 5.18 A) and decrease the ratio of embryos with CNC migration defect from 57% to 39% (N=4,n=250), similar to the rescue effect obtained by E-cadMu (fl) (Fig 5.18 A, C).

Surprisingly, co-injection of 25 pg E-cadMuΔC mRNA restores CNC migration even better as the percentage of embryos with migration defect decreases to only 20% (Fig 5.18 A, C). Additionally, when injected alone, neither DN E-cadMu nor E-cadMuΔC has influence on CNC migration (Fig 5.18 A, C). Taken together, these results suggest that both E-cadherin mutants are able to rescue the E-cad MO phenotype and an E-cadherin with functional EC1 domain, but lacks the cytoplasmic domain achieves the best rescue effect for reconstitution CNC migration in E-cadherin morphants.

5.2.8 Extracellular domain of E-cadherin is sufficient to rescue cell protrusion formation *in vitro*

Since the cytoplasmic domain deleted E-cadherin construct (E-cadMuΔC) rescues CNC migration *in vivo*, the question raises whether cell protrusion formation can also be rescued *in vitro*. Therefore, embryos are injected with 8 ng E-cad MO along with either 25 pg DN E-cadMu or E-cadMuΔC mRNA at 16-cell stage. Injection of E-cad MO alone serves as control (Fig 5.19 A).
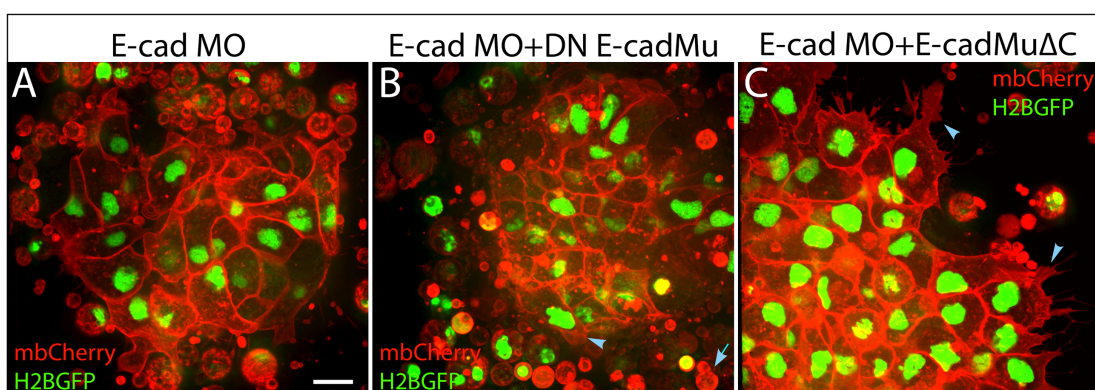
Fig5.19 E-cadMuΔC restores protrusion formation in CNC cells *in vitro*. Embryos are injected with indicated constructs and the corresponding CNC explants are shown. (B) Cells injected with DN E-cadMu and E-cad MO fail to form proper protrusion and show cell blebbing (arrowhead). Also, cells do not survival well and dead cells are often observed (arrow). (C) Co-injection of E-cadMuΔC rescues protrusion formation. DN E-

cadMu and E-cadMuΔC are injected as 25 pg mRNA. All constructs are injected at 16-cell stage along with membrane cherry (mbcherry) and H2B GFP mRNA as lineage tracer. Scale bar = 20 µm

CNC cells from DN E-cadMu co-injected embryos display cell blebbing and less protrusion formation (Fig 5.19 B, Movie 3). On the contrary, co-expressing E-cadMuΔC restores largely the protrusion formation of CNC cells (Fig 5.19 C Movie 4). This result indicates that the cytoplasmic domain of E-cadherin is expendable for cell protrusion formation, and a functional extracellular domain is required for CNC cells to maintain normal cell morphology *in vitro*.

5.2.9   E-cadherin knockdown do not disturb early CNC specification

Until now, it is shown that E-cadherin is involved in CNC migration. To confirm that the CNC cells are indeed properly formed at premigratory stage, and that the migration defects are not due to disturbed CNC specification, the expression of several neural crest specifier genes are analyzed in E-cadherin knockdown embryos. *C-myc* is one of the earliest neural crest specifier in *Xenopus*, which is expressed first in a broad domain at the neural plate border and later becomes restricted to newly formed neural crest cells (Bellmeyer et al., 2003). Another neural crest specifier is *AP2,* which is strongly expressed during neural crest formation (de Crozé et al., 2011). Additionally, *twist* serves as a neural crest specifier active at premigratory stage of CNC (Prasad et al., 2012).
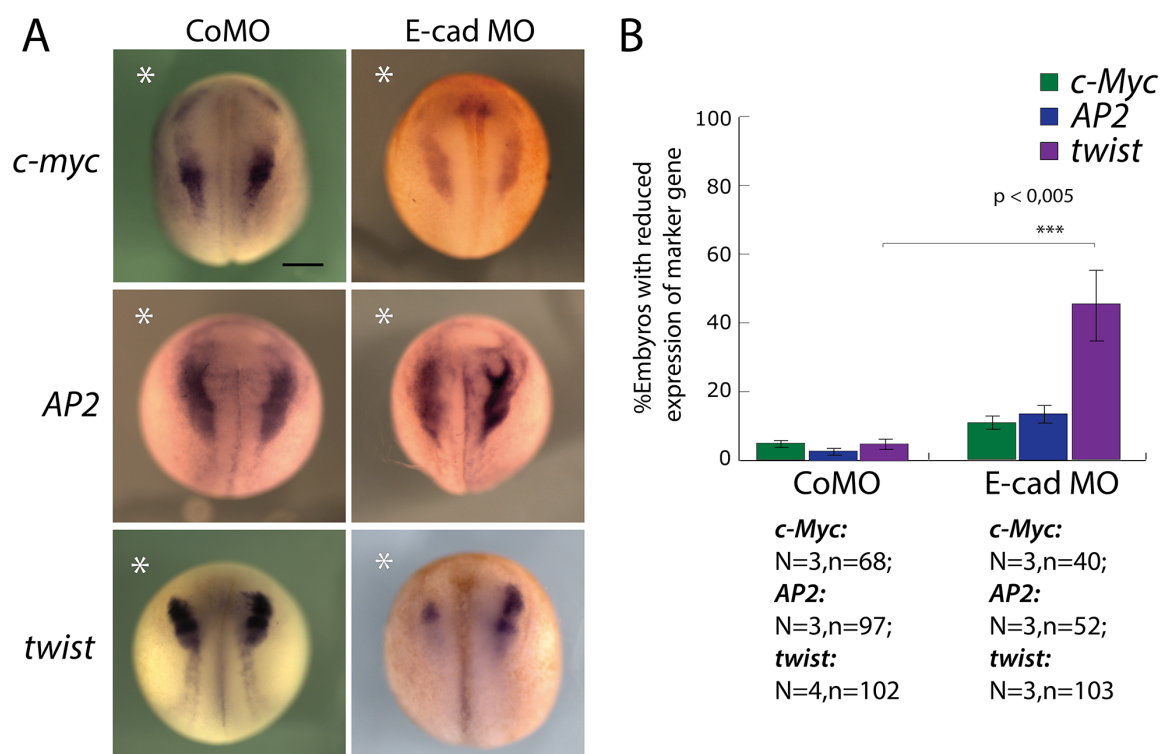
Fig5.20 The early specification of E-cadherin knockdown CNC cells at premigratory stage is not impaired. (A) Embryos are injected with 8 ng E-cad MO at 16-cell stage. Injected embryos are fixed at stage 17 and *in situ* hybridisation is performed using *c-myc*, *AP2* and *twist* as probe. * indicates the injected site. **(B)** Bars indicate the percentage of embryos with reduced expression of marker gene. At least three independent experiments are performed and the average percentage is shown with standard deviations. Scale bar = 100 µm. Significance is calculated by one-tailed test (Wissenschaftliche Arbeit, V. Knotz, 2013).

To assess the expression of these genes, 8 ng E-cad MO is injected in the same manner as described above at 16-cell stage and the embryos are raised up until stage 17. *In situ* hybridization is performed using *c-myc*, *AP2* and *twist* as probe, respectively. Embryos injected with CoMO are served as control. As shown in Fig 5.20, the expression of *c-myc* and *AP2* is not influenced by the injection of E-cad MO. Interestingly, *twist* expression is significantly reduced in 45% (N=3, n=103) of E-cad MO injected embryos. These results suggest that upon E-cadherin knockdown, the CNC cells are formed at premigratory stage, since the expression of *c-myc* and *AP2* are not impaired. However, the *twist* expressing CNC population is disturbed.

5.2.10   N-cadherin and E-cadherin have distinct functions in CNC migration

The role for N-cadherin during CNC migration has been shown by *in vivo* and *in vitro* studies and both overexpression and MO knockdown of N-cadherin block CNC migration (Theveneau et al., 2010). Considering the overlap of their expressions during CNC migration and the inhibitive effect on CNC migration, there is likely to be a functional redundancy between N-cadherin and E-cadherin in mediating CNC cell migration, which would have also explained the relative weak phenotype in loss of function experiment when a single gene is targeted. To test whether an additive effect by simultaneously knockdown of both E-cadherin and N-cadherin can be observed, different combinations of N-cadherin MO (N-cad MO) and E-cad MO is co-injected in embryo (Fig 5.21 B).
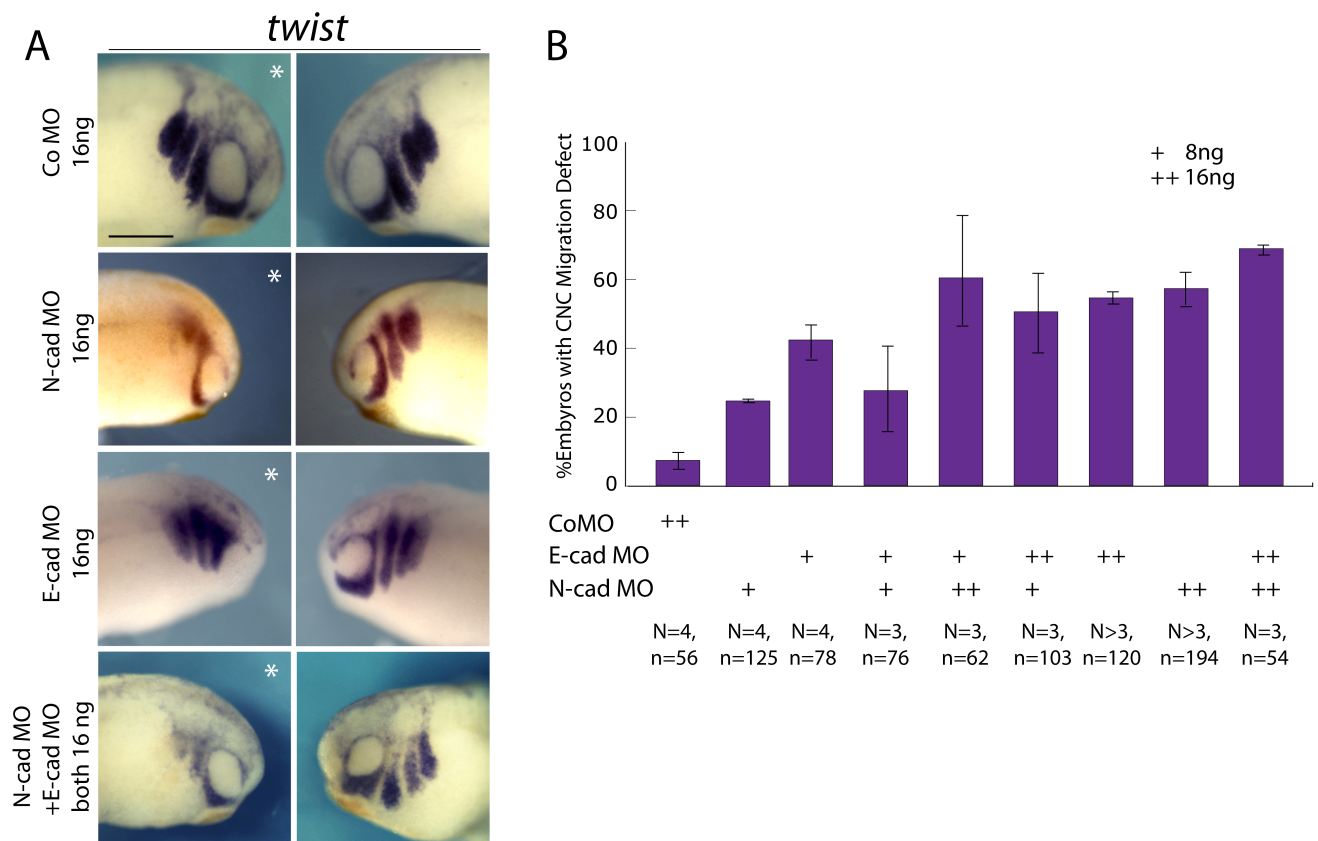
Fig5.21 Double knockdown of E-cadherin and N-cadherin does not achieve an additive effect in regard to loss of CNC migration. (A) MOs are injected in the dorsal animal blasotomere in 16-cell stage embryos. Embryos are fixed at stage 25 and *in situ* hybridisation is performed using *twist* as probe. * indicates the injected site. **(B)** "+" symbolizes for 8 ng morpholino injection and "++" symbolizes for 16 ng morpholino injection. Bars indicate the percentages of embryos with CNC migration defect. At least three independent experiments are performed and the average percentage is shown with standard deviations. Significance is calculated by one-tailed test (Wissenschaftliche Arbeit, V. Knotz, 2013). Scale bar = 200 µm.

As expected, embryos injected with double amount of MO exhibit more severe migration defect compared to 8 ng (E-cad MO shown in Fig 5.13, N-cad MO not shown). By increasing E-cad MO dose from 8 ng to 16 ng, the ratio of embryos with CNC migration defect rises from 43% (N=4, n=78) to 55% (N=7, n=120) (Fig 5.21 B). A similar result is observed by doubling the doses for N-cad MO, which increases the number of embryos with migration defect from 24% (N=4, n=125) to 57% (N=6, n=194) (Fig 5.21 B). This indicates that the severity and frequency of the phenotypes is dose dependent. However, when either of E-cad MO or N-cad MO is given additionally to the full dose (16 ng) of the other morpholino, the frequency of the phenotype changes lightly. For example, embryos injected with 8 ng E-cad MO and 16 ng N-cad MO display 61% (N=3, n=62) migration defect, comparable to 57% (N=6, n=194) from 16 ng N-cad MO alone (Fig 5.21 B). Similarly, injection of 8 ng N-cad MO additional to the 16 ng E-cad MO results

in 51% (N=3, n=103) migration defect compared to 55% (N=7, n=120) by 16 ng E-cad MO alone (Fig 5.21 B). Injecting 16 ng of both morpholinos increases the migration defect phenotype to 69% (N=3, n=54), which is only slightly higher than other MO combinations. Co-injection of both morpholinos do not lead to additive effects in the phenotype of disturbed CNC migration pointing to independent function of both cadherins.

On the cellular level, it is described in (Theveneau et al., 2010) that the CNC cells injected with N-cad MO are more motile and disperse more rapidly than control cells *in vitro*. In this work, it is observed that the N-cadherin knockdown CNC cells display mostly normal cell protrusion formation (Fig 5.22 C).
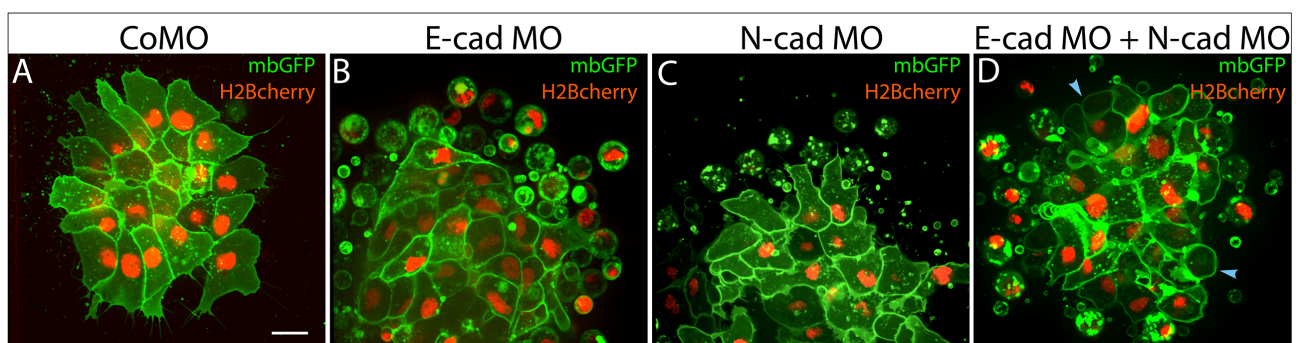
Fig5.22 CNC cells treated with both E-cadherin and N-cadherin morpholino display E-cadherin knockdown phenotype *in vitro*. (A) Control morpholino and **(B)** E-cadherin morpholino alone are injected for comparison. **(C)** N-cadherin MO injected cells exhibit normal cell protrusion formation. **(D)** Double knockdown for both E-cadherin and N-cadherin display an E-cadherin knockdown phenotype with less protrusions and cell blebbing (arrowheads). All morpholinos are injected in 16-cell stage embryos and explanted at stage 17. Membrane cherry (mbcherry) and H2B GFP mRNA are co-injected as lineage tracer. Scale bar = 20 µm

However, when E-cad MO is co-injected, the cells appear more like E-cadherin knockdown phenotype with cell blebbing and lack of cell protrusion formation (Fig 5.22 D). Taken these results together, E-cadherin and N-cadherin seems to have distinct function in mediating CNC cell migration.

5.2.11 CNC migration defect caused by E-cadherin knockdown cannot be rescued by other cadherins

To test whether E-cadherin has a unique function in CNC migration, substitution experiments are performed with XB-cadherin, Cadherin-11 and N-cadherin. Accordingly, 25 pg of XB-cadherin,

Cadherin-11 and N-cadherin mRNA is co-injected with 8 ng of E-cad MO in 16-cell stage embryos, respectively.
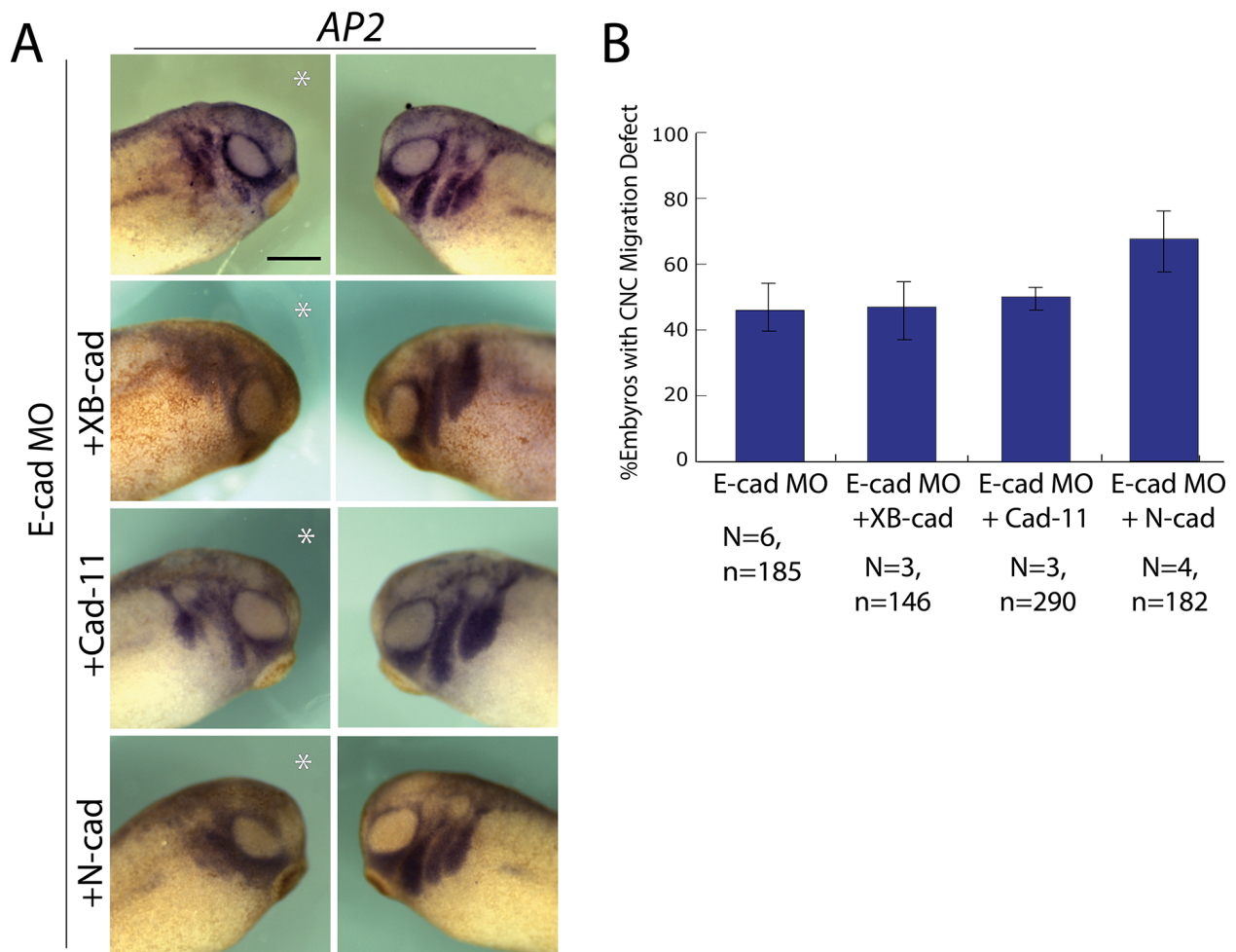
Fig5.23 E-cadherin knockdown resulted CNC migration defects cannot be rescued by overexpression of other classical cadherins. (A) 8 ng E-cad MO are injected with 25 pg of XB-cadherin, Cadherin-11 and N-cadherin mRNA respectively at 16-cell stage. Injected embryos are fixed at stage 25 and *in situ* hybridisation is performed using *AP2* as probe. * indicates the injected site. **(B)** Bars indicate the percentage of embryos with CNC migration defect. At least three independent experiments are performed and the average percentage is shown with standard deviations. Significance is calculated by one-tailed test (Wissenschaftliche Arbeit, V. Knotz, 2013). Scale bar = 200 µm.

As shown in Fig 5.23, the impaired invasion of the pharyngeal pouches caused by injection of E-cad MO (45%, N=6, n=185) can neither be rescued by co-injection of the the classical type I XB-cadherin (46%, N=3,n=146) and N-cadherin (67%, N=4, n=182) nor by the classical type II Cadherin-11 (50%, N=3, n=290), as demonstrated by whole mount *in situ* hybridizations with the

CNC marker *AP2*. Importantly, co-injection of N-cadherin results in a more severe effect underlying the distinct role of E-cadherin and N-cadherin.

5.2.12 N-cadherin and Cadherin-11 show partially redundacy in mediating CNC migration *in vivo*

Since E-cadherin depletion is not rescued by other cadherins, the question arises whether this is a common phenomenon in CNC migration. Therefore the ability of N-cadherin and Cadherin-11 to replace each other is investigated. *In vivo*, CNC migration is inhibited by blocking either N-cadherin or Cadherin-11. 16 ng of Cadherin-11 morpholino (Cad11 MO) is injected in the dorsal animal blastomere D1.2 in 16-cell stage embryo, resulting in 95% (N=4, n=81) embryos with migration defect (Fig 5.24 A).
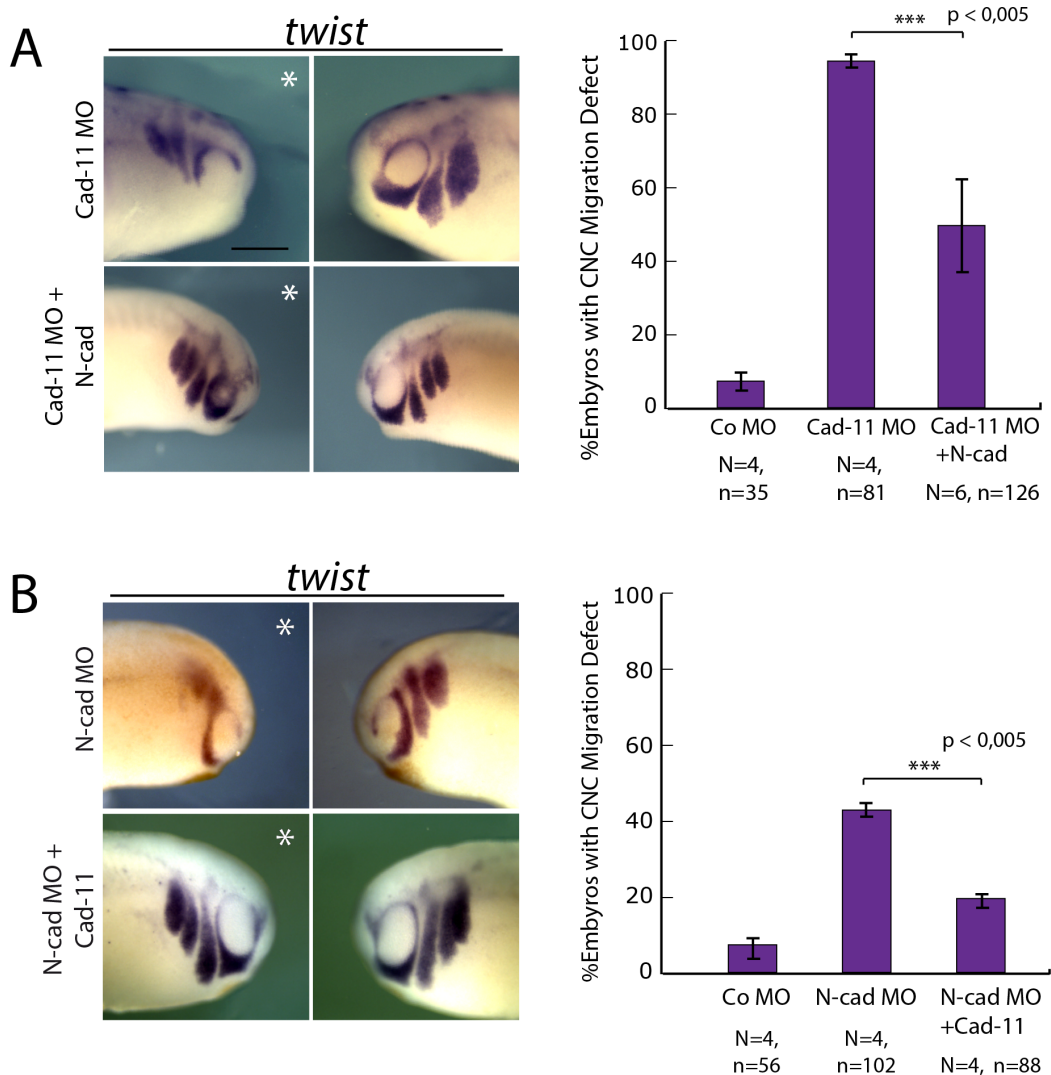
Fig5.24 N-cadherin and Cadherin-11 act redundant in mediating CNC migration *in vivo.* (A) *In situ* hybridisation of embryos injected with 200pg N-cadherin mRNA and Cadherin-11 morpholino (Cad-11 MO). Embryos that injected only with Cad-11 MO alone serve as control. **(B)** *In situ* hybridisation of embryos injected with 200 pg Cadherin-11 mRNA and N-cadherin morpholino (N-cad MO). Embryos with N-cad MO alone serve as control. Morpholinos and mRNAs are injected as indicated in 16-cell stage embryos. Embryos are fixed at stage 25 and *in situ* hybridisation is performed using *twist* as probe. * indicates the injected site. Bars indicate the percentages of embryos with CNC migration defect. At least three independent experiments are performed and the average percentage is shown with standard deviations. Significance is calculated by one-tailed test (Wissenschaftliche Arbeit, V. Knotz, 2013). Scale bar = 200 µm.

Surprisingly, co-injection of 200 pg N-cadherin mRNA with Cad 11 MO is able to decreases the ratio of embryos with migration defect to 49% (N=6, n=126) (Fig 5.24 A). Vice versa, when 200 pg of Cadherin-11 mRNA is co-injected with 16 ng of N-cad MO, the percentage of phenotype declines from 42% (N=4, n=102) to 20% (N=4,n=88) (Fig 5.24 B). This mutual rescue effect points to a partial redundant function of N-cadherin and Cadherin-11 in mediating CNC cell migration and underlines the uniqueness of E-cadherin function in CNC cells.

6   Discussion

6.1   E-cadherin, XB/C-cadherin and PAPC identified as new cadherin family members expressed in CNC cells

The expression of several cadherin subtypes are described in *Xenopus* CNC cells including N-cadherin, Cadherin-11 and PCNS (Hadeball et al., 1998; Rangarajan et al., 2006; Theveneau et al., 2010). N-cadherin is involved in CIL, implying its requirement during CNC cell migration (Theveneau et al., 2010). Cadherin-11 is known to be expressed strongly in CNC in later stages during CNC migration and depletion of Cadherin-11 inhibits the migration of CNC cells (Hadeball et al., 1998). PCNS shows a very prominent expression in CNC cells from premigratory until tailbud stages, revealed by *in situ* hybridization, and the inhibition of this molecule severely disrupts the migration of CNC cells (Rangarajan et al., 2006). However, which particular cadherin(s) promotes CNC migration during distinct phases of migration remains unclear. Also, a quantitative comparison of different cadherin subtypes, in regard to their changes in the expression level during CNC migration, as well as their transcripts abundance on the cellular level within CNC cells, has not been reported yet. In this work, CNC cells from three distinctive stages are analysed to demonstrate respectively their expression profile through the premigratory, emigrating and migrating state during CNC migration. Interestingly, RT-qPCR analyses not only confirmed the expression of the three cadherins mentioned above (N-cadherin, Cadherin-11 and PCNS) during CNC migration, also three other cadherin family members, namely E-cadherin, XB/C-cadherin and PAPC, are for the first time identified in *Xenopus* CNC cells.

Xenopus Cadherin-11 is a classical type II cadherin and so far the most investigated cadherin in regard to its function in CNC cell migration. The expression of Cadherin-11 in CNC cells has been described (Hadeball et al., 1998) and it is necessary for the protrusion activity of CNC cells (Kashef et al., 2009). Also, Cadherin-11 mediated cell-cell adhesion is required for CIL during CNC migration (Becker et al., 2013). In whole embryos, a basal maternal expression of Cadherin-11 is found before mid-blastula-transition (MBT), but zygotic transcription begins at mid-gastrulation. Its expression decreases afterwards but rises up again at stage 18, and reaches its maximum at the tailbud stage (Hadeball et al., 1998). Subsequently, *in situ* hybridization shows that CNC transcripts are localised in migrating CNC cells and in the entire lateral mesoderm in the truck region (Hadeball et al., 1998). In this work, RT-qPCR analyses

demonstrate the up-regulation of Cadherin-11 expression from stage 17 to stage 23 in whole embryos and in CNC cells. The expression of Cadhein-11 in whole embryos may correspond to its expression in the lateral mesoderm as revealed by *in situ* detection (Hadeball et al., 1998). RT-qPCR data in this work show that Cadherin-11 is present with very few transcripts at stage 17, suggesting that this mesenchymal cadherin plays a minor role in CNC delamination. This is further supported by loss-of-function experiments, where depletion of Cadherin-11 does not effect the delamination of CNC cells (Kashef et al., 2009). Compared with other cadherins, Cadherin-11 clearly shows the most dramatic change on its expression level during CNC migration, which is consist with its multiple roles in regulating CNC migration. Besides its requirement in protrusion formation, Cadherin-11 is also essential in cell-substrate adhesion, which is as well necessary for CNC to populate the pharyngeal pouches (Kashef et al., 2009); Langhe et al., in revision). Consistent with its localization in cell protrusions (Becker et al., 2012; Kashef et al., 2009), Cadherin-11 mediated CIL is not only a crucial mechanism involved in collective migration, but also important for single cell migration as well (Becker et al., 2013). Interestingly, a gene with such functional significance is expressed with very few transcripts in CNC cell, as showed by the RT-qPCR data in this work. This could suggest a unique role of Cadherin-11 in the migration process. Additionally, up-regulation of Cadherin-11 is also observed in tumour progression (Chu et al., 2008; Pishvaian et al., 1999) and cartilage invasion in inflammatory arthritis (Lee et al., 2007), indicating that besides its function of promoting cell migration during development, aberrant expression of Cadherin-11 also leads to increased invasiveness in tumour cells.

Xenopus N-cadherin is a classical type I cadherin and as a zygotic cadherin, its expression begins at neurula stage, associated with neural plate and neural tube formation (Detrick et al., 1990; Nandadasa et al., 2009). After neurula, N-cadherin is primary found in neural tissue but also in CNC cells (Theveneau et al., 2010). In this work, transcripts of N-cadherin are detected in premigratory and migratory CNC cells. Both knockdown and overexpression of N-cadherin inhibit CNC migration (Theveneau et al., 2010), indicating that balanced N-cadherin level is necessary for migration. The continuous expression of N-cadherin supports its role in mediating CIL between placodes and CNC together with the Wnt/PCP signalling pathway (Theveneau et al., 2013). On cellular level, endogenous N-cadherin is localized at cell-cell contact indicated by immunofluorescence staining on CNC explant in this work. This is consistent with the observation that N-cadherin mediated cell-cell adhesion is required for CIL between CNC cells (Theveneau et al., 2010), as well as between placodes and CNC cells during the chase-and-run behaviour (Theveneau et al., 2013).

Quantification via RT-qPCR in this work is able to confirm the expression of PCNS in CNC cells through all stages. When compared to the expression level in whole embryos, PCNS shows a clear enrichment in CNC cells, which is also exhibited by its very high copy number on the cellular level. When average copy numbers in CNC cells are compared, PCNS expression is approximately three fold higher than N-cadherin and 30 folds higher than Cadherin-11. The enrichment of PCNS in CNC cells consist also with the known expression pattern of PCNS as revealed by *in situ* hybridisation, which detects strong signal of PCNS transcripts and its prominently expression in CNC region (Rangarajan et al., 2006). Inhibition of PCNS function results in failure of CNC migration *in vivo*, causing severe defects in the craniofacial skeleton (Rangarajan et al., 2006). Furthermore, PCNS morphant CNC cells explanted on fibronectin show a round cell shape and no formation of cell protrusions (Rangarajan et al., 2006). This can be caused by cell death or disturbed cell-substrate adhesion. Considering its localization within cell protrusions (in this work), PCNS could be involved in protrusion formation in CNC cells. Also, protocadherins generally display weak homophilic adhesion properties (Halbleib and Nelson, 2006). Considering the rounded and apoptotic PCNS deficient cells observed *in vitro*, it is likely that the expression of PCNS is closely related to cell survival, which would explain the high abundance of PCNS transcripts detected in CNC cells. Thus, future rescue experiments with different deletion constructs will help elucidate the role of PCNS in CNC cell migration.

Interestingly, in this work, the protocadherin PAPC is additionally identified in CNC cells via RT-qPCR. PAPC shows an overall 65% amino acid identity with PCNS, but its expression in CNC cells has not been described until now. PAPC is expressed prominently in mesoderm tissues and it is best known for its interaction with the Wnt/PCP pathway regulating cell polarity and convergent extension movements during *Xenopus* gastrulation (Kim et al., 1998; Unterseher et al., 2004). In this work, PAPC transcripts are detected in premigratory and migratory CNC cells. This adds a new expression domain to the so far known expression pattern of PAPC. Quantification data also show its low copy number in CNC cells compared to other cadherins, which might be the reason for lack of detection by *in situ* hybridization due to its limited sensitivity. Though present in very low abundance, particularly when compared to the abundance of PCNS, overexpression of PAPC is able to compensate the loss of PCNS in CNC migration. Knockdown of PAPC has no effect on cell migration, indicating that for normal CNC migration PAPC is dispensable (Schneider et al., 2014). Recent studies have shown that PAPC regulates cell adhesion indirectly by controlling the membrane localization and turnover of C-cadherin (Kraft et al., 2012), implying a role for PAPC in CNC cells in context with modulating the adhesive function of classical cadherins.

XB-cadherin and C-cadherin are classical type I cadherins maternally expressed in early *Xenopus* embryos (Ginsberg et al., 1991; Muller et al., 1994). A sequence divergence of about 8-10% between XB- and C-cadherin characterizes them as pseudoallele (Kühl and Wedlich, 1996). They both are expressed in all cells until neurula stage and are thought to diminish afterwards in most of the tissue except in the epidermis (Kühl and Wedlich, 1996). This is the first time these two cadherins has been identified in CNC cells. Interestingly, immunofluorescence staining in this work shows that they are both localized at the cell-cell contacts of CNC cells. C-cadherin contributes to the major part of the cadherin protein pool (Muller et al., 1994). This is consistent with the absolute quantification showing that XB/C-cadherin has relative high copy numbers in CNC cells as well as in whole embryos. Despite of targeted injection for future neural crest region in 16-cell stage, knockdown of C-cadherin leads to severe tissue dissociation and high lethality in early developmental stages of *Xenopus* (data not shown), indicating that C-cadherin could have a general adhesive functions in maintaining tissue integrity by presenting in close association with the cell membrane (Levi et al., 1991). C-cadherin shares comparable homology with mouse E- and P-cadherin (Ginsberg et al., 1991), whereas XB-cadherin represents the *Xenopus* homolog of the mammalian P-cadherin (Redies and Muller, 1994). P-cadherin is reported to be an enhancer of migration and invasion of breast cancer cell, with correlation to tumour aggressiveness (Paredes et al., 2007). The function of XB-cadherin or C-cadherin in CNC cell migration has not been described, probably due to the low survival rate of embryos when XB-cadherin or C-cadherin is deprived.

Xenopus E-cadherin is known as an epithelial cadherin and is required for maintaining the integrity of the ectoderm during epiboly (Levine et al., 1994) and the assembly of F-actin in non-neural ectorderm (Nandadasa et al., 2009). Recent studies demonstrate the expression of E-cadherin in placodes (Theveneau et al., 2013). It is shown that E-cadherin expression results in cohesion between placodal cells and in CNC cells, when E-cadherin is ectopically expressed (Theveneau et al., 2013). But blocking E-cadherin with an specific antibody in placodes does not effect the interaction between CNC cells and placodes (Theveneau et al., 2013), implying the absence of E-cadherin in CNC cells is necessary for CIL between CNC cells as well as for CIL between CNC and placodes.

In this work, the expression of E-cadherin in CNC cells is demonstrated not only on the transcriptional level using RT-qPCR, but also on the protein level, as shown by immunofluorescence staining of CNC explants and in whole embryo sections. Additionally, western blot analysis performed on CNC explants lysates confirmed the expression of E-cadherin in CNC. By applying multiple CNC markers as positive controls, the specificity of the

CNC tissue used for RT-qPCR is validated to further support the striking expression of E-cadherin in CNC. As negative controls served the mesoderm marker *xbra*, the epithelial marker *xK81* and the placodal marker *xeya1*. All of them are detected in very few amounts confirming the specificity of CNC in the isolated tissue. The placodal tissue remains intact after dissection of CNC, indicating that the detected transcripts of E-cadherin are not from placodes. RT-qPCR analyses reveal that E-cadherin transcripts are present in relatively high abundance in CNC cells during all stages, with average copy number similar to N-cadherin but half as many as that of PCNS. However, in comparison to its expression in whole embryos, E-cadherin expression in CNC comprises a fairly small proportion compared to the whole E-cadherin pool in *Xenopus* embryos, which is expected, when considering the abundance of E-cadherin in the epidermis. Nevertheless, the presence of abundant transcripts of E-cadherin probably explains the relatively low knockdown efficiency in the CNC tissue. As shown by the specificity test of the E-cadherin morpholino, with injection of 16 ng morpholino, a low E-cadherin expression can still be detected. 16 ng morpholino causes relatively high death rate after neurula stage, and the head region of the embryos are often deformed. Moreover, most CNC cells treated with 16 ng E-cadherin morpholino could not survive more than two hours in culture. All these imply that E-cadherin is involved in fundamental functions such as cell cohesion in CNC cells as well as in the whole embryo (Levine et al., 1994). Additionally, the up-regulation of E-cadherin from premigration to migration phase suggests that the E-cadherin expression might be necessary for migrating CNC cells. This is contradictory to the previous EMT model, which claims the annihilation of E-cadherin in mesenchymal tissue once the migration begins (Shook and Keller, 2003; Theveneau and Mayor, 2012b). In this work, it is shown that E-cadherin protein is localized at cell-cell contacts in premigratory CNC explant as well as in migrating CNC segments. Interestingly, heterogeneously expressed E-cadherin is detected in mandibular, hyoid and branchial streams of CNC, indicating that different CNC subpopulations exhibit distinctive E-cadherin expression. This suggests the expression level of E-cadherin could correlate to specific function in the derivatives of these different CNC subpopulations.

The quantification of different cadherin molecules in CNC cells performed by RT-qPCR demonstrates the expression level of distinctive cadherin subtypes during CNC migration, which could be linked to their specific function in mediating cell migration. But more important, the quantitative analyses and the subsequent comparison of the molecule numbers are able to provide a unique view about the distribution and abundance of distinctive cadherins subtypes. Although the quantification is carried out in an amphibian cell system, a comparison to the mammalian cells provides nevertheless some hint about the abundances of mRNA populations.

A total of 10,000 to 20,000 different mRNA species are normally observed in each mammalian cell and mRNA populations in the cells can be usually sorted into three classes: Scarce, intermediate and abundant mRNAs (Tab 6.1) (Alberts, 2002).

	Copies/cell#/class	Total	mRNA molecules/class
Abundant	12,000	4	= 48,000
Intermediate	300	500	= 150,000
Scarce	15	11,000	= 165,000

Tab6.1 Populations of mRNA molecules in a typical mammalian cell. (Adopted from Alberts, 2002)

The majority of mRNA species" presents with 5 to 15 molecules per cell and is classified as "scarce abundance mRNAs (scarce as less copy number per cell). In this work, most of the identified cadherin subtypes belong to this class of mRNA population except for PCNS. With average more than 30 copies per cell, the abundance of PCNS transcripts is much higher than other cadherins and reaches the copy number of mRNA with "intermediate abundance" mRNAs. As indicated in the Tab 6.1, the majority of the genes that are transcribed give rise to very few mRNA molecules. The fact that PCNS is transcribed at much higher rates than others could imply that it is needed in multiple cellular processes or have essential functions related to cell proliferation and survival.

6.2 E-cadherin promotes CNC cell migration

In this work, loss-of-function experiments show that the inhibition of E-cadherin blocks CNC migration *in vivo*. Due to the prominent expression of E-cadherin in *Xenopus*, the morpholino concentration for loss-of-function experiments is reduced. Though the E-cadherin morpholino induced knockdown effect seems to vary in different batches of embryos, a 40% to 70% phenotype frequency can still be observed. The variation could be caused by insufficient knockdown using low dose of morpholino. The CNC cell migration defect can be partially rescued by reintroducing full length E-cadherin, indicating a specific function of E-cadherin in mediating CNC cell migration. It is likely that the partial rescue is due to the heterogeneous expression pattern of E-cadherin in CNC. Therefore, the titration of the optimal does is critical to achieve a better rescue effect.

Since the migration defect of CNC cells can be caused by defect in early specification of neural crest prior to migration, *in situ* hybridization is performed on E-cadherin knockdown embryos with CNC specification markers. The expressions of two early CNC specifiers *c-myc* and *AP2* are not impaired by E-cadherin knockdown, indicating that CNC cells are correctly formed at premigratory stage. Though *twist* signal at stage 17 is reduced upon E-cadherin knockdown, it could be an effect caused by delayed twist expression, because a reduction of twist expression is not observed in later migration stages. However, the unimpaired expressions of *c-myc* and *AP2* upon E-cadherin knockdown suggest that E-cadherin is specifically needed for migratory CNC cells.

The requirement of E-cadherin in migratory CNC cells contradicts to the commonly accepted premise that E-cadherin is down-regulated in the process of epithelial-mesenchymal transition (EMT) in CNC emigration (Pla et al., 2001; Shook and Keller, 2003). Likewise, in the context of cancer, E-cadherin is traditionally categorized as a tumor suppressor, as decreased E-cadherin level is often associated with cell motility, invasion and metastasis (Hazan et al., 2004; Jeanes et al., 2008). However, recent investigations about the role of E-cadherin in cancer indicate that the presence of E-cadherin does not preclude cell migration or invasion during tumour progression. Carcinoma of the breast is for example a tumor type in which the EMT is usually associated with down-regulation of E-cadherin (Berx et al., 1995), However, recent studies show that a predominant subtype of breast cancer, the invasive ductal carcinoma, not only consistently expresses E-cadherin, but in their distant metastases even higher amounts of E-cadherin are found than in the primary tumor (Kowalski et al., 2003). Moreover, E-cadherin is overexpressed in the inflammatory carcinoma (Hoffmeyer et al., 2005; Kleer et al., 2001) and introduction of dominant negative mutant E-cadherin is able to decrease the invasion (Dong et al., 2007). As epithelial properties are not always lost in progressive tumours, invasion in the form of aggregates with cells remaining closely together may enable the spread of specific tumour types, including the well-differentiated carcinomas, melanomas and rhadomyosarcomas (Friedl and Gilmour, 2009). CNC cells are pre-segmented in different populations prior to their emigration from the neural tube and each segment migrates collectively as aggregate but individually from other segments along different routes (Sadaghiani and Thiébaud, 1987). These characters suggest that preservation of cell-cell cohesion could be facilitating the collective cell migration, in that E-cadherin stabilizes interactions between cells such that the traction forces generated by the leading edge cells are able to pull the adherent following cells along. Such mechanism is experimentally demonstrated in carcinoma cells, whereby intact E-cadherin mediated cell junctions and p120 catenin are required for collective invasion (Macpherson et al., 2007). In this

work, it is observed that reduced E-cadherin expression does not cause dissociation of cells. However, other cadherins expressed in the CNC cells for instance XB/C-cadherin or N-cadherin, also mediate cell-cell adhesion and thereby maintain cell clustering. To determine whether the E-cadherin mediated adhesion between CNC cells is important for the migration, adhesion force measurements (Mège et al., 2006) in E-cadherin knockdown cells are required.

The migration of border cells on the surface of germline cells during *Drosophila* oogenesis provides an example, where E-cadherin itself could provide cell-cell adhesion and traction during cell migration. It has been shown that the *Drosophila* E-cadherin homologue, *D*E-cadherin, is required in border cells as well in germline cells for migration (Niewiadomska et al., 1999). In fact, *D*E-cadherin is not essential for adhesion between border cells, but for the *D*E-cadherin mediate interactions between cell surfaces of border cells and germline cells, as *D*E-cadherin deficient border cells cannot use the germline cells as a substratum for migration (Niewiadomska et al., 1999). This is reminiscent of the "chase and run" behaviour between CNC cells and placodes. Since placode cells express E-cadherin (Theveneau et al., 2013), the E-cadherin mediated interaction between CNC cells and placodes could be important to drive the migration of CNC cells. It would be for example interesting to show, whether CNC cells in the absence of E-cadherin can still engage the "chase and run" behaviour with placodal cells. In this case, the migration of CNC cells could rely on E-cadherin in different ways. E-cadherin itself may also mediate CIL between CNC cells and placodal cells. Alternatively, E-cadherin mediated contact and mechanical coupling between cells may be required for generating traction force that move cells forward. This is observed for example in single germ cell migration in zebrafish embryos, where E-cadherin-mediated adhesion is required, both for the interaction between migrating cells and their neighbouring cells, but also for generating traction force upon actin-rich structure (Kardash et al., 2010). Here, it is noteworthy that the adhesive function of E-cadherin seems to be required for mediating traction forces, since blocking of the homophilic interaction of E-cadherin by overexpression of a dominant-negative mutant lacking the extracellular domains, "uncouples" the actin-rich structure and inhibit cell motility (Kardash et al., 2010). This finding is consistent with the observation in this work, that a better rescue of CNC migration is achieved with the cytoplasmic domain deleted form of E-cadherin (E-cadMuΔC), rather than the extracellular domain mutated dominant-negative form of E-cadherin (DN E-cadMu), indicating that an unimpaired extracellular domain of E-cadherin is essential for the migration of cells. Surprisingly, E-cadMuΔC achieves a better rescue effect than full length E-cadherin (EcadMu). One speculation is that p120 catenin regulated cell motility might be involved. It has been shown that elevated level of unbound p120 promotes cell migration by activating cdc42 and Rac activity

(Grosheva et al., 2001). However, formation of cadherin-mediated cell-cell contacts sequester p120 to the junction region, abolishing the effects of p120 on cell morphology (Grosheva et al., 2001). Moreover, in E-cadherin expressed breast cancer cells, p120 disperse also in the cytoplasm and nucleus apart from cell-cell contacts and p120-mediated Rac1 activation is required for HER2/ErB2 signalling-induced cell migration (Johnson et al., 2010). It is also reported that the extracellular fragment of E-cadherin promotes cell migration by activating ErbB signalling (Najy et al., 2008). The proposed hypothesis is that the cytoplasmic domain depleted E-cadherin in this work might promote CNC cell migration by "free" the p120 from the sequestering effect, which normally caused by E-cadherin-mediated cell adhesion. Earlier study has also reported the requirement of p120 in *Xenopus* CNC migration (Ciesiolka et al., 2004). However, how p120 function is correlated with cadherins to promote CNC migration remains unclear and needs to be investigated. Additionally, it is still not clear how the E-cadherin mediated cell-cell adhesion act together with actin to generate traction force that drives migration of CNC cells. Furthermore, the signalling function of E-cadherin is demonstrated by its regulation role at inhibitory GABAergic synapse in cortical neurons, whereby E-cadherin signalling might directly affect synapse vesicle clustering and regulate synapse vesicle cycle (Fiederling et al., 2011).

Additionally, it is also shown in this work that E-cadherin knockdown CNC cells *in vitro* fail to form stable cell protrusions and show cell blebbing, which could be due to two reasons. Cadherin clusters anchor contractile actomyosin network in cells, removal this anchorage by depletion of E-cadherin from cell membrane may disturb the actomyosin structure. This could result in increased cortical tension, which might be responsible for blebbing formation (Paluch et al., 2005). Additionally, it is shown that in the cell-cell contact formation, E-cadherin mechanically couple the adhering cells, allowing cortex tension to control contact expansion (Maitre et al., 2012). In this work, since introducing the DN E-cadMu with disruptive adhesive function fails to restore protrusions in CNC cells, suggesting that E-cadherin mediated adhesion is in some way necessary for protrusion formation. This is verified by the fact that with intact adhesive function is able to largely restore the protrusion formation of CNC cells. The cytoplasmic domain of E-cadherin seems in this case dispensable.

The blebbing phenotype of E-cadherin knockdown can also be caused by reduced cell-substrate adhesion. It is recently reported that Cadherin-11 mediates cell-substrate adhesion, and when the focal adhesion formation is compromised in Cadherin-11 depleted CNC cells *in vitro*, protrusions could not be formed and cells show blebbing (Langhe et al., in revision). It would be interesting to test whether E-cadherin knockdown reduces focal adhesion formation as well.

Recent study shows E-cadherin-mediated contact and mechanical coupling between cells are required for the traction force between cell and fibronectin, which involved Src and PI3K activities (Jasaitis et al., 2012). Similar observation is also made in collective directional migration of epithelial sheets, where cells in the leading rows exert traction force on the substratum to coordinate in directional re-orientation (Li et al., 2012). Thus, traction force measurements of E-cadherin expressed/deficient CNC cells on fibronectin surface should be able to clarify whether E-cadherin stimulate traction force at focal adhesion in CNC cells as well. Taken together, these results suggest a unique function of E-cadherin in mediating collective CNC cell migration. E-cadherin mediated contact seems to be necessary for cells to migrate *in vivo* as well as to form protrusions *in vitro*.

Classical cadherins have in general very similar structures, which raises the question, whether some of them could have redundant function in promoting CNC migration. However, reconstitution experiments in this work demonstrate that the loss of E-cadherin cannot be rescued by other cadherins. Furthermore, double knockdown of E-cadherin and N-cadherin reveals that E-cadherin and N-cadherin have distinct function in mediating CNC migration as well as cell protrusion formation. However, another reconstitution experiments in this work could demonstrate that Cadherin-11 and N-cadherin are indeed mutually interchangeable in their function in mediating CNC migration. Interestingly, both Cadherin-11 and N-cadherin promote CIL in CNC cells (Becker et al., 2013; Theveneau et al., 2010). Also, it is recently demonstrated that PAPC can compensate for the loss of PCNS in regulating CNC migration (Schneider et al., 2014). And PCNS is also able to replace the function of PAPC in inner ear development (Jung et al., 2011). These results imply that cadherins from the same subfamily with analogous structure could employ more resembling mechanism for their conserved function. Chimera constructs combining different domains of N-cadherin and Cadherin-11 could further elucidate the functional discrepancies and similarities in those two cadherins.

6.3 E-cadherin positive CNC cells may contribute to the development of the *Xenopus* ear

As reported by the amphibian fate map, the three CNC streams contribute to cartilage formation in the middle and external ear (Cerny et al., 2004). The mandibular CNC subpopulation forms the tympanic annulus (external ear), supporting the surrounding cartilage and a cartilaginous

tympanic disk. The hyoidal CNC subpopulation gives rise to the pars externa plectri (extrastapes) and pars media plectri (stapes). The branchial subpopulation forms the pars interna plectri (stapedial footplate) that inserts in to the oval window (Gross et al., 2006). Stapes is the only ear ossicle in *Xenopus* (Mason et al., 2009), although the extrastapes of frogs function as a second ossicle (Mason and Narins, 2002). In addition, the anterior and posterior domains of the otic capsule, which surrounds and protects the inner ear, arise also from the branchial subpopulation (Gross and Hanken, 2008; Gross et al., 2006). The malformation of outer or middle ear structure is related with conductive hearing loss in human (Ruckenstein, 1995). In this work, the immunofluorescence staining in whole embryo section shows a heterogeneous expression of E-cadherin in different subpopulation of CNC cells, with strong expression particularly in the branchial subpopulation. This implies a possible role of E-cadherin in the middle ear development. Therefore, histological sections of E-cadherin deficient embryo should able to display whether E-cadherin is involved in the middle ear formation.

In this work, E-cadherin positive branchial CNC cells are observed in the otic vesicle, indicating CNC cells contribute directly in the otic vesicle formation. It is generally accepted that the otic placode ectoderm is the only source for the inner ear, except melanocytes and glia cells derived from NC cells. However, it is recently reported in mice that the neuroepithelial cells, including NC cells, contribute directly to the otic vesicle from the neural tube. Using transgenic mice to fate map the neuroepithelial cells, it is demonstrated that these cells incorporate into the otic epithelium after otic placode induction and their derivatives give rise to hair cells and supporting cells within sensory epithelia, neuralblasts in the otic vesicle and cochleovestibular ganglion (Freyer et al., 2011). The E-cadherin positive CNC population observed in the otic vesicle could represent such incorporation of CNC cells into the otic vesicle after the induction occurred. This implies that besides the well established contribution of CNC to middle ear, CNC cells may also contribute to the inner ear formation in *Xenopus*. Furthermore, E-cadherin expressed in CNC cells could have specific function for the incorporation of CNC into otic vesicle, since otic vesicle itself expresses E-cadherin as well during its formation (own unpublished observations). Additionally, PAPC and C-cadherin are also present during otic vesicle formation in *Xenopus* (Jung et al., 2011); and own unpublished observations) and PAPC is required for the invagination of otic vesicle (Jung et al., 2011). In zebrafish, N-cadherin and Cadherin-11 (Novince et al., 2003) are expressed in the otic placode and N-cadherin is required for the elongation of placodal cells and its subsequent invagination in chicken (Christophorou et al., 2010). Recent studies reveal that mutation of Cadherin-23 is associated with deafness due to its structural role in the tip-links of inner ear hair cells (Giacomello et al., 2012). Cadherin-23 and the

protocadherin-15, both involved in forming the tip-link, are suggested for their function in mechanotransduction (Müller, 2008).

To determine whether an incorporation of CNC cells to the otic vesicle occurs *in vivo*, live tracking analysis of both labeled CNC cells and ectoderm originated otic vesicle should be performed. In addition, the function of E-cadherin in the otic vesicle formation has to be investigated. It has been shown that E-cadherin interacts with Myosin VI, which is required for normal hair cell formation and mutations cause deafness in mice (Geisbrecht and Montell, 2002). Therefore, investigation of E-cadherin function in ear development could provide new insights into the understanding of deafness.

7   Summary

In this present work, quantitative analysis of six different cadherin superfamily members provides a novel cadherin expression profile in *Xenopus* CNC cells. Interestingly, XB/C-cadherins, E-cadherin and PAPC are identified for the first time in CNC cells. Furthermore, knockdown analysis of E-cadherin allocates a novel function of this cadherin in mediating CNC migration.

The expression of Cadherin-11, N-cadherin and PCNS in CNC cells is confirmed via quantitative real-time PCR (RT-qPCR). Additionally, transcripts of XB/C-cadherin, E-cadherin and PAPC are newly identified in CNC cells. Relative quantification reveals the change of expression level in each cadherin subtype in premigratory (stage 17), emigrating (stage 20) and migratory (stage 23) CNC cells. The copy number of each cadherin is determined via absolute quantification, allowing a direct comparison of cadherin abundance in CNC cells as well as in whole embryo. Immunofluorescence staining on CNC explants verifies the expression of XB/C-cadherin, N-cadherin and E-cadherin in CNC cells, and demonstrates their prominent sub-cellular localization at cell-cell contacts.

E-cadherin is expressed at cell-cell contacts in premigratory CNC cells as well as in migratory CNC, which is shown by the immunofluorescence staining performed on CNC transplanted whole embryo sections. Distinct CNC subpopulations express E-cadherin heterogeneously, with the strongest expression found in branchial streams of CNC cells. Knockdown of E-cadherin inhibits CNC migration *in vivo* and protrusion formation *in vitro*. In the reconstitution experiment, it is shown that both CNC migration and cell protrusion formation relies on the intact extracellular domain of E-cadherin, instead of the cytoplasmic domain. Reconstitution experiments with other classical cadherins are not able to restore the E-cadherin knockdown induced CNC migration defect, indicating a unique function of E-cadherin during CNC migration.

8   Zusammenfassung

Die in der vorliegenden Arbeit durchgeführten quantitativen Analysen von sechs verschiedenen Cadherinen ergeben ein bis dato noch nicht vorhandenes Cadherin-Expressionsprofil in den cranialen Neuralleistenzellen (cNLZ) von *Xenopus*. Vor allem konnten dabei XB/C-cadherin, E-cadherin und PAPC zum ersten mal in den cNLZ beschrieben werden. Des Weiteren konnte eine neue Rolle von E-cadherin in der Migration der cNLZ zugeordnet werden.

Durch die quantitative RT-PCR konnte die bereits bekannte Expression von Cadherin-11, N-cadherin und PCNS in cNLZ bestätigt werden, während Transkripte von XB/C-cadherin, E-cadherin und PAPC zum ersten Mal in cNLZ identifiziert wurden. Mittels der relativen Quantifizierung konnte die dynamische Veränderung der Expressionslevel der einzelnen Cadherine vor der Migration (Stadium 17), während der Emigration (Stadium 20) und der Migration (Stadium 23) der cNLZ veranschaulicht werden. Durch die absolute Quantifizierung konnte zusätzlich die genaue Kopienanzahl der einzelnen Cadherine ermittelt werden, sodass ein direkter Vergleich der Expression verschiedenen Cadherine durchgeführt werden konnte. Durch Immunfluoreszenzfärbung auf cNLZ Explantaten wurde des Weiteren die Lokalisation von XB/C-cadherin, N-cadherin und E-cadherin an Zell-Zell Kontakte gezeigt. Mit Hilfe von Immunfluoreszenzfärbungen auf Gefrierschnitten konnte eine verstärkte Expression von E-cadherin in den branchialen Kiemenbögen *in vivo* beobachtet werden. Transplantationsanalysen und Ganzkeim-ISH mit cNLZ Markern zeigten, dass die Injektion eines antisense Morpholino-Oligonukleotids gegen E-cadherin die Migration der cNLZ blockiert. Zeitrafferaufnahmen von explantierten cNLZ konnten weiterhin eine Funktion von E-cadherin im Ausbilden von Zellausläufern aufdecken. Rekonstitutionsversuche mit E-cadherin Deletionskon-strukten veranschaulichten, dass die Migration der cNLZ in die Kiemenbögen und das Ausbilden von Zellausläufern vor allem von der Anwesenheit der extrazellulären Domäne und nicht der zytoplasmatischen Domäne abhängig ist. Rekonstitutionsversuche mit anderen klassichen Cadherine konnten die durch den Verlust von E-cadherin bedingten Migrationsdefekte der cNLZ nicht wiederherstellen, das auf eine spezifische Funktion von E-cadherin in der Migration der cNLZ hindeutet.

9   References

Abercrombie, M. (1979). Contact inhibition and malignancy. Nature *Sep 27;281(5729):259-62.*

Ahlstrom, J.D., and Erickson, C.A. (2009). The neural crest epithelial-mesenchymal transition in 4D: a `tail' of multiple non-obligatory cellular mechanisms. Development *136*, 1801-1812.

Alberts B, J.A., Lewis J, et al. (2002). Molecular Biology of the Cell. 4th edition. New York: Garland Science.

Alfandari, D., Cousin, H., Gaultier, A., Hoffstrom, B.G., and DeSimone, D.W. (2003). Integrin α5β1 supports the migration of Xenopus cranial neural crest on fibronectin. Developmental Biology *260*, 449-464.

Alfandari, D., Cousin, H., and Marsden, M. (2010). Mechanism of Xenopus cranial neural crest cell migration. Cell adhesion & migration *4*, 553-560.

Anastasiadis, P.Z., and Reynolds, A.B. (2000). The p120 catenin family: complex roles in adhesion, signaling and cancer. Journal of cell science *113*, 1319-1334.

Arboleda-Estudillo, Y., Krieg, M., Stühmer, J., Licata, N.A., Muller, D.J., and Heisenberg, C.-P. (2010). Movement Directionality in Collective Migration of Germ Layer Progenitors. Current Biology *20*, 161-169.

Aubry, M.F.M., and Morand (1964). [THE EPIBULBAR DERMOID-AURICULAR APPENDIX-PREAURICULAR FISTULA TRIAD OR FRANCHESCETTI-GOLDENHAR SYNDROME]. Ann Otolaryngol Chir Cervicofac *81*, 69-71.

Baltzinger, M., Ori, M., Pasqualetti, M., Nardi, I., and Rijli, F.M. (2005). Hoxa2 knockdown in Xenopus results in hyoid to mandibular homeosis. Developmental Dynamics *234*, 858-867.

Becker, S.F., Langhe, R., Huang, C., Wedlich, D., and Kashef, J. (2012). Giving the right tug for migration: Cadherins in tissue movements. Archives of biochemistry and biophysics *524*, 30-42.

Becker, S.F.S., Mayor, R., and Kashef, J. (2013). Cadherin-11 Mediates Contact Inhibition of Locomotion during <italic>Xenopus</italic> Neural Crest Cell Migration. PLoS ONE *8*, e85717.

Bellmeyer, A., Krase, J., Lindgren, J., and LaBonne, C. (2003). The Protooncogene c-Myc Is an Essential Regulator of Neural Crest Formation in Xenopus. Developmental cell *4*, 827-839.

Berx, G., Cleton-Jansen Am Fau - Nollet, F., Nollet F Fau - de Leeuw, W.J., de Leeuw Wj Fau - van de Vijver, M., van de Vijver M Fau - Cornelisse, C., Cornelisse C Fau - van Roy, F., and van Roy, F. (1995). E-cadherin is a tumour/invasion suppressor gene mutated in human lobular breast cancers.

Berx, G., and van Roy, F. (2009). Involvement of Members of the Cadherin Superfamily in Cancer. Cold Spring Harbor perspectives in biology *1*.

Bio-Rad applications guide (2006).

Blaschuk, O.W., Sullivan, R., David, S., and Pouliot, Y. (1990). Identification of a cadherin cell adhesion recognition sequence. Developmental Biology *139*, 227-229.

Boggon, T.J., Murray, J., Chappuis-Flament, S., Wong, E., Bm, G., and Shapiro, L. (2002). C-cadherin ectodomain structure and implications for cell adhesion mechanisms. science.

Borchers, A., David, R., and Wedlich, D. (2001). Xenopus cadherin-11 restrains cranial neural crest migration and influences neural crest specification. Development *128*, 3049-3060.

Bouwmeester, T., Kim, S.-H., Sasai, Y., Lu, B., and Robertis, E.M.D. (1996). Cerberus is a head-inducing secreted factor expressed in the anterior endoderm of Spemann's organizer. Nature *382*, 595-601.

Brieher, W.M., and Gumbiner, B.M. (1994). Regulation of C-cadherin function during activin induced morphogenesis of Xenopus animal caps. The Journal of Cell Biology *126*, 519-527.

Bustin, S. (2000). Absolute quantification of mRNA using real-time reverse transcription polymerase chain reaction assays. Journal of Molecular Endocrinology *25*, 169-193.

Carmona-Fontaine, C., Matthews, H.K., Kuriyama, S., Moreno, M., Dunn, G.A., Parsons, M., Stern, C.D., and Mayor, R. (2008). Contact inhibition of locomotion in vivo controls neural crest directional migration. Nature *456*, 957-961.

Carmona-Fontaine, C., Theveneau, E., Tzekou, A., Tada, M., Woods, M., Page, Karen M., Parsons, M., Lambris, John D., and Mayor, R. (2011). Complement Fragment C3a Controls Mutual Cell Attraction during Collective Cell Migration. Developmental cell *21*, 1026-1037.

Cavey, M., Rauzi, M., Lenne, P.-F., and Lecuit, T. (2008). A two-tiered mechanism for stabilization and immobilization of E-cadherin. Nature *453*, 751-756.

Cerny, R., Meulemans, D., Berger, J., Wilsch-Bräuninger, M., Kurth, T., Bronner-Fraser, M., and Epperlein, H.-H. (2004). Combined intrinsic and extrinsic influences pattern cranial neural crest migration and pharyngeal arch morphogenesis in axolotl. Developmental Biology *266*, 252-269.

Charrasse, S., Comunale, F., Fortier, M., Portales-Casamar, E., Debant, A., and Gauthier-Rouvière, C. (2007). M-Cadherin Activates Rac1 GTPase through the Rho-GEF Trio during Myoblast Fusion. Molecular Biology of the Cell *18*, 1734-1743.

Chidgey, M., and Dawson, C. (2007). Desmosomes: a role in cancer? Br J Cancer *96*, 1783-1787.

Choi, Y.S., and Gumbiner, B. (1989). Expression of cell adhesion molecule E-cadherin in Xenopus embryos begins at gastrulation and predominates in the ectoderm. The Journal of Cell Biology *108*, 2449-2458.

Choi, Y.S., Sehgal, R., McCrea, P., and Gumbiner, B. (1990). A cadherin-like protein in eggs and cleaving embryos of Xenopus laevis is expressed in oocytes in response to progesterone. The Journal of Cell Biology *110*, 1575-1582.

Christophorou, N.A.D., Mende, M., Lleras-Forero, L., Grocott, T., and Streit, A. (2010). Pax2 coordinates epithelial morphogenesis and cell fate in the inner ear. Developmental Biology *345*, 180-190.

Chu, K., Cheng, C.-J., Ye, X., Lee, Y.-C., Zurita, A.J., Chen, D.-T., Yu-Lee, L.-Y., Zhang, S., Yeh, E.T., Hu, M.C.-T.*, et al.* (2008). Cadherin-11 Promotes the Metastasis of Prostate Cancer Cells to Bone. Molecular Cancer Research *6*, 1259-1267.

Chu, Y.-S., Thomas, W.A., Eder, O., Pincet, F., Perez, E., Thiery, J.P., and Dufour, S. (2004). Force measurements in E-cadherin–mediated cell doublets reveal rapid adhesion strengthened by actin cytoskeleton remodeling through Rac and Cdc42. The Journal of Cell Biology *167*, 1183-1194.

Ciesiolka, M., Delvaeye, M., Van Imschoot, G., Verschuere, V., McCrea, P., van Roy, F., and Vleminckx, K. (2004). p120 catenin is required for morphogenetic movements involved in the formation of the eyes and the craniofacial skeleton in Xenopus. Journal of cell science *117*, 4325-4339.

Corey, D., and Abrams, J. (2001). Morpholino antisense oligonucleotides: tools for investigating vertebrate development. Genome Biology *2*, reviews1015.1011 - reviews1015.1013.

David, R., Ahrens K Fau - Wedlich, D., Wedlich D Fau - Schlosser, G., and Schlosser, G. (2001). Xenopus Eya1 demarcates all neurogenic placodes as well as migrating hypaxial muscle precursors.

Davis, M.A., Ireton, R.C., and Reynolds, A.B. (2003). A core function for p120-catenin in cadherin turnover. The Journal of Cell Biology *163*, 525-534.

de Crozé, N., Maczkowiak, F., and Monsoro-Burq, A.H. (2011). Reiterative AP2a activity controls sequential steps in the neural crest gene regulatory network. Proceedings of the National Academy of Sciences *108*, 155-160.

Deprez, P., Mandine, E., Vermond, A., and Lesuisse, D. (2002). Imidazole-based ligands of the Src SH2 protein. Bioorganic & Medicinal Chemistry Letters *12*, 1287-1289.

Desai, R.A., Gao, L., Raghavan, S., Liu, W.F., and Chen, C.S. (2009). Cell polarity triggered by cell-cell adhesion via E-cadherin. Journal of cell science *122*, 905-911.

Detrick, R.J., Dickey, D., and Kintner, C.R. (1990). The effects of N-cadherin misexpression on morphogenesis in xenopus embryos. Neuron *4*, 493-506.

DiGeorge, A. (1968). Congenital absence of the thymus and ist immunologic consequences:

concurrence with congenital hypoparathyroidism. NY: March of Dimes Birth Defects Foundation *116*, 21.

Dong, H.-M., Liu, G., Hou, Y.-F., Wu, J., Lu, J.-S., Luo, J.-M., Shen, Z.-Z., and Shao, Z.-M. (2007). Dominant-negative E-cadherin inhibits the invasiveness of inflammatory breast cancer cells in vitro. J Cancer Res Clin Oncol *133*, 83-92.

Drees, F., Pokutta, S., Yamada, S., Nelson, W.J., and Weis, W.I. (2005). α-Catenin Is a Molecular Switch that Binds E-Cadherin-β-Catenin and Regulates Actin-Filament Assembly. Cell *123*, 903-915.

El-Amraoui, A., and Petit, C. (2010). Cadherins as Targets for Genetic Diseases. Cold Spring Harbor perspectives in biology *2*.

Freyer, L., Aggarwal, V., and Morrow, B.E. (2011). Dual embryonic origin of the mammalian otic vesicle forming the inner ear. Development *138*, 5403-5414.

Friedl, P., and Gilmour, D. (2009). Collective cell migration in morphogenesis, regeneration and cancer. Nature reviews Molecular cell biology *10,* 445-457.

Friedl, P., Noble, P.B., Walton, P.A., Laird, D.W., Chauvin, P.J., Tabah, R.J., Black, M., and Zänker, K.S. (1995). Migration of Coordinated Cell Clusters in Mesenchymal and Epithelial Cancer Explants in Vitro. Cancer Research *55*, 4557-4560.

Fujimori, T., and Takeichi, M. (1993). Disruption of epithelial cell-cell adhesion by exogenous expression of a mutated nonfunctional N-cadherin. Molecular Biology of the Cell *4*, 37-47.

Gammill, L.S., and Bronner-Fraser, M. (2003). Neural crest specification: migrating into genomics. Nat Rev Neurosci *4*, 795-805.

Geiger, B., and Ayalon, O. (1992). Cadherins. Annual Review of Cell Biology *8*, 307-332.

Geisbrecht, E.R., and Montell, D.J. (2002). Myosin VI is required for E-cadherin-mediated border cell migration. Nat Cell Biol *4*, 616-620.

Giacomello, M., De Mario, A., Primerano, S., Brini, M., and Carafoli, E. (2012). Hair cells, plasma membrane Ca2+ ATPase and deafness. The International Journal of Biochemistry & Cell Biology *44*, 679-683.

Ginsberg, D., DeSimone, D., and Geiger, B. (1991). Expression of a novel cadherin (EP-cadherin) in unfertilized eggs and early Xenopus embryos. Development *111*, 315-325.

Gorfinkiel, N., and Arias, A.M. (2007). Requirements for adherens junction components in the interaction between epithelial tissues during dorsal closure in Drosophila. Journal of cell science *120*, 3289-3298.

Gorfinkiel, N., Blanchard, G.B., Adams, R.J., and Martinez Arias, A. (2009). Mechanical control of global cell behaviour during dorsal closure in Drosophila. Development *136*, 1889-1898.

Grosheva, I., Shtutman, M., Elbaum, M., and Bershadsky, A. (2001). p120 catenin affects cell motility via modulation of activity of Rho-family GTPases: a link between cell-cell contact formation and regulation of cell locomotion. Journal of cell science *114*, 695 - 707.

Gross, J.B., and Hanken, J. (2008). Segmentation of the vertebrate skull: neural-crest derivation of adult cartilages in the clawed frog, Xenopus laevis. Integrative and Comparative Biology *48*, 681-696.

Gross, J.B., Hanken, J., Oglesby, E., and Marsh-Armstrong, N. (2006). Use of a ROSA26:GFP transgenic line for long-term Xenopus fate-mapping studies. Journal of Anatomy *209*, 401-413.

Haas, P., and Gilmour, D. (2006). Chemokine Signaling Mediates Self-Organizing Tissue Migration in the Zebrafish Lateral Line. Developmental cell *10*, 673-680.

Hadeball, B., Borchers, A., and Wedlich, D. (1998). Xenopus cadherin-11 (Xcadherin-11) expression requires the Wg/Wnt signal.

Halbleib, J.M., and Nelson, W.J. (2006). Cadherins in development: cell adhesion, sorting, and tissue morphogenesis. Genes & Development *20*, 3199-3214.

Hall, B. (1979). Choanal atresia and associated multiple anomalies. J Pediatr 95(3): 395-398.

Hall, B.K. (2000). The neural crest as a fourth germ layer and vertebrates as quadroblastic not triploblastic. Evolution & Development *2*, 3-5.

Harland, R.M. (1991). In situ hybridization: an improved whole-mount method for Xenopus embryos. Methods Cell Biol *36:685*, 95.

Harrison, O.J., Jin, X., Hong, S., Bahna, F., Ahlsen, G., Brasch, J., Wu, Y., Vendome, J., Felsovalyi, K., Hampton, C.M.*, et al.* (2011). The Extracellular Architecture of Adherens Junctions Revealed by Crystal Structures of Type I Cadherins. Structure *19*, 244-256.

Häussinger, D., Ahrens, T., Aberle, T., Engel, J., Stetefeld, J., and Grzesiek, S. (2004). Proteolytic E‐cadherin activation followed by solution NMR and X‐ray crystallography, Vol 23.

Hazan, R.B., Qiao, R.U.I., Keren, R., Badano, I., and Suyama, K. (2004). Cadherin Switch in Tumor Progression. Annals of the New York Academy of Sciences *1014*, 155-163.

Hegerfeldt, Y., Tusch, M., Bröcker, E.-B., and Friedl, P. (2002). Collective Cell Movement in Primary Melanoma Explants: Plasticity of Cell-Cell Interaction, β1-Integrin Function, and Migration Strategies. Cancer Research *62*, 2125-2130.

Hoffmeyer, M., Wall, K., and Dharmawardhane, S. (2005). In vitro analysis of the invasive phenotype of SUM 149, an inflammatory breast cancer cell line. Cancer Cell International *5*, 11.

Hong, S., Troyanovsky, R.B., and Troyanovsky, S.M. (2010). Spontaneous assembly and active disassembly balance adherens junction homeostasis. Proceedings of the National Academy of Sciences.

Hopwood, N.D., Pluck, A., and Gurdon, J.B. (1989). A Xenopus mRNA related to Drosophila twist is expressed in response to induction in the mesoderm and the neural crest. Cell *59*, 893-903.

Hoshino, T., Sakisaka, T., Baba, T., Yamada, T., Kimura, T., and Takai, Y. (2005). Regulation of E-cadherin Endocytosis by Nectin through Afadin, Rap1, and p120ctn. Journal of Biological Chemistry *280*, 24095-24103.

Hulpiau, P., and van Roy, F. (2009). Molecular evolution of the cadherin superfamily. The International Journal of Biochemistry & Cell Biology *41*, 349-369.

Hyafil, F., Babinet, C., and Jacob, F. (1981). Cell-cell interactions in early embryogenesis: A molecular approach to the role of calcium. Cell *26*, 447-454.

Jaffe, A.B., and Hall, A. (2005). RHO GTPASES: Biochemistry and Biology. Annual Review of Cell and Developmental Biology *21*, 247-269.

Jamrich, M., Sargent, T., and Dawid, I.B. (1987). Cell-type-specific expression of epidermal cytokeratin genes during gastrulation of Xenopus laevis.

Jasaitis, A., Estevez, M., Heysch, J., Ladoux, B., and Dufour, S. (2012). E-Cadherin-Dependent Stimulation of Traction Force at Focal Adhesions via the Src and PI3K Signaling Pathways. Biophysical journal *103*, 175-184.

Jeanes, A., Gottardi, C.J., and Yap, A.S. (2008). Cadherins and cancer: how does cadherin dysfunction promote tumor progression[quest]. Oncogene *27*, 6920-6929.

Johnson, E., Seachrist, D., DeLeon-Rodriguez, C.M., Lozada, K., Miedler, J., Abdul-Karim, F.W., and Keri, R.A. (2010). HER2/ErbB2-induced breast cancer cell migration and invasion require p120 catenin activation of Rac1 and Cdc42.

Jung, B., Kohler, A., Schambony, A., and Wedlich, D. (2011). PAPC and the Wnt5a/Ror2 pathway control the invagination of the otic placode in Xenopus. BMC Developmental Biology *11*, 36.

Kalcheim, C., and Le Douarin, N.M. (1986). Requirement of a neural tube signal for the differentiation of neural crest cells into dorsal root ganglia. Developmental Biology *116*, 451-466.

Kametani, Y., and Takeichi, M. (2007). Basal-to-apical cadherin flow at cell junctions. Nat Cell Biol *9*, 92-98.

Kardash, E., Reichman-Fried, M., Maitre, J.-L., Boldajipour, B., Papusheva, E., Messerschmidt, E.-M., Heisenberg, C.-P., and Raz, E. (2010). A role for Rho GTPases and cell-cell adhesion in single-cell motility in vivo. Nat Cell Biol *12*, 47-53.

Kashef, J., Köhler, A., Kuriyama, S., Alfandari, D., Mayor, R., and Wedlich, D. (2009). Cadherin-11 regulates protrusive activity in Xenopus cranial neural crest cells upstream of Trio and the small GTPases. Genes & Development *23*, 1393-1398.

Kee, Y., and Bronner-Fraser, M. (2005). To proliferate or to die: role of Id3 in cell cycle progression and survival of neural crest progenitors. Genes & Development *19*, 744-755.

Khan, K., Hardy, R., Haq, A., Ogunbiyi, O., Morton, D., and Chidgey, M. (2006). Desmocollin switching in colorectal cancer. Br J Cancer *95*, 1367-1370.

Kim, S.H., Yamamoto, A., Bouwmeester, T., Agius, E., and Robertis, E.M. (1998). The role of paraxial protocadherin in selective adhesion and cell movements of the mesoderm during Xenopus gastrulation. Development *125*, 4681-4690.

Kitt, K.N., and Nelson, W.J. (2011). Rapid Suppression of Activated Rac1 by Cadherins and Nectins during *De Novo* Cell-Cell Adhesion. PLoS ONE *6*, e17841.

Kleer, C., van Golen, K., Braun, T., and Merajver, S. (2001). Persistent E-cadherin expression in inflammatory breast cancer. Mod Pathol *14*, 458 - 464.

Kovacs, E.M., Ali, R.G., McCormack, A.J., and Yap, A.S. (2002). E-cadherin Homophilic Ligation Directly Signals through Rac and Phosphatidylinositol 3-Kinase to Regulate Adhesive Contacts. Journal of Biological Chemistry *277*, 6708-6718.

Kowalski, P., Rubin, M., and Kleer, C. (2003). E-cadherin expression in primary carcinomas of the breast and its distant metastases. Breast Cancer Res *5*, R217 - R222.

Kraft, B., Berger, C.D., Wallkamm, V., Steinbeisser, H., and Wedlich, D. (2012). Wnt-11 and Fz7 reduce cell adhesion in convergent extension by sequestration of PAPC and C-cadherin. The Journal of Cell Biology *198*, 695-709.

Kühl, M., and Wedlich, D. (1996). Xenopus cadherins: Sorting out types and functions in embryogenesis. Developmental Dynamics *207*, 121-134.

Kulesa, P.M., and Gammill, L.S. (2010). Neural crest migration: Patterns, phases and signals. Developmental Biology *344*, 566-568.

LaBonne, C., and Bronner-Fraser, M. (1998). Neural crest induction in Xenopus: evidence for a two-signal model. Development *125*, 2403-2414.

LaBonne, C., and Bronner-Fraser, M. (1999). MOLECULAR MECHANISMS OF NEURAL CREST FORMATION. Annual Review of Cell and Developmental Biology *15*, 81-112.

Ladoux, B., Anon, E., Lambert, M., Rabodzey, A., Hersen, P., Buguin, A., Silberzan, P., and Mège, R.-M. (2009). Strength Dependence of Cadherin-Mediated Adhesions. Biophysical journal *98*, 534-542.

le Duc, Q., Shi, Q., Blonk, I., Sonnenberg, A., Wang, N., Leckband, D., and de Rooij, J. (2010). Vinculin potentiates E-cadherin mechanosensing and is recruited to actin-anchored sites within adherens junctions in a myosin II–dependent manner. The Journal of Cell Biology *189*, 1107-1115.

Lee, D.M., Kiener, H., Agarwal, S., Noss, E.H., Watts, G.F.M., Chisaka, O., Takeichi, M., and Brenner, M.B. (2007). Cadherin-11 in synovial lining formation and pathology in arthritis.

Lee, S.-H., Bédard, O., Buchtová, M., Fu, K., and Richman, J.M. (2004). A new origin for the maxillary jaw. Developmental Biology *276*, 207-224.

Levi, G., Ginsberg, D., Girault, J.M., Sabanay, I., Thiery, J.P., and Geiger, B. (1991). EP-cadherin in muscles and epithelia of Xenopus laevis embryos. Development *113*, 1335-1344.

Levine, E., Lee, C.H., Kintner, C., and Gumbiner, B.M. (1994). Selective disruption of E-cadherin function in early Xenopus embryos by a dominant negative mutant. Development *120*, 901-909.

Li, L., Hartley, R., Reiss, B., Sun, Y., Pu, J., Wu, D., Lin, F., Hoang, T., Yamada, S., Jiang, J.*, et al.* (2012). E-cadherin plays an essential role in collective directional migration of large epithelial sheets. Cell Mol Life Sci *69*, 2779-2789.

Liu, Z., Tan, J.L., Cohen, D.M., Yang, M.T., Sniadecki, N.J., Ruiz, S.A., Nelson, C.M., and Chen, C.S. (2010). Mechanical tugging force regulates the size of cell–cell junctions. Proceedings of the National Academy of Sciences *107*, 9944-9949.

Livak, K.J., and Schmittgen, T.D. (2001). Analysis of Relative Gene Expression Data Using Real-Time Quantitative PCR and the 2−ΔΔCT Method. Methods *25*, 402-408.

Locascio, A., Manzanares, M., Blanco, M.J., and Nieto, M.A. (2002). Modularity and reshuffling of Snail and Slug expression during vertebrate evolution. Proceedings of the National Academy of Sciences of the United States of America *99*, 16841-16846.

Macpherson, I.R., Hooper, S., Serrels, A., McGarry, L., Ozanne, B.W., Harrington, K., Frame, M.C., Sahai, E., and Brunton, V.G. (2007). p120-catenin is required for the collective invasion of squamous cell carcinoma cells via a phosphorylation-independent mechanism. Oncogene *26*, 5214-5228.

Magie, C.R., Pinto-Santini, D., and Parkhurst, S.M. (2002). Rho1 interacts with p120ctn and α-catenin, and regulates cadherin-based adherens junction components in Drosophila. Development *129*, 3771-3782.

Maitre, J.L., Berthoumieux, H., Krens, S., Salbreux, G., Julicher, F., Paluch, E.K., and Heisenberg, C.P. (2012). Adhesion functions in cell sorting by mechanically coupling the cortices of adhering cells.

Martin, A.C., Gelbart, M., Fernandez-Gonzalez, R., Kaschube, M., and Wieschaus, E.F. (2010). Integration of contractile forces during tissue invagination. The Journal of Cell Biology *188*, 735-749.

Martin, A.C., Kaschube, M., and Wieschaus, E.F. (2009). Pulsed contractions of an actin-myosin network drive apical constriction. Nature *457*, 495-499.

Mason, M., Wang, M., and Narins, P. (2009). STRUCTURE AND FUNCTION OF THE MIDDLE EAR APPARATUS OF THE AQUATIC FROG, XENOPUS LAEVIS.

Mason, M.J., and Narins, P.M. (2002). Vibrometric studies of the middle ear of the bullfrog Rana catesbeiana I. The extrastapes. Journal of Experimental Biology *205*, 3153-3165.

McCusker, C., Cousin, H., Neuner, R., and Alfandari, D. (2009). Extracellular Cleavage of Cadherin-11 by ADAM Metalloproteases Is Essential for Xenopus Cranial Neural Crest Cell Migration. Molecular Biology of the Cell *20*, 78-89.

McCusker, C.D., and Alfandari, D. (2009). Life after proteolysis: Exploring the signaling capabilities of classical cadherin cleavage fragments. Communicative & Integrative Biology *2*, 155-157.

Mège, R.-M., Gavard, J., and Lambert, M. (2006). Regulation of cell–cell junctions by the cytoskeleton. Current opinion in cell biology *18*, 541-548.

Milet, C., and Monsoro-Burq, A.H. (2012). Neural crest induction at the neural plate border in vertebrates. Developmental Biology *366*, 22-33.

Moll, I., Houdek, P., Schafer, S., Nuber, U., and Moll, R. (1999). Diversity of desmosomal proteins in regenerating epidermis: immunohistochemical study using a human skin organ culture model. Arch Dermatol Res 1999 Jul-Aug;291(7-8):437-46, 437-446.

Montell, D.J. (1994). Moving right along: regulation of cell migration during Drosophila development.

Montell, D.J. (2003). Border-cell migration: the race is on. Nature reviews Molecular cell biology *4*, 13-24.

Muller, H., Kuhl, M., Finnemann, S., Schneider, S., van der Poel, S., Hausen, P., and Wedlich, D. (1994). Xenopus cadherins: the maternal pool comprises distinguishable members of the family. Mech Dev *47*, 213 - 223.

Müller, U. (2008). Cadherins and mechanotransduction by hair cells. Current opinion in cell biology *20*, 557-566.

Nabeshima, K., Inoue, T., Shimao, Y., Kataoka., and Koono, M. (1999). Cohort migration of carcinoma cells: differentiated colorectal carcinoma cells move as coherent cell clusters or sheets. Histol Histopathol 1999 Oct;14(4):1183-97.

Nagar, B., Overduin, M., Ikura, M., and Rini, J.M. (1996). Structural basis of calcium-induced E-cadherin rigidification and dimerization. Nature *380*, 360-364.

Najy, A.J., Day Kc Fau - Day, M.L., and Day, M.L. (2008). The ectodomain shedding of E-cadherin by ADAM15 supports ErbB receptor activation.

Nakagawa, M., Fukata, M., Yamaga, M., Itoh, N., and Kaibuchi, K. (2001). Recruitment and activation of Rac1 by the formation of E-cadherin-mediated cell-cell adhesion sites. Journal of cell science *114*, 1829-1838.

Nakagawa, S., and Takeichi, M. (1995). Neural crest cell-cell adhesion controlled by sequential and subpopulation-specific expression of novel cadherins. Development *121*, 1321-1332.

Nakagawa, S., and Takeichi, M. (1998). Neural crest emigration from the neural tube depends on regulated cadherin expression. Development *125*, 2963-2971.

Nandadasa, S., Tao, Q., Menon, N.R., Heasman, J., and Wylie, C. (2009). N- and E-cadherins in Xenopus are specifically required in the neural and non-neural ectoderm, respectively, for F-actin assembly and morphogenetic movements. Development *136*, 1327-1338.

Ng, M.R., Besser, A., Danuser, G., and Brugge, J.S. (2012). Substrate stiffness regulates cadherin-dependent collective migration through myosin-II contractility. The Journal of Cell Biology *199*, 545-563.

Niessen, C.M., Leckband, D., and Yap, A.S. (2011). Tissue Organization by Cadherin Adhesion Molecules: Dynamic Molecular and Cellular Mechanisms of Morphogenetic Regulation, Vol 91.

Nieuwkoop, P., and Faber, J. (1967). Normal Tables of Xenopus laevis (Daudin). North Holland Publishing Cy.

Niewiadomska, P., Godt, D., and Tepass, U. (1999). DE-Cadherin Is Required for Intercellular Motility during Drosophila Oogenesis. The Journal of Cell Biology *144*, 533-547.

Noren, N.K., Niessen, C.M., Gumbiner, B.M., and Burridge, K. (2001). Cadherin Engagement Regulates Rho family GTPases. Journal of Biological Chemistry *276*, 33305-33308.

Nose, A., Tsuji, K., and Takeichi, M. (1990). Localization of specificity determining sites in cadherin cell adhesion molecules. Cell *61*, 147 - 155.

Novince, Z.M., Azodi, E., Marrs, J.A., Raymond, P.A., and Liu, Q. (2003). Cadherin expression in the inner ear of developing zebrafish. Gene Expression Patterns *3*, 337-339.

Oda, H., Uemura, T., Harada, Y., Iwai, Y., and Takeichi, M. (1994). A Drosophila Homolog of Cadherin Associated with Armadillo and Essential for Embryonic Cell-Cell Adhesion. Developmental Biology *165*, 716-726.

Ozaki, C., Obata, S., Yamanaka, H., Tominaga, S., and Suzuki, S.T. (2010). The extracellular domains of E- and N-cadherin determine the scattered punctate localization in epithelial cells and the cytoplasmic domains modulate the localization. Journal of Biochemistry *147*, 929.

Pacquelet, A., and Rørth, P. (2005). Regulatory mechanisms required for DE-cadherin function in cell migration and other types of adhesion. The Journal of Cell Biology *170*, 803-812.

Paluch, E., Sykes, C., Prost, J., and Bornens, M. (2005). Dynamic modes of the cortical actomyosin gel during cell locomotion and division. Trends in cell biology *16*, 5-10.

Paredes, J., Correia, A., Ribeiro, A., Albergaria, A., Milanezi, F., and Schmitt, F. (2007). P-cadherin expression in breast cancer: a review. Breast Cancer Research *9*, 214.

Patel, S.D., Ciatto, C., Chen, C.P., Bahna, F., Rajebhosale, M., Arkus, N., Schieren, I., Jessell, T.M., Honig, B., Price, S.R.*, et al.* (2006). Type II Cadherin Ectodomain Structures: Implications for Classical Cadherin Specificity. Cell *124*, 1255-1268.

Peyrieras, N., Hyafil, F., Louvard, D., Louvard D Fau - Ploegh, H.L., Ploegh Hl Fau - Jacob, F., and Jacob, F. (1983). Uvomorulin: a nonintegral membrane protein of early mouse embryo. Proc Nat Acad Sc U S *80*.

Pishvaian, M.J., Feltes, C.M., Thompson, P., Bussemakers, M.J., Schalken, J.A., and Byers, S.W. (1999). Cadherin-11 Is Expressed in Invasive Breast Cancer Cell Lines. Cancer Research *59*, 947-952.

Pla, P., Moore, R., Morali, O.G., Grille, S., Martinozzi, S., Delmas, V., and Larue, L. (2001). Cadherins in neural crest cell development and transformation. Journal of Cellular Physiology *189*, 121-132.

Pokutta, S., Herrenknecht, K., Kemler, R., and Engel, J. (1994). Conformational changes of the recombinant extracellular domain of E-cadherin upon calcium binding.

Prasad, M.S., Sauka-Spengler, T., and LaBonne, C. (2012). Induction of the neural crest state: Control of stem cell attributes by gene regulatory, post-transcriptional and epigenetic interactions. Developmental Biology *366*, 10-21.

Rangarajan, J., Luo, T., and Sargent, T.D. (2006). PCNS: A novel protocadherin required for cranial neural crest migration and somite morphogenesis in Xenopus. Developmental Biology *295*, 206-218.

Rappolee, D.A., Mark, D., Banda, M., and Werb, Z. (1988). Wound macrophages express TGF-alpha and other growth factors in vivo: analysis by mRNA phenotyping. Science *Aug 5 (4866)*, 708.

Rasmussen, L.D., F., E., Hansen, L., Sj., S., and Johnsen, K. (2001). Group-Specific PCR Primers to Amplify 24S a-Subunit rRNA Genes from Kinetoplastida (Protozoa) Used in Denaturing Gradient Gel Electrophoresis. Microb Ecol 2001 Aug;42(2):109-115.

Redies, C., and Muller, H.A. (1994). Similarities in structure and expression between mouse P-cadherin, chicken B-cadherin and frog XB/U-cadherin.

Ririe, K.M., Rasmussen, R.P., and Wittwer, C.T. (1997). Product Differentiation by Analysis of DNA Melting Curves during the Polymerase Chain Reaction. Analytical Biochemistry *245*, 154-160.

Rørth, P. (2009). Collective Cell Migration. Annual Review of Cell and Developmental Biology *25*, 407-429.

Ruckenstein, M.J. (1995). Hearing loss. A plan for individualized management.

Sadaghiani, B., and Thiébaud, C.H. (1987). Neural crest development in the Xenopus laevis embryo, studied by interspecific transplantation and scanning electron microscopy. Developmental Biology *124*, 91-110.

Sano, K., Tanihara H Fau - Heimark, R.L., Heimark Rl Fau - Obata, S., Obata S Fau - Davidson, M., Davidson M Fau - St John, T., St John T Fau - Taketani, S., Taketani S Fau - Suzuki, S., and Suzuki, S. (1993). Protocadherins: a large family of cadherin-related molecules in central nervous system. EMBO.

Schneider, M., Huang, C., Becker, S.F.S., Gradl, D., and Wedlich, D. (2014). Protocadherin PAPC is expressed in the CNC and can compensate for the loss of PCNS. genesis *52*, 120-126.

Shewan, A.M., Maddugoda, M., Kraemer, A., Stehbens, S.J., Verma, S., Kovacs, E.M., and Yap, A.S. (2005). Myosin 2 Is a Key Rho Kinase Target Necessary for the Local Concentration of E-Cadherin at Cell–Cell Contacts. Molecular Biology of the Cell *16*, 4531-4542.

Shook, D., and Keller, R. (2003). Mechanisms, mechanics and function of epithelial–mesenchymal transitions in early development. Mechanisms of Development *120*, 1351-1383.

Smith, A.L., Dohn, M.R., Brown, M.V., and Reynolds, A.B. (2012). Association of Rho-associated protein kinase 1 with E-cadherin complexes is mediated by p120-catenin. Molecular Biology of the Cell *23*, 99-110.

Smith, J.C., Price Bm Fau - Green, J.B., Green Jb Fau - Weigel, D., Weigel D Fau - Herrmann, B.G., and Herrmann, B.G. (1991). Expression of a Xenopus homolog of Brachyury (T) is an immediate-early response to mesoderm induction.

Smutny, M., Cox, H.L., Leerberg, J.M., Kovacs, E.M., Conti, M.A., Ferguson, C., Hamilton, N.A., Parton, R.G., Adelstein, R.S., and Yap, A.S. (2010). Myosin II isoforms identify distinct functional modules that support integrity of the epithelial zonula adherens. Nat Cell Biol *12*, 696-702.

Solon, J., Kaya-Çopur, A., Colombelli, J., and Brunner, D. (2009). Pulsed Forces Timed by a Ratchet-like Mechanism Drive Directed Tissue Movement during Dorsal Closure. Cell *137*, 1331-1342.

Sonnenberg-Riethmacher, E., Miehe, M., Stolt, C.C., Goerich, D.E., Wegner, M., and Riethmacher, D. (2001). Development and degeneration of dorsal root ganglia in the absence of the HMG-domain transcription factor Sox10. Mechanisms of Development *109*, 253-265.

Spritz, R.A. (1997). Piebaldism, Waardenburg syndrome, and related disorders of melanocyte development.

Takeichi, M. (1990). Cadherins: a molecular family important in selective cell-cell adhesion. Annu Rev Biochem *59*, 237 - 252.

Takeichi, M. (1995). Morphogenetic roles of classic cadherins. Current opinion in cell biology *7*, 619-627.

Theveneau, E., Marchant, L., Kuriyama, S., Gull, M., Moepps, B., Parsons, M., and Mayor, R. (2010). Collective Chemotaxis Requires Contact-Dependent Cell Polarity. Developmental cell *19*, 39-53.

Theveneau, E., and Mayor, R. (2011). Can mesenchymal cells undergo collective cell migration? The case of the neural crest. Cell adhesion & migration *5*, 490-498.

Theveneau, E., and Mayor, R. (2012a). Cadherins in collective cell migration of mesenchymal cells. Current opinion in cell biology *24*, 677-684.

Theveneau, E., and Mayor, R. (2012b). Neural crest delamination and migration: From epithelium-to-mesenchyme transition to collective cell migration. Developmental Biology *366*, 34-54.

Theveneau, E., Steventon, B., Scarpa, E., Garcia, S., Trepat, X., Streit, A., and Mayor, R. (2013). Chase-and-run between adjacent cell populations promotes directional collective migration. Nat Cell Biol *15*, 763-772.

Thompson, E.W., and Price, J.T. (2002). Mechanisms of tumour invasion and metastasis: emerging targets for therapy. Expert Opinion on Therapeutic Targets *6*, 217-233.

Ulrich, F., Krieg, M., Schötz, E.-M., Link, V., Castanon, I., Schnabel, V., Taubenberger, A., Mueller, D., Puech, P.-H., and Heisenberg, C.-P. (2005). Wnt11 Functions in Gastrulation by Controlling Cell Cohesion through Rab5c and E-Cadherin. Developmental cell *9*, 555-564.

Unterseher, F., Hefele, J.A., Giehl, K., De Robertis, E.M., Wedlich, D., and Schambony, A. (2004). Paraxial protocadherin coordinates cell polarity during convergent extension via Rho A and JNK, Vol 23.

Waardenburg, P.J. (1951). A new syndrome combining developmental anomalies of the eyelids, eyebrows and nose root with pigmentary defects of the iris and head hair and with congenital deafness. Am J Hum Genet Sep 1951; 3(3): 195–253, 195–253.

Wagner, G.P. (1990). Hall, B. K. and S. Hörstadius 1988. The Neural Crest. Oxford University Press, London, New York, Tokyo, Toronto, viii + 302 pp. Journal of Evolutionary Biology *3*, 482-483.

Weber, Gregory F., Bjerke, Maureen A., and DeSimone, Douglas W. (2012). A Mechanoresponsive Cadherin-Keratin Complex Directs Polarized Protrusive Behavior and Collective Cell Migration. Developmental cell *22*, 104-115.

Wheelock, M.J., Shintani, Y., Maeda, M., Fukumoto, Y., and Johnson, K.R. (2008). Cadherin switching. Journal of cell science *121*, 727-735.

Whelan, J.A., Russell, N.B., and Whelan, M.A. (2003). A method for the absolute quantification of cDNA using real-time PCR. Journal of Immunological Methods *278*, 261-269.

Wilhelm, J., and Pingoud, A. (2003). Real-Time Polymerase Chain Reaction. ChemBioChem *4*, 1120-1128.

Wollner, D., and Nelson, W. (1992). Establishing and maintaining epithelial cell polarity. Roles of protein sorting, delivery and retention. Journal of cell science *102*, 185-190.

Xiao, K., Oas, R.G., Chiasson, C.M., and Kowalczyk, A.P. (2007). Role of p120-catenin in cadherin trafficking. Biochimica et Biophysica Acta (BBA) - Molecular Cell Research *1773*, 8-16.

Yamada, S., and Nelson, W.J. (2007). Localized zones of Rho and Rac activities drive initiation and expansion of epithelial cell–cell adhesion. The Journal of Cell Biology *178*, 517-527.

Yap, A.S., Niessen, C.M., and Gumbiner, B.M. (1998). The Juxtamembrane Region of the Cadherin Cytoplasmic Tail Supports Lateral Clustering, Adhesive Strengthening, and Interaction with p120ctn. The Journal of Cell Biology *141*, 779-789.

Yonemura, S. (2011). Cadherin–actin interactions at adherens junctions. Current opinion in cell biology *23*, 515-522.

Yu, Z., Michel, F.C., Hansen, G., Wittum, T., and Morrison, M. (2005). Development and Application of Real-Time PCR Assays for Quantification of Genes Encoding Tetracycline Resistance. Applied and Environmental Microbiology *71*, 6926-6933.

Supplementary CD

Contents of the enclosed DVD:

Movie1: E-cadMO explant

Movie2: E-cadMO + E-cadMu explant

Movie3: E-cadMO + DN E-cadMu explant

Movie4: E-cadMO + E-cadMu ΔC explant

The time laps movies show the cell morphology of the CNC cells injected with the indicated constructs. Cell membranes are labelled with either mbGFP or mbCherry, and nuclei are labelled with either H2B GFP or H2B cherry. The movies are 15 minutes to 30 minutes long and the images are taken in three minutes time interval using Axio Observer Z1 Spinning Disc Confocal microscope (40× fluid object).

Publications

Scientific Articles

Becker SF, Langhe R, **Huang C**, Wedlich D and Kashef J (2012)

Giving the right tug for migration: cadherins in tissue movements.

Arch Biochem Biophys 524: 30-42

Schneider M, **Huang C**, Becker SF, Gradl D and Wedlich D (2014)

Protocadherin PAPC is expressed in the CNC and can compensate for the loss of PCNS.

Genesis 52: 120-6

Posters

EMBO Conference Series: Morphogenesis and Dynamics of Multicellular Systems

EMBL Heidelberg, Deutschland, 7.9.2012 - 9.9.2012

13th Young Scientist Meeting oft he German Society for Cell Biology (DGZ)

"Cell Biology shapes the Embryo", Jena, Deutschland, 20.9.2012 – 22.9.2012

Joint meeting FOR1759 and SFB937

"Physics of the embryo", Göttingen, Deutschland, 29.9.2013 – 1.10.2013